X-Linked Inhibitor of Apoptosis (XIAP) in Colorectal Cancer Models

Kathryn C Connolly

Doctor of Medicine (MD) – The University of Edinburgh – 2008

Declaration

Dr Kathryn Connolly has performed the work described in this thesis and composed this thesis in its entirety. Where others have contributed to the work, this has been specifically acknowledged. This thesis has not been accepted in any previous application for a degree.

Dr Kathryn Connolly

March 2008

Contents

List of Figures

List of Tables

Abbreviations

5FU	5 Fluorouracil
AE	Adverse Event
ALP	Alkaline Phosphatase
ALT	Alanine Aminotransferase
Apaf1	Apoptotic Peptidase Activating Factor 1
AST	Aspartate Aminotransferase
AV	Annexin Five
BCL2	B-Cell Lymphoma 2
BioB	Biotinylated hybridisation control
BIR	Baculovirus IAP Repeats
CIAP1	Cellular Inhibitor of Apoptosis 1
CIAP2	Cellular Inhibitor of Apoptosis 2
CPT-11	Irinotecan
CTC	Common Toxicity Criteria
Cyt-C	Cytochrome C
DcR1	Decoy Receptor 1
DcR2	Decoy Receptor 2
DLT	Dose Limiting Toxicity
DNA	Deoxyribonucleic Acid
DR4	Death Receptor 4
DR5	Death Receptor 5
EGFR	Epidermal Growth Factor Receptor
FA	Folinic Acid
GGT	Gamma Glutamyl Transpeptidase
Gy	Gray
HtrA2	High temperature requirement protein A2
IAP	Inhibitor of Apoptosis
IRES	Internal Ribosome Entry Site
JNK	Jun N-terminal Kinase
MAPK6	Mitogen Activated Protein Kinase 6
MLH1	mutL homolog 1
MSH2	mutS homolog 2
MSI	Microsatellite Instability
MTD	Maximum Tolerated Dose
MTT	3-(4,5-dimethylthiazol-2-yl)-2,5-diphenyltetrazolium bromide
NC	No Change
NE	Not Evaluable
NF-κB	Nuclear Factor Kappa B
NHL	Non-Hodgkins Lymphoma
OGN	Oligonucleotide

OS	Overall Survival
PARP	Poly ADP Ribose Polymerase
PBMC	Peripheral Blood Mononuclear Cells
PD	Pharmacodynamic
PD	Progressive Disease
PI	Propidium Iodide
PK	Pharmacokinetic
PR	Partial Response
qRT-PCR	Quantitative Real Time Polymerase Chain Reaction
RECIST	Response Evaluation Criteria in Solid Tumours
RFU	Relative Fluorescence Units
RING	Really Interesting New Gene
RNA	Ribonucleic Acid
SAE	Serious Adverse Event
SD	Stable Disease
smac/Diablo	Second Mitochondria-derived Activator of Caspase/ Direct IAP Binding Protein with Low PI
SRB	Sulforhodamine B
TNF	Tumour Necrosis Factor
TNFα	Tumour Necrosis Factor alpha
Topo1	Topoisomerase 1
TRAIL	TNF Related Apoptosis Inducing Ligand
TTP	Time To Progression
VEGF	Vascular Endothelial Growth Factor
XAF1	XIAP Associated Factor 1
XIAP	X-Linked Inhibitor of Apoptosis

Acknowledgements

The Cancer Research UK (CRUK) Pharmacology and Drug Development Group has been a steady source of advice both technical and personal. In particular, Janet Macpherson who patiently taught me the intricacies of RNA extraction and RT-PCR, Rhona Aird whose skill in cell culture made my experiments relatively easy and Dr Stephanie Arnould for her advice and teaching on protein extraction and Western blotting.

Dr Sylvie Guichard directed my scientific studies and without her help an uninitiated medic would be lost in the world of science. Her expertise in data analysis and statistics was particularly valuable, as was her skill in flow cytometry which made a complicated machine less frightening. She supervised the first *in vivo* antisense study which meant that the project was already underway prior to my arrival in the group.

The members of the CRUK Clinical Trials Unit have been very generous with their time; John Curran looked after the patients on the Phase I XIAP Antisense study, Ron Rye taught me the importance of accuracy in data management and Patty Campbell's dedication ensured the smooth running of the project.

I would like to thank Eric Lacasse, Jon Durkin and Jacques Jolivet of Aegera Therapetics Inc for constructive advice on experimental design and provision of the AEG compounds. They also provided the shXIAP construct which has been one of the most valuable assets of the project.

The members of the CRUK Biomedical Research Facility skilfully performed the animal experiments and I am grateful for advice on experimental planning and execution to Morwenna Muir. I would like to express my thanks to Richard Mitter of

CRUK Bioinformatics and Biostatistics Group, London who performed the statistical analysis of the microarray data, a highly complex area which requires specialist input.

Professor Duncan Jodrell has been a pillar of support throughout, protecting my time from clinical commitments and advising on the 'bigger' picture. He first inspired me to become an oncologist as a third year medical student and has encouraged my research career over the last ten years. I am particularly grateful for his fast turn-around of the multiple drafts of this thesis as I struggled to meet a self-imposed deadline.

My parents' encouragement has made me believe that I can achieve my goals with hard work and perseverance. My husband, Russell Jamieson, has patiently proof-read this entire document and supported me throughout the last few years, despite all the ups and downs. I now look forward to spending more time with our son, Hamish who was born on 14th June 2007 and is changing every day.

Abstract

X-linked inhibitor of apoptosis (XIAP) is the most potent endogenous caspase inhibitor, preventing cell death via the caspase-9, -7 and -3 (initiator and executioner) pathways. The project aimed to determine whether XIAP down regulation alone, or in combination with existing therapeutic agents, is a potential treatment for patients with colorectal cancer. Two methods of XIAP down regulation were considered; transient knock down using antisense (AS) oligonucleotides (OGNs) and stable down regulation by generating short hairpin RNA expressing cells.

AEG35156 (Aegera Therapeutics Inc), a 2nd generation mixed backbone AS OGN, binds specifically to the sense XIAP mRNA strand, stimulating its breakdown and preventing translation into protein. During its development, AEG35156 showed efficacy *in vitro* in a variety of cancer cell lines. *In vivo* efficacy was seen in the human colon cancer model, LS174T and synergy was seen in combination with docetaxel in a prostate cancer model. A clinical phase I trial of AEG35156 was undertaken in patients with advanced cancer, in Manchester and Edinburgh. The maximum tolerated dose was 96 mg/m^2/day of AEG35156, using a 7 day continuous infusion regimen. Dose limiting toxicities were all abnormal laboratory values, reported at higher dose levels (125mg/m^2/day and 160mg/m^2/day).

In laboratory studies, a panel of colorectal cell lines (Colo205, HT29, SW620, HCT15, HCT116) have been characterised according to p53, MLH1 and XIAP status. The HCT116 cell line is mismatch repair deficient (MLH1-) but has a normal functioning p53. It expresses XIAP at levels similar to other members of the cell line panel and is up regulated when compared to normal tissue. HCT116 is a well characterised cell line which is easy to grow *in vitro* and as a xenograft model. It is readily modifiable, making it a good candidate for further study.

A method of transient transfection of XIAP AS (AEG35156) *in vitro* was developed which achieved 81% down regulation of XIAP mRNA using the AEG35156 compound. Down regulation of XIAP mRNA was also seen with the missense (MS) OGN, AEG35187. Specific down regulation of XIAP with the AS (and not MS) was achieved using a 24 hour transfection at 400nM, but knockdown seen in this case was only 33%. Cytotoxicity experiments showed no significant therapeutic benefit of AS over MS. Investigation of stimulation of the extrinsic apoptotic pathway with TRAIL following 33% XIAP down regulation did not confer a significant increase in apoptosis when compared to the MS control. The anti-tumour efficacy and pharmacodynamic effect of AEG35156 *in vivo* in a colorectal cancer xenograft model was also investigated. AEG35156 had a significant effect on tumour growth in the HCT116 xenograft, but a subsequent study was unable to confirm this. AS directed against human XIAP caused target knockdown in mouse liver despite a 3 base pair mismatch, but no XIAP down regulation was seen in the human tumour xenografts.

Using short hairpin RNA (shRNA) against XIAP, stably expressed in a parent HCT116 human colon cancer cell line, a series of clones were developed. XIAP mRNA levels were established by RT-PCR, the 4 X (XIAP knockdown) clonal cell lines showing 82-93% reduction in XIAP mRNA when compared to the 4 L (luciferase control) cell lines. Immunoblot analysis showed a 67-89% reduction in XIAP protein in X cell lines compared to L. Results of RNA microarray analysis of the clonal cell lines confirmed down regulation of XIAP at early and late passage although some of the fold change effect was lost over time. There were no compensatory changes in genes currently documented to have an association with XIAP function.

Therefore a colorectal cancer model has been developed using isogenic cell lines which differ only in their XIAP status. The *in vitro* characterisation of these cell lines show differences in cell growth, plating efficiency and morphology in the XIAP deficient cell lines. The X23 cell line showed a 3-fold increase in sensitivity to

rhTRAIL. A 20% increase in sensitivity to radiotherapy was seen in the XIAP deficient cell lines and a >2-fold increase in sensitivity to paclitaxel and docetaxel. All 8 shRNA cell lines can be established *in vivo*, the L8 and X23 cell lines showing a similar growth pattern. XIAP knockdown is maintained at the mRNA level for 26 days after implantation, though the down regulation is less than that seen *in vitro*. However, treatment of X23 and L8 xenografts with docetaxel showed no significant differential effect on growth.

Further investigation should focus on increasing the magnitude of XIAP knock down, to lower the threshold of apoptosis inhibition in the colorectal cancer model.

Chapter 1

Introduction

1 Introduction

1.1 Cancer and Apoptosis Pathways

When considering strategies to eliminate malignant cells it is first important to consider the ways in which these cells differ from healthy cells. In this way therapies may be targeted towards differences between cancer and normal cells, thus avoiding the elimination of normal cells. Hanahan and Weinburg (1) describe six essential alterations in cell physiology which cancer cells develop that distinguish them from normal cells – of which one of the most important is the ability to evade apoptosis. Apoptosis, also described as programmed cell death, is a key regulator of physiological growth control and normal tissue homeostasis. As a result, abnormalities in this process contribute to tumour formation.

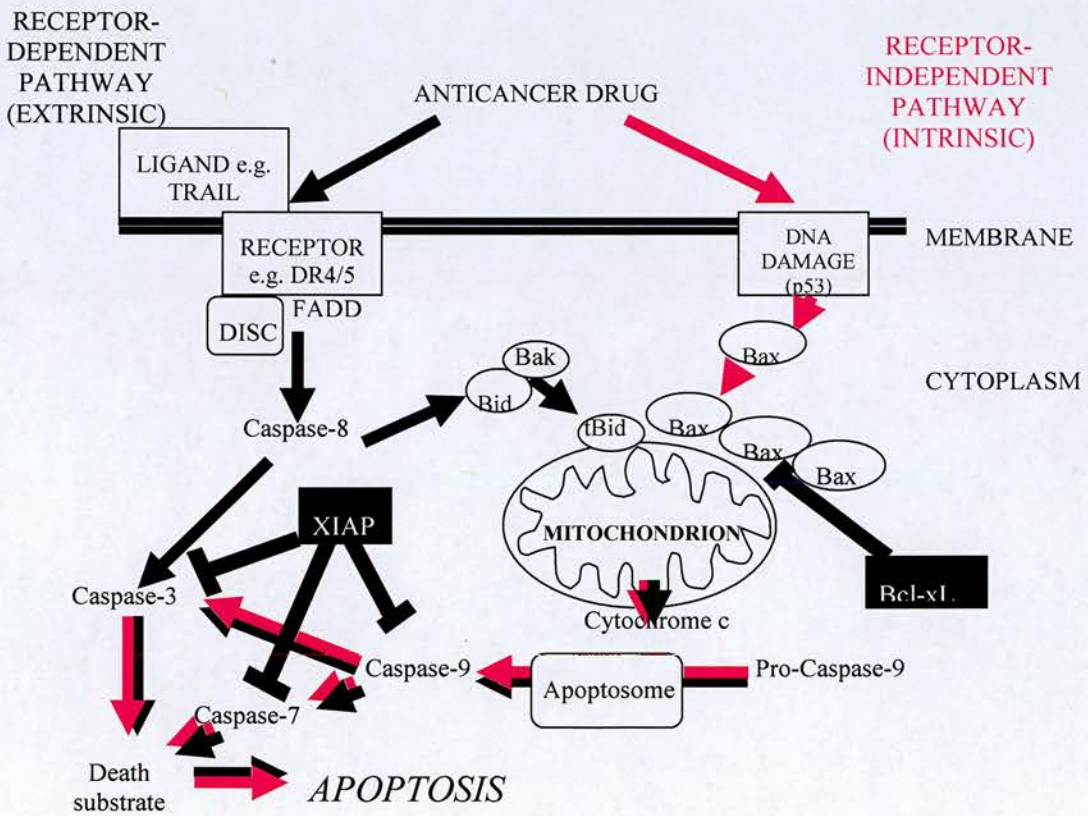

Figure 1: The Apoptotic Pathway

A complex pathway as illustrated in Figure 1 leads to apoptosis. Central to apoptosis are the caspases – a family of cysteine proteases which trigger the apoptotic program and dismantle the cell in an orderly fashion without inflammation. Failure to activate caspases may account for cellular resistance to apoptosis and current treatments; this will be discussed in more detail below.

Caspases lie in a latent (zymogen) state in cells but become activated in response to a wide variety of cell death stimuli. This activation may broadly be divided into two pathways – intrinsic and extrinsic – although links between them exist at different levels (2).

The intrinsic pathway involves the mitochondrion, with caspase activation linked to the permeability of the mitochondrial membrane. Mitochondrial permeability is controlled by members of the B-cell lymphoma 2 (BCL2) family and the pathway is initiated by the release of cytochrome C, second mitochondria-derived activator of caspases/direct IAP binding protein with low pI (smac/DIABLO) and high temperature requirement protein A2 (HtrA2) from the mitochondrion (3). Most conventional chemotherapeutic agents including etoposide, doxorubicin, cisplatin and paclitaxel induce mitochondrial permeability indirectly by affecting the BCL2 proteins or inducing p53 expression (4). Apoptotic protease-activating factor 1 (Apaf1) binds to cytochrome C and oligomerises to form the apoptosome (5) which triggers caspases resulting in apoptosis.

The extrinsic pathway involves the Death Receptors which are members of the TNF (Tumour Necrosis Factor) receptor superfamily. An inducer of the extrinsic pathway relevant to this work is TRAIL (TNF-related apoptosis-inducing ligand) which binds to Death Receptors 4 and 5 (DR4 and DR5) (6). These are the only death receptors with an intracellular death domain. Activation of the Death Receptors results in cleavage of procaspase 8, the initiator caspase, which propagates apoptosis. Decoy

receptors (DcR1 and DcR2) compete for binding of TRAIL but do not have the necessary death domain to initiate apoptosis. Therefore by regulating the expression of DR4 and 5 and DcR1 and 2 a cell may modify its response to apoptosis (7).

1.2 Colorectal Cancer and its Treatment

Colorectal cancer is the 3rd commonest cancer in the UK (after breast and lung cancer). There are almost 34,900 cases diagnosed in the UK each year. 13,300 of these are in the rectum and the rest in the colon (Cancer Research UK Cancer Stats). For patients in Scotland current guidance for the management of colorectal cancer is produced by the Scottish Intercollegiate Guidelines Network www.sign.ac.uk/guidelines/fulltext/67/section9.html.

The Dukes' Staging system (Figure 2) is useful for predicting any further treatment which may be required after surgery and also the prognosis of the patient. Five year survival rates are 83%, 64%, 38% and 3% and the frequency of diagnosis is 11%, 35%, 26% and 29% for Dukes Stage A - D tumours respectively (taken from http://info.cancerresearchuk.org/cancerstats/types/bowel/survival/). Therefore approximately 20,000 people currently die each year from the disease. Advances in clinical treatment of colorectal cancer have reduced deaths from large bowel cancer in the UK despite increasing incidence. Between 1995 and 2004, the male age-standardised rates fell by 16% and the female rates by 21% (taken from Cancer Research UK CancerStats http://info.cancerresearchuk.org/cancerstats/mortality/timetrends/). However, further development of emerging therapies and strategies to overcome tumour resistance to current treatment regimes is required to continue the improvement in patient survival.

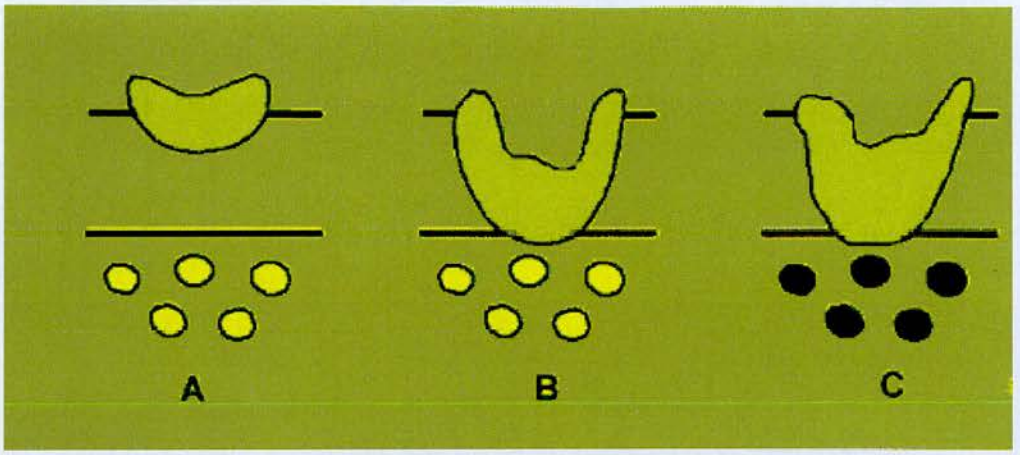

Figure 2: The Dukes' Staging System for Colorectal Cancer. Dukes' A: Tumour confined to the mucosa. Dukes' B: Tumour infiltrating through muscle. Dukes' C: Lymph node metastasis present. Dukes' D: Metastatic disease.

1.2.1 Cytotoxic Chemotherapy

Surgery remains the mainstay of treatment for patients with Dukes stage A and B disease. The value of adjuvant chemotherapy for patients with Dukes B tumours is controversial (8) and current guidelines advise discussion on an individual case basis depending on poor prognostic risk factors (bowel obstruction, tumour adhesion, invasion, perforation or aneuploidy). Further clinical trials are warranted to identify which patients might benefit from current chemotherapy and novel therapeutic strategies.

In the absence of significant co-morbidity, adjuvant chemotherapy is recommended for patients with Dukes' C disease; there is a 4-13% increase in 5 year survival (9). The principal chemotherapeutic agent has been intravenous 5- fluorouracil (5-FU) but it is being increasingly replaced by capecitabine (a 5-FU prodrug) due to the latter's tablet formulation and outpatient administration (10). 5-FU is a potent anti-tumour agent that affects pyrimidine synthesis by inhibiting thymidylate synthase

thus depleting intracellular dTTP pools. It is also metabolised to fluoro-ribonucleotides and deoxyribonucleotides, which can be incorporated into RNA and DNA. Treatment of cells with 5-FU leads to an accumulation of cells in S-phase and has been shown to induce p53 dependent apoptosis.

More recently oxaliplatin has been added to 5-FU based regimes in the adjuvant setting for patients with Dukes' C tumours and it is associated with increased disease free survival in the combination therapy group (11). Oxaliplatin is a third generation platinum compound which, unlike its parent cisplatin, is active in colorectal cancer. Platinum compounds form adducts with cellular DNA and the type of adduct formed with cisplatin differs from oxaliplatin (12). Oxaliplatin carries the diaminocyclohexane (DACH) ligand which allows DNA lesions to avoid mismatch repair and damage recognition pathways. This results in DNA strand breaks leading to the induction of apoptosis (13). Loss of mismatch repair proteins results in low level resistance to cisplatin but not oxaliplatin (14) and these proteins are implicated in a subset of colorectal cancers.

Chemotherapy for metastatic disease has been shown to improve overall survival; in a meta analysis of 5-FU based chemotherapy versus no treatment, the 1 year mortality was significantly reduced (15). Scottish guidelines state that all patients should be offered this treatment if medically fit. Two newer drugs irinotecan (CPT-11) and oxaliplatin have also been evaluated in the first-line treatment of patients with metastatic colorectal cancer. In a trial of irinotecan in addition to 5-FU folinic acid, improvements were seen in the combination arm with increased response rate, time to progression and overall survival (16). A randomised comparison of 5-FU and folinic acid in combination with either oxaliplatin or irinotecan showed no difference in overall response rate, time to progression or overall survival (17). The toxicities of the two regimens were also similar and both are therefore licensed in the UK for use as first line therapy in patients with metastatic disease. In Edinburgh, oxaliplatin is preferred as it is easier to combine with capecitabine.

Topoisomerase 1 is an enzyme which allows the DNA helix to unwind in order for a cell to divide normally (18). Irinotecan is converted into its active form (SN-38) in-vivo by carboxylesterase enzymes in the liver. SN-38 binds irreversibly to the DNA-topoisomerase I complex, inhibiting the reassociation of DNA after cleavage by topoisomerase I and traps the enzyme in a covalent linkage with DNA. The enzyme complex is ubiquitinated and destroyed by the 26S proteasome, thus depleting cellular topoisomerase 1. This blocks the cell cycle in S-phase at low dose and induces apoptosis (19).

Second-line chemotherapy with irinotecan after failure of 5-FU based regimes prolongs survival, improves symptom control and quality of life (20). The addition of oxaliplatin to 5-FU showed no significant increase in overall survival though response rate and time to progression were improved (21). With both drugs there were significant increases in toxicity and therefore the current recommendation for treatment depends on the fitness of the patient.

1.2.2 Radiotherapy

For rectal cancer, pre-operative radiotherapy with 3 or 4 fields is recommended for local disease control in patients undergoing curative resections. Post-operative radiotherapy may be given in cases where patients are at high risk of local relapse. The schedule is 45 Gray (Gy) in 25 fractions over 5 weeks. Evidence from a prospective cohort study suggests synchronous 5-FU based chemotherapy and radiotherapy improves the complete response rate and resectability rate in more advanced tumours and randomised Phase 3 data is awaited (22).

Radiotherapy has three roles in advanced rectal cancer; to downsize tumours to allow attempts at curative resection, potentially curative treatment of inoperable disease, and symptom control in persistent or locally recurrent disease. In the case of inoperable rectal disease combined chemo-radiotherapy showed improved overall survival in the subgroup where response to treatment and tumour downsizing

allowed surgical intervention (23). For the palliation of symptoms in rectal cancer 44Gy in 12 fractions over 10 to 12 weeks was shown to minimize early and late toxic effects (24) but the regimen used will vary according to centre and patient condition.

Radiotherapy damages DNA by directly or indirectly ionising the atoms which make up the DNA chain. Indirect ionisation is more common and happens as a result of water forming free radicals which then damage DNA. Cells have mechanisms for repairing the DNA damage and therefore double strand DNA breaks are the most lethal. Fractionation of approximately 2 Gy per day of the total dose allows normal cells time to recover. Shinomiya advocates a theory of pre and post mitotic cell death which describes two modes of apoptosis in radiation damaged cells (25). Premitotic apoptosis is induced by high dose irradiation (20Gy), mainly occurs in the S phase and leads to rapid apoptosis via the activation of caspase 3. Postmitotic apoptosis is induced by low dose irradiation (5Gy), mainly occurs in the G_1 phase and leads to apoptosis after 24 hours associated with the down regulation of genes such as bcl-2 and mitogen-activated protein kinase 6 (MAPK6) which play an important role in the mitochondrial (intrinsic) pathway of apoptosis. There is also evidence to suggest a role for the extrinsic pathway of apoptosis in γ radiation treated cells (26). Reap *et al* have shown that surface Fas expression increases on normal lymphocytes exposed to radiation and that radiation-induced apoptosis can be blocked with high concentrations of a Fas–Fc fusion protein.

1.2.3 Targeted Antibodies in Colorectal Cancer

Cetuximab (Erbitux, Merck KGaA, Darmstadt, Germany) is a monoclonal EGFR antibody licensed in 2004 for use as second line therapy in irinotecan resistant colon cancer. Cunningham *et al* described a response rate of 23% in the irinotecan plus cetuximab group compared to 11% in the cetuximab alone group. There were also significant improvements in the time to progression (4.1 vs 1.5 months) in the combination treatment group (27). Cetuximab is currently under investigation as first line therapy in the MRC COIN study which compares continuous chemotherapy (oxaliplatin and 5-FU) with or without cetuximab with intermittent combination

chemotherapy. The results of the EPIC trial of irinotecan with or without cetuximab as second line therapy in metastatic colorectal cancer were recently presented (28). This showed a significantly longer progression free survival and higher response rate in the cetuximab combination arm though no difference in overall survival was seen. Currently, cetuximab is licenced as 3rd line treatment in metastatic colorectal cancer.

Bevacizumab (Avastin, Roche, Basel, Switzerland) is a monoclonal antibody against VEGF inhibiting the angiogenesis pathway. Benefits have been shown with the addition of bevacizumab to 5-FU/folinic acid and 5-FU/folinic acid plus irinotecan in the first-line treatment of metastatic colorectal cancer (29) and therefore this drug is licensed for first line treatment in the UK.

There are significant development costs involved with targeted agents and therefore health care providers are increasingly seeking economic evaluation prior to the approval of these drugs for clinical use (30). Neither of the above antibody treatments are currently approved by the National Institute for Clinical Excellence (NICE) and therefore are not routinely used in the UK.

1.2.4 Other agents relevant to Apoptosis

rhTRAIL (recombinant human tumour necrosis factor-related apoptosis-inducing ligand) binds to death receptors (DR4 and DR5) on the cell surface, directly stimulating the extrinsic apoptotic pathway. Targeting the extrinsic pathway is attractive as most known mechanisms of resistance to chemotherapy and radiotherapy are related to abnormalities in the intrinsic pathway (31). Monoclonal antibodies activating the death receptors DR4 and DR5 are also in early clinical development (32, 33). This is particularly promising for colorectal cancer as TRAIL receptor antibodies have been shown to delay xenograft tumour growth *in vivo* (34). Combinations of TRAIL pathway stimulation and an IAP antagonist would therefore be a rational step forward in targeted therapy.

The taxanes (paclitaxel and docetaxel) bind to tubulin and interfere with the function of the mitotic spindle blocking cells at the metaphase-anaphase junction (35). Paclitaxel has also been shown to induce NFkB expression and increase levels of XIAP in addition to other apopotic and inflammatory markers (36). These drugs are not routinely used in the treatment of colorectal cancer; an infusion of paclitaxel failed to show significant clinical benefit in a Phase 2 trial in patients with metastatic disease (37). A number of resistance mechanisms to taxanes have been described, including overexpression of the P-glycoprotein efflux pump and alterations of assembly or stability of microtubules (38). Tortora *et al* (39) were able to show sensitisation of an oral taxane with a combination of an antisense targeting protein kinase A and an EGFR inhibitor in xenografts of colon cancer. In addition, XIAP antisense has been shown to enhance the activity of docetaxel in prostate tumour xenografts (40) and breast cancer RNAi XIAP cells were sensitised to taxanes (41). In this thesis data from combination studies of taxane therapy and XIAP knockdown in a colorectal cancer model will be described.

1.3 Apoptosis and outcome in colorectal cancer

Biomarkers are anatomic, physiologic, biochemical, or molecular parameters associated with the presence and severity of specific disease states. They are detectable and measurable by a variety of methods including physical examination, laboratory assays and medical imaging. Biomarkers have been developed to identify individuals at risk for cancer, to detect disease earlier, determine prognosis (and potentially avoid toxic therapy), detect recurrence, predict response to therapeutic agents and monitor response to treatment (42). Discovery, testing and validation of tumour biomarkers markers should permit individualisation of therapy.

The development of biomarkers for routine clinical use requires a reproducible test which is standardised, cost effective and quality controlled. Standardised specimen collection and processing, together with measurement of physiological variation is

essential. For routine use outside a research environment rigorous testing to set standards is vital to ensure a high lab to lab concordance (42).

Early clues for genetic defects in colorectal cancer arose from clinical diagnostic identification of families with hereditary colorectal cancer. Lynch and de la Chapelle describe a theory that such cancers may be broadly divided into two groups; proximal and distal colonic tumours (43). Proximal tumours behave in a less aggressive manner; possess microsatellite instability and mutations in the mismatch repair genes. Distal tumours tend to be more aggressive and have mutations of p53 (44).

An area of microsatellite instability arises during DNA replication where short nucleotide repeat sequences (microsatellites) undergo mutation and therefore become mis-aligned (unstable). These areas would usually be repaired by the mismatch repair proteins, however if mutations in these repair proteins are present the defect is allowed to persist and a tumour propagates. Deficiency in mismatch repair is characterised by mutations of MLH1 (mutL homolog 1) in 50% and MSH2 (mutS homolog 2) in 40% of cases of hereditary colon cancer and in 15% of sporadic cases mismatch repair deficiencies may be identified (45).

Funaiola *et al* reviewed the literature for biomarkers which had prognostic significance in early colorectal cancer and found that favourable microsatellite instability status, as assessed by MLH1 and MSH2, correlated with better prognosis (46). This is consistent with previously described data (44), however they did not find a correlation with p53, BCL2 or thymidylate synthase status by immunohistochemistry. Magrini *et al* described the response to irinotecan chemotherapy in HCT116 colon cancer cell lines according to p53 and MLH1 status which could be useful for designing rational therapies. They found that the apoptotic response to irinotecan was enhanced in cells which were deficient in MLH1 or p53 (47).

Apoptosis requires a functioning p53 protein and tumours with p53 gene mutations may display resistance to programmed cell death. p53 can be activated by a large number of cellular stresses including DNA damage (caused by chemotherapy and radiotherapy) which promotes apoptosis. A mutation of p53 has been shown to correlate with poor patient survival in distal colorectal tissue samples (48) which would agree with Lynch's theory (44). Mutations in p53 have been shown to confer chemoresistance (49) in breast cancer. The prediction of response to chemotherapy according to p53 status is more controversial. Ahnen *et al* showed that patients with p53 over expression in colorectal tumours did not benefit from 5FU based chemotherapy (50) however a further study was unable to confirm this (51). The role of p53 in apoptosis is continually unfolding and increasingly complex. It does not function in isolation therefore it is unlikely that a simple correlation with prognosis and resistance to treatment will exist (52).

1.4 Apoptosis and Inhibitor of Apoptosis Proteins (IAP)

Apoptosis is tightly controlled and may be considered a binary life or death decision (53). In each cell there is a balance between pro- and anti-apoptotic signals and in cancer cells the balance is weighted towards anti-apoptosis – the cells are unable to die. There are likely to be many mechanisms involved and no one component will be entirely responsible for the ultimate outcome, however, if the cell is near the tipping point of the balance it may be possible to alter one variable and allow the cell to tip into apoptosis. In order to identify useful therapeutic targets, cells, which are sensitive to therapy, may be compared with those which are resistant in order to identify potential mechanisms preventing the apoptotic balance swinging in favour of apoptosis. As shown earlier (Figure 1) apoptotic cell death relies on a caspase controlled cascade which is tightly regulated. One of the regulatory mechanisms identified are a family of proteins – the inhibitors of apoptosis (IAP) which have been shown to have an important role in preventing cell death.

The IAP family is characterised by one to three Baculovirus IAP Repeat (BIR) domains at the NH_2 terminus of the polypeptide chain (Figure 3) (54). These domains specifically bind the functional units of caspases and allow inhibition. At present IAPs are the only known intracellular inhibitors of apoptosis. They inhibit two effector caspases, 3 and 7 (55) and one initiator caspase 9 (56). Caspase 9 is responsible for the intrinsic mitochondrial death pathway (Figure 1) triggered by chemotherapy and radiotherapy. IAPs also block the extrinsic pathway triggered by ligands such as TRAIL and FAS binding to death receptors by inhibiting caspase 3 (the target of caspase 8).

The IAPs were first discovered in baculoviruses where it was noted that a gene containing a zinc finger-like motif was able to regulate apoptosis (57). The mammalian BIR domains show structural similarity to zinc fingers. Evolutionary conservation suggests that these genes have an important role (58). Caspase inhibition is not the only known function of these proteins, for example survivin is known to regulate cell division (58). Some IAPs function as co-factors of signal transduction pathways (59) and others play a part in cell division and cytokinesis (60).

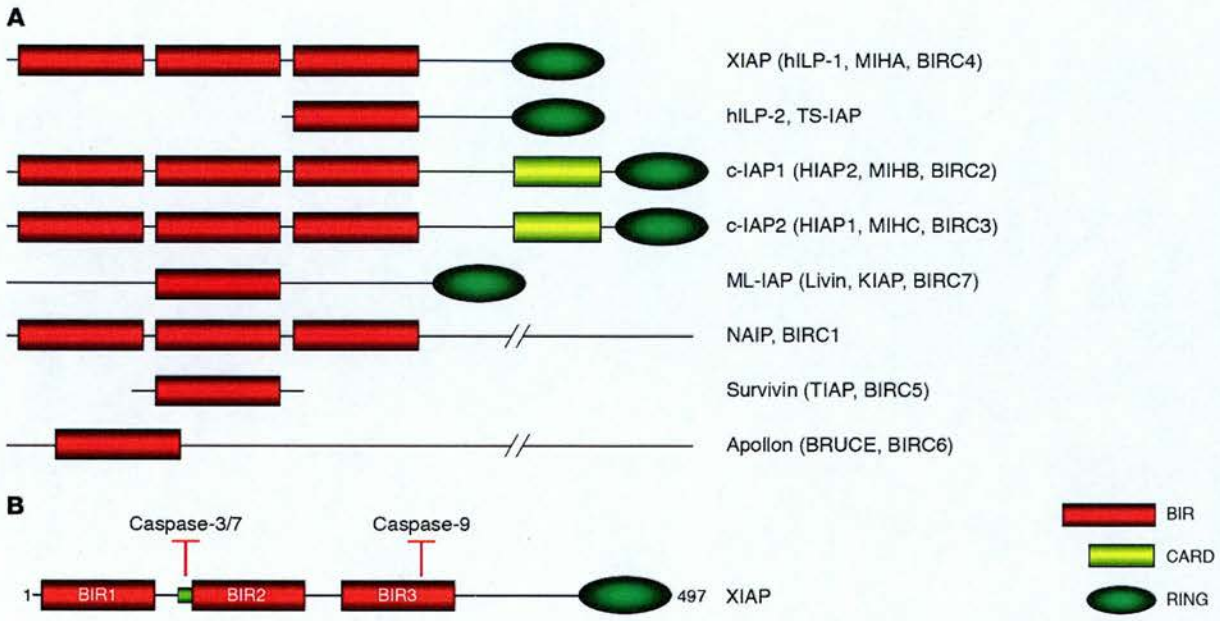

Figure 3A: The Structure of IAP Family Members with alternate names. Figure 3B: XIAP structure in detail showing the three BIR (Baculovirus IAP Repeat) domains and the sites of caspase inhibition. CARD (CAspase Recruitment Domain). RING (Really Interesting New Gene). Taken from the Journal of Clinical Investigation, 2005 (54).

One of the key players in the IAP family is XIAP which is the most potent known endogenous caspase inhibitor (54). Other members of the IAP family have a role in cellular immunity. Cellular Inhibitor of Apoptosis 2 (CIAP2) has been found to have a critical role in the maintenance of normal innate immune inflammatory response (61). This may be relevant in the clinical setting; a decrease in IAP could trigger an undesirable immune response or lead to immunocompromise in a patient.

1.5 XIAP structure and function

The XIAP gene is located on chromosome Xq25 (62) and to date no mutations or chromosomal abnormalities have been identified implying that mutation of XIAP is not an initiating event in the formation of cancer (54). The control of XIAP expression is essential for a cell to be able to modulate its response to apoptotic stimuli. A general response to cellular stress is to decrease cap-dependant protein synthesis but XIAP is translated through an internal ribosome entry site (IRES), and this alternative translation mechanism allows XIAP protein to be expressed under conditions of cell stress such as serum withdrawal (63). This expression of XIAP will transiently protect the cell from programmed cell death and plays a role in disease progression and resistance to therapy. The 57kDa XIAP protein contains three BIR domains and a RING (Really Interesting New Gene) domain. The RING domain has structural similarities to a zinc finger and is thought to provide a scaffold for complex cellular processes (64). The functions of the XIAP domains are described below.

1.5.1 Caspase Inhibition

XIAP inhibits caspase 3 and 7 via the linker region between BIR domains 1 and 2 (55), caspase 9 inhibition is via a hydrophobic pocket in the surface groove of the BIR3 domain of XIAP (65). It is the most potent member of the IAP family with caspase 3 and 7 inhibition constants of 0.2 – 0.7 nM (55). In comparison, survivin, another member of the IAP family which contains only the BIR2 domain, has inhibition constants of 10-20nM (66). Further experiments measuring caspase activity by cleavage of the fluorescent compound DEVD-AFC after incubation of recombinant caspase 3 and 7 with fragments of the XIAP protein, showed that the BIR2 domain was sufficient to inhibit these proteases at concentrations of 1-5nM (56, 67).

Cancer cells are specifically under stress and primed for apoptosis due to genetic and chromosomal aberrations. XIAP down regulation alone can tip the balance in favour

of apoptosis in tumour cells suggesting that the caspases must already be active in tumour cells compared to normal and the activity is suppressed by the IAPs (68). Removing inhibition of caspase 3 and 7 at the distal end of the apoptotic cascade allows these cells to undergo apoptosis (68). Thus XIAP antagonism alone may have therapeutic effects as a single agent ethically justifying a Phase 1 clinical trial.

XIAP is characterised by its role in caspase inhibition (as described above), however, more recently it has been found to have a role in multiple cellular events which may contribute to its overall anti-apoptotic activity (69).

1.5.2 Ubiquitination

The functional relevance of the carboxyl terminal RING domain of XIAP is that it shows E3 ubiquitin ligase activity. This allows XIAP to catalyse ubiquitination, targeting proteins for degradation in the proteosome. In addition, XIAP catalyses its own ubiquitination, a process which is dependent on the RING domain allowing regulation of apoptosis. Stably expressed XIAP, which lacks this domain, was more resistant to degradation implying auto-ubiquitination and degradation are key events in apoptosis (70). The ability to activate NF-κB (Nuclear Factor-kappa B) depends on the ubiquitin ligase activity of the RING suggesting that this occurs as a result of ubiquitination of a regulator of the NF-κB signalling pathway.

1.5.3 Signaling Pathways

Signalling properties of XIAP can be mapped to different regions of the protein which are not involved in caspase inhibition. This is shown by Lewis *et al* in experiments where mutations in different regions of XIAP were introduced and, although caspase inhibition was lost, the ability to activate NF-κB and JNK (Jun N-terminal Kinase) pathways was retained (69). Ability of XIAP to participate in signalling is an evolutionarily conserved mechanism with the regions of the molecule required for signalling highly conserved. The role for the integration of these functions into a single molecule remains unclear.

NF-κB is a transcription factor which induces expression of target genes; XIAP represents one of the NF-κB regulated genes in addition to CIAP1 and CIAP2 (71). Many human tumours have constitutively active NF-κB which turns on the expression of genes preventing cell death. It counteracts the apoptotic signals caused by TNFα and thereby prevents the cell from undergoing programmed cell death. Aggarwal *et al* have shown that paclitaxel induces expression of XIAP amongst other antiapoptotic proteins via the activation of NF-κB (36). Treatment with curcumin suppressed the expression of NF-κB gene products *in vitro* and *in vivo* in a breast cancer model and synergy was shown with paclitaxel. Using curcumin in combination with paclitaxel lowers the cytotoxic dose required to be effective therefore reducing potential toxicity (36).

JNK is a member of the MAP (Mitogen Activated Protein) kinase family which are responsive to stress stimuli such as cytokines and involved in apoptosis. There have been several reports of XIAP interacting with the JNK pathway but the mechanism is yet to be elucidated (72).

Akt is a protein kinase which is known to mediate a number of anti-apoptotic mechanisms. The BIR1 domain of XIAP contains an Akt phosphorylation site that is involved in protein stabilisation (73); Akt phosphorylates XIAP protecting it from ubiquitination and degradation. XIAP down regulation is associated with Akt cleavage and apoptosis and has a role in cisplatin resistance in an ovarian cancer model (74). Cisplatin decreased XIAP protein levels and induced Akt cleavage and apoptosis in chemosensitive, but not in resistant, ovarian cancer cells.

A novel role for XIAP in copper homeostasis through MURR1 has recently been identified (75). This was first discovered in the cells and tissues of XIAP deficient mice (76) which were found to have reduced copper levels.

1.6 The Endogenous Regulation of XIAP

Multiple mechanisms exist for increasing IAP activity in a cell further adding to the evidence for the importance of XIAP in cancer. The anti-apoptotic activity of XIAP can be suppressed by two proteins localised to the mitochondria; smac/DIABLO (77) and HtrA2/Omi (78). These molecules are released into the cytoplasm during apoptosis where they bind to the same hydrophobic pocket in BIR3 which interacts with caspase 9 (79). XIAP may bind either smac/DIABLO, Omi/HtrA2 or caspase 9 – they are mutually exclusive (80). Therefore these molecules are negative regulators of XIAP and can release XIAP from caspases.

XAF-1 binds to XIAP via the zinc finger region antagonising caspase activity and causing nuclear translocation of XIAP (81). In normal tissues levels of XAF-1 are abundant compared to the NCI 60 panel of cancer cell lines (82). In cancer cell lines the alteration in XIAP and XAF-1 levels may lead to increased apoptotic resistance due to unregulated XIAP function. XAF-1 protein over expression has been shown to induce G1 cell cycle arrest (82), consequently increased cellular proliferation may be a direct result of XAF-1 down regulation.

Other members of the IAP family cIAP1 and cIAP2 can be shown to degrade XIAP as they also contain RING E3 ubiquitin ligase activity (83). XIAP and cIAP1 RING domains heterodimerise and induce protein degradation. Therefore abundance of XIAP can be regulated in a proteasome dependent manner. The RING domain of cIAP1 has a pro-apoptotic function (84); Clem *et al* have shown that the cleaved RING domain is capable of killing cells *in vitro*. XIAP also auto-ubiquitinates (as described in section 1.5.2) controlling its own regulation though this process is less efficient than the heterodimerisation described between XIAP and CIAP1 (83).

GSPT1/Efr3 contains a conserved four residue IAP binding motif (like smac/Diablo and Htra2/omi) and functions as an IAP binding protein (85). In its processed form it binds to IAPs to release them from caspases.

1.7 Evidence for XIAP as a therapeutic target

The evidence would suggest that cancer cells use XIAP to evade extrinsic and intrinsic cues that would normally lead to their demise. In almost all of the 60 cell lines of the NCI panel across multiple tumour types XIAP mRNA, as quantified by RT-PCR, is over-expressed in comparison to normal human liver (82). This has been confirmed in an RNase protection assay (86). Elevation of XIAP has also been detected in human malignancy including prostate (87) and colorectal tumours (88), and AML (86) where XIAP levels were found to be increased in comparison to adjacent normal tissue. This implies that malignant cells increase the levels of XIAP to avoid apoptosis. If levels could be reduced the cells would undergo programmed cell death, either spontaneously if their caspases were activated or in response to a cytotoxic stimulus, for example chemo- or radiotherapy.

1.7.1 Prognosis

XIAP has been identified as a useful therapeutic target by its involvement in resistance to apoptosis (54). High XIAP levels correlate with poor prognosis implying that a tumour is more aggressive, able to metastasise earlier or grow faster. Human tissue from patients with pancreatic adenocarcinoma was compared to healthy controls at the mRNA and protein levels for XIAP expression, XIAP levels were found to be 2.1 fold higher in the malignant group which correlated with a less favourable survival (13.4 compared to 16.1 months) (89). However, a paper by Krajewska *et al* (88) was unable to correlate overall survival with XIAP in human colorectal cancer samples by immunohistochemistry.

Increased XIAP expression correlates with poor clinical outcome in several disease types and has been used as a prognostic indicator. In AML patients with high XIAP protein levels had significantly poorer prognosis (86). Yamamoto *et al* were able to identify an increase in XIAP mRNA levels in patients who underwent transformation of disease from pre-leukeamic to myelodysplastic to AML and in de novo AML (90). This suggests that up-regulation of XIAP is a mechanism for preventing cell death in

clinical samples. However these results were not reproduced at the protein level when assessed by immunohistochemistry.

Anoikis may be defined as apoptosis in response to detachment of an epithelial cell from its matrix. Most epithelial cancer cells die on entering the blood stream but tumour cells may escape this mechanism and invade other tissues. Up-regulation of XIAP is seen in anoikis of normal intestinal epithelial cells (91) implying a transient attempt at survival which is eventually overcome. The evidence for the role of XIAP in the progression of colorectal cancer has been documented in clinical samples; XIAP levels increase from adenoma to carcinoma to hepatic metastasis (92). This implies a role for XIAP in the ability for cancer cells to metastasise from the area of origin through the blood and a mechanism of resistance to anoikis. Increased expression of XIAP has also been shown to contribute to anoikis resistance in a prostate cancer model (93).

1.7.2 Resistance to Therapies

In an isogenic *in vitro* ovarian cancer model of A2780 and A2780cp (cisplatin resistant) cells XIAP was found to be over expressed in the A2780cp cells and when XIAP was down regulated with antisense the cells were sensitised to cisplatin treatment (94). Shrikhande *et al* were able to demonstrate an increase in sensitivity to gemcitabine when XIAP was silenced in two pancreatic tumour cell lines (89). Down regulation of XIAP with antisense oligonucleotides in combination with radiotherapy shows decreased cell survival in non-small-cell lung cancer cell lines *in vitro* and in a xenograft model (95). In addition breast cancer cells expressing shRNA to XIAP were sensitised to TRAIL (41).

These results support XIAP downregulation strategies in combination with other therapeutic agents; cytotoxic agents or radiotherapy which stimulate the intrinsic or extrinsic pathway. The above evidence would suggest that inhibition of XIAP

activity would facilitate the execution of the pro-apoptotic signals when challenged by chemotherapeutic agents.

1.8 Strategies to antagonise XIAP

Strategies that modulate the effects of XIAP may be divided into those that regulate the amount of XIAP available and those that block its function. To date use of an antisense oligonucleotide (OGN) is the only strategy in clinical development and this will be discussed in more detail in Chapter 2.

1.8.1 Regulation of protein abundance

1.8.1.1 Antisense Oligonucleotides

Antisense oligonucleotides are synthetic oligonucleotides which bind in a complementary fashion to messenger RNA and induce its degradation through ribonuclease H (Rnase H). In order to effectively inhibit gene expression, an antisense must be resistant to nucleases, be taken up efficiently by cells, hybridize efficiently with the target mRNA and activate selective degradation of the target mRNA or block its translation without causing undesirable side effects (96).

1.8.1.1.1 Antisense as a therapy

Antisense drugs are being studied in oral, intravenous, subcutaneous, intravitreal and enema formulations in clinical trials. Fomivirsen (Vitravine™) is a licenced antiviral drug used for the treatment of CMV retinitis in immunocompromised patients with AIDS. The oligonucleotide is targeted against the coding region of the major immediate-early gene of the human cytomegalovirus (97); it was the first antisense drug, approved by the FDA in 1998 (98).

AEG35156/GEM640 (XIAP antisense) was developed by Aegera Therapeutics Inc in collaboration with Hybridon Inc (now Idera Pharma). It is an anti-XIAP antisense oligonucleotide synthesised with second generation antisense chemistry. The pre-clinical and early clinical development will be described in Chapter 2.

1.8.1.1.2 Antisense in target validation

The mapping of the human genome unveiled an abundance of potential molecular targets. The challenge for the pharmaceutical industry is to gain valuable insight into the role these targets play in the body and their viability as drug targets. Ultimately, scientists seek to understand which genes are directly involved in disease pathways in order to develop drugs specific to key gene targets in a timely manner. This overall task is referred to as functional genomics. Traditional drug discovery screening methods are time-consuming, often requiring years to identify lead drug candidates.

Antisense oligonucleotides are excellent tools in the laboratory for the identification of gene function and help to assess whether a specific gene is a good drug target. However, the non specific effects of phosphorothioate oligonucleotides have been previously documented (99) and include effects on cell proliferation. Therefore it is important to include a control oligonucleotide which is not complementary to the mRNA of interest in laboratory studies.

1.8.1.2 Short Hairpin RNA

Short hairpin RNA (shRNA) is a short sequence of RNA that makes a tight hairpin turn and can be used to silence gene expression. In this work a small insert encoding a short hairpin RNA sequence targeting the gene of interest (XIAP) was cloned into the pCDNA3 vector. The insert-containing vector was then transfected into the colorectal cancer cell line HCT116. The insert is transcribed in the cells from a DNA template as a single stranded RNA molecule of approximately 50 to 100 bases.

Complementary regions spaced by a 'loop' region cause the transcript to fold back on itself forming a 'short hairpin'. Processing by the cell's machinery converts the shRNA into the corresponding short interfering RNA (siRNA). siRNA assembles into RNA-induced silencing complexes (RISCs) and activates the complex by unwinding its RNA strands. The unwound strands guide the complex to the complementary RNA molecules where the complex cleaves and destroys the target mRNA.

Vector based siRNA is easily transfected and the sustained repression is propagated indefinitely (100). A stable cell line may be established which allows observation of the long term effects of XIAP down regulation. However, construction of shRNA may be associated with technical difficulties (101) and we are therefore grateful to Aegera Oncology for the supply of the insert-containing vector which had previously been validated (41).

1.8.1.3 Translational Inhibitors

Inhibitors of XIAP translation may block the expression of the protein in cancer cells under stress via internal ribosome entry site (IRES) based control mechanisms. Mammalian Target of Rapamycin (mTOR) inhibitors such as sirolimus (Rapamune™) inhibit the translation of antiapoptotic proteins including XIAP (102). Synergy has been shown between mTOR inhibitors and dexamethasone in a multiple myeloma model *in vivo* (102) and the mechanism is dependent on down regulation of XIAP.

1.8.1.4 Compounds which Decrease Protein Half Life

Protein half life may be reduced as a further strategy for regulating the abundance of XIAP. Akt kinase inhibitors have been shown to destabilise XIAP by leaving the

protein hypophosphorylated and therefore more susceptible to ubiquitin-mediated degradation (73).

1.8.2 Functional Inhibitors

Polyphenylurea compounds have been developed which antagonise the ability of XIAP to inhibit caspase 3 (103). They bind and inhibit the BIR2 domain of XIAP responsible for suppressing caspase 3 and 7. Karikari *et al* describe good *in vitro* and *in vivo* activity in pancreatic cancer models alone and in combination with TRAIL, radiotherapy and gemcitabine, the clinical standard of care (104).

Small molecule antagonists of XIAP BIR3 domain (smac peptidomimetics) have also been developed (105, 106). XIAP BIR3 domain is important for caspase 9 inhibition and the tetra peptide small molecule can displace caspase 9 from XIAP and activate the caspase cascade.

1.9 Aim of the Project

The aim of this project is to determine whether XIAP down regulation alone, or in combination with other therapeutic agents, is a potential treatment for patients with colorectal cancer. To achieve this aim, the following studies have been undertaken and will be discussed in this thesis.

- The characterisation of colorectal cell lines according to p53, MLH1 and XIAP status.
- The effects of transient transfection of XIAP antisense (AEG35156) *in vitro* as a method of XIAP down regulation.
- The anti-tumour efficacy and pharmacodynamic effect of AEG35156 *in vivo* in a colorectal cancer xenograft model.
- The development and characterisation of stable XIAP knock down cell lines using short hairpin RNA.
- The *in vitro* response of stable XIAP knock down cell lines to therapeutic agents.
- The establishment and treatment of shXIAP-expressing cell lines as xenografts.

Chapter 2

Development of AEG35156

2 Development of AEG35156

2.1 Preclinical Development of AEG35156

AEG35156 is a second generation 19-mer oligonucleotide (OGN) in which the core 11 DNA bases are flanked by four 2'-O-methyl-modified RNA residues at the 3' and 5' ends (Figure 4).

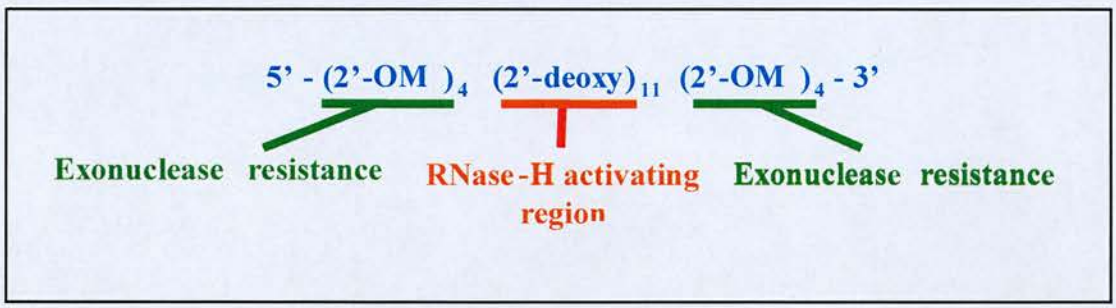

Figure 4: Structure of AEG35156

First generation oligonucleotides have shown dose dependant side effects of liver transaminitis, thrombocytopenia, hyperplasia of reticuloendothelial organs, prologation of APTT, activation of complement and renal tubular changes (107). Second generation chemistry was developed to improve both the pharmacokinetics and the toxicity profile of antisense compounds (107).

In second generation OGNs, the 2'-O-methyl groups introduced at the ends of the oligos are necessary for resistance to exonucleases which cleave nucleotides from the end of an RNA chain and therefore this aids stability of the OGN *in vivo*. The central part of the oligonucleotides activates RNase H, this recognises RNA-DNA duplexes and hydrolyses the mRNA strand thereby achieving down regulation of XIAP.

There has been concern regarding the immunostimulation which may arise from the presence of CpG residues (96) and this compound was specifically optimised for potency and specificity in the absence of CpG residues. The oligo is phosphorothioated where the nonbridging oxygen in the normal phosphate backbone is replaced by sulphur. The reduction of continuous length of phosphorothioate (PS) linkages in second generation chemistry leads to improvements in the effects on lymphocyte proliferation, thrombocytopenia, liver transaminases and renal tubular changes (107).

The sequence of AEG35156 was selected from a screen of more than one hundred second generation compounds. The preclinical development is fully described by LaCasse *et al* (40) in work by Aegera Therapeutics Inc and will be summarised here.

2.2 Anti-tumour activity of AEG35156 in vitro

The down regulation of XIAP mRNA expression *in vitro* was seen across five human cancer cell lines; lung, breast, pancreas, ovary and prostate. There was no colorectal cell line included in these *in vitro* transfection studies. The effect was dose dependant in 2/5 cell lines (pancreas and ovary). The EC50 was in the range 8-32nM for all five cell lines. Of note, a reduction of up to 22% in XIAP mRNA levels was described with the non-sense control AEG35185 indicating a non specific effect of the OGN. RNase H assays were performed and showed the specific degradation of XIAP mRNA from total cellular RNA in comparison to GAPDH and cIAP1 mRNA which remained intact. In pancreatic carcinoma cells (Panc1) a synergistic effect of XIAP down regulation by antisense was seen with TRAIL when neither of these agents had an effect on cell survival alone. This effect was associated with loss of XIAP protein and increased PARP cleavage.

2.3 Anti-tumour effects of AEG35156 in vivo

AEG35156 was found to have anti tumour effects as a single agent in a xenograft model of human colon cancer (LS174T). This effect was dose dependent with 60% reduction in tumour volume relative to saline control seen at a dose of 25mg/kg/dx5 for 3 weeks. In a prostate cancer model (PC-3) a similar effect was seen though not in a lung model (H460). However, in the H460 model, synergy was seen with docetaxel and XIAP protein knockdown identified in the xenografts using immunohistochemistry. In the prostate cancer model the most impressive example of synergy was seen in combination with docetaxel. Complete regression of the xenografts was seen and after cessation of treatment the re-growth was minimal.

2.4 Preclinical toxicology of AEG35156

Body weight loss was measured as a sign of toxicity and <10% was seen after prolonged exposure to AEG35156 but was non specific in that the control oligonucleotides showed greater loss. Body weight recovered after the treatment phase.

The immunostimulatory effect was assessed by spleen weight measurements and compared to an 18-mer CpG oligonucleotide control. There was a 6% increase in spleen weight in the AEG35156 group relative to the saline controls which was found to be insignificant; the CpG treated group showed an 82% increase in spleen weight.

On the basis of the above *in vitro* and *in vivo* data a Phase 1 clinical trial was proposed to investigate AEG35156 as a single agent.

2.5 Phase 1 clinical trial AEG35156

2.5.1 Introduction

XIAP antisense (AEG35156) entered Phase 1 clinical trial in March 2004. The trial was conducted under the auspices of Cancer Research UK and two centres participated: Christie Hospital Manchester (Prof M Ranson, Principal Investigator) and Edinburgh Cancer Centre (Prof D Jodrell, Principal Investigator). As a Clinical Research Fellow, I was responsible for the management of the patients in Edinburgh and I am grateful to Prof M. Ranson and Cancer Research UK for allowing me to discuss data from patients entered in Manchester. Patients 05, 08, 10, 11, 12, 17 (not treated, replaced) 18, 22 and 24, a total of eight patients, were treated in Edinburgh.

The preliminary results of this trial were reported at AACR-NCI-EORTC International Conference Molecular Targets and Cancer Therapeutics Nov 2005 (108) and ASCO Annual Meeting 2006 (109). The primary objectives were to establish the safety and toxicity profile, the dose limiting toxicity of AEG35156 and to establish the maximum tolerated dose (MTD) in order to propose a safe dose for Phase II evaluation. The secondary objectives were to determine the pharmacokinetic and pharmacodynamic properties and document potential anti-tumour activity. Although not included in the objectives of this Phase I Trial, clearly the data accrued will be useful in developing combination protocols with cytotoxic agents. The data presented here are taken from the study report prepared by the CRUK Drug Development Office (personal communication, Ms L Robson).

2.5.2 Methods

Dose levels were selected based on data from regulatory pre-clinical studies in primates utilising the same route of administration and dosing schedule. The starting dose of 48mg/m^2/day selected for this study was one tenth of the maximum tolerated dose (MTD) observed in primate pre-clinical studies (480mg/m^2/day), thus allowing a margin of safety.

The schedule was based on the consideration of tissue sequestration and the two week tissue half-life of the study drug (personal communication, Aegera Therapeutics Inc). The seven day continuous infusion schedule was designed to address the toxicity associated with high plasma levels of antisense agents with short infusion regimens. The study schedule was aimed at minimising plasma levels whilst achieving therapeutic levels of AEG35156/GEM640.

The drug was administered as a 7 day continuous intravenous infusion every 3 weeks at dose levels of 48, 96, 125 and 160 mg/m^2/day. Single patient cohorts were treated until a toxicity of grade 2 or higher was observed, the cohort was then expanded to 3-6 patients per dose level. The MTD was defined as the dose level below that at which more than 30% of the cohort developed a dose limiting toxicity (DLT). DLT was defined as grade 3 or 4 non-haematologic toxicity, grade 4 thrombocytopenia or grade 3 thrombocytopenia for 7 or more days or associated with bleeding, grade 3 anaemia or grade 4 neutropenia, drug related death or increase in complement levels greater than twice baseline. Toxicity was assessed weekly and graded according to common toxicity criteria (CTC) version 2.0. Safety was assessed through adverse events (AE), serious adverse events (SAE), DLT, abnormal laboratory findings, deaths, study withdrawals due to toxicity and changes in vital signs. Tumour assessments were determined using the response evaluation criteria in solid tumours (RECIST) criteria. Tumour response results were compiled on all patients evaluable in terms of overall response, time to progression and survival.

Samples were taken for pharmacokinetic (PK) and pharmacodynamic (PD) markers during cycle 1. Aegera Therapeutics Inc performed PK and RT-PCR assays, the Paterson Institute for Cancer Research (Manchester) was responsible for the M30/M65 assay, the XIAP IHC method was developed by Aegera Therapeutics Inc and validated by the Paterson Institute.

Pharmacokinetic samples were taken at 3, 6, 24, 72, and 168 hours after the start of infusion and at 0.5, 1, 1.5, 2, 4, 6 and 24 hours after the end of infusion. The plasma was analysed for levels of drug and major metabolites using capillary gel electrophoresis.

PD assessments included mRNA knockdown of XIAP by RT-PCR in peripheral blood lymphocytes (a surrogate marker) and circulating tumour cells (NHL patients) and paired tumour biopsies were sought at the predicted MTD. In addition serial M30/M65 cytokeratin 18, a marker of apoptosis, was assessed in patients with epithelial tumours although the data is not currently available for presentation.

2.5.3 Results

2.5.3.1 Safety

In total 24 patients were enrolled in the Phase 1 trial between March 2004 and July 2006. The safety population consisted of 22 patients, as a result of two patients (17 and 19) at the 125mg/m^2/day dose level, being excluded as treatment with the study drug was not commenced.

All 22 treated patients completed the first cycle. Two patients (patients 8 and 22) only completed one cycle. Ten patients completed two cycles of study drug and a further ten patients completed three cycles. No patients received treatment beyond Cycle 3, as all patients had withdrawn from the study.

The primary reason for discontinuation was disease progression (16 patients). Although one patient withdrew consent, there was also documented evidence of disease progression. Two patients were withdrawn from the study by the Investigator, and again there was evidence that the decision was based on deterioration of the patient's condition. Therefore a total of 19 patients withdrew as a result of their underlying disease (Table 1).

Three patients withdrew from the study due to toxicity. Two patients experienced persistent transaminitis and ALT elevations which were associated with study drug treatment. One patient experienced a pulmonary embolism which was reported as a SAE, and was considered unlikely to be related to study drug.

	48 mg/m^2/day (N=1)	96 mg/m^2/day (N=3)	125 mg/m^2/day[d] (N=12)	160 mg/m^2/day (N=6)	Overall (N=22)
Progressive Disease	1	3	8	4	16
Unacceptable Toxicity	0	0	2	1	3
Requirement for > 1 dose level reduction	0	0	0	0	0
Slow recovery from toxicity requiring > 2 week delay	0	0	0	0	0
Patient Request/ Consent	0	0	1[a]	0	1
Physician decision	0	0	1[b]	1[c]	2
Patient non-compliance	0	0	0	0	0
Administrative decision	0	0	0	0	0

a) Patient 24 withdrew consent but had documented disease progression

b) Documented clinical progression confirmed as the reason for Investigator withdrawing patient

c) Patient too unwell to continue and related to underlying disease

d) Patients 17 and 19 did not receive study drug

Table 1: Reason for Treatment Discontinuation (Safety Population)

All patients experienced at least one treatment emergent AE during the study. The most common treatment emergent AEs were abnormal laboratory values, including anaemia (16 patients), raised AST (15 patients), raised ALT (14 patients), lymphocytopenia (14 patients), raised GGT (12 patients), thrombocytopenia (12 patients), hyponatraemia (ten patients) and raised urea (ten patients).

The most common non-laboratory events included fatigue (15 patients), nausea (11 patients) and anorexia (11 patients). The majority of AEs reported were mild to moderate (grade 1 or 2) in severity. Adverse events were more commonly reported in the two higher dose levels (doses 125mg/m^2/day and 160mg/m^2/day).

All grade 3/4 events reported were grade 3 severities, with the exception of two AEs (raised ALT – patient 7 and hypophosphataemia – patient 16). All grade 3 and 4 events were abnormal laboratory values. Considering the overall incidence of these AEs (all grades), the proportion of grade 3 and 4 events were small in relation to the overall population. Hypophosphataemia was the only abnormality where all drug-related events reported were considered to be grade 3 or 4 in severity. Grade 3 and 4 events were reported only in the higher dose levels (125mg/m^2/day and 160mg/m^2/day). No grade 3 or 4 drug-related AE was reported in the lower dose levels (48mg/m^2/day and 96mg/m^2/day).

The most common grade 3/4 non-haematological DLT was raised ALT, followed by hypophosphataemia, raised AST, raised GGT and raised alkaline phosphatase. All these events were abnormal laboratory values and are consistent with the AEs reported in this study (Table 2).

Dose limiting toxicities were reported primarily in the higher dose levels (125mg/m^2/day and 160mg/m^2/day), and were identified in 33% of patients receiving 125mg/m^2/day and 67% of patients receiving 160mg/m^2/day reporting DLTs.

Symptom Adverse Event	**48 mg/m^2/day (N=1)**		**96 mg/m^2/day (N=3)**		**125 mg/m^2/day (N=12)**		**160 mg/m^2/day (N=6)**		**Overall (N=22)**	
	Pts[a]	**Eve[b]**	**Pts**	**Eve**	**Pts**	**Eve**	**Pts**	**Eve**	**Pts**	**Eve**
Raised AST	0	0	0	0	1	1	1	1	2	2
Raised ALT	0	0	0	0	2	2	2[c]	2	4	4
Raised GGT	0	0	0	0	1	1	1	1	2	2
Reduced Platelets	0	0	0	0	1	2	2	2	3	4
Reduced Lymphocytes	0	0	0	0	0	0	1	1	1	1
Raised Alkaline Phosphatase	0	0	0	0	1	1	0	0	1	1
Hypophosphataemia	0	0	0	0	1[c]	5	1	1	2	6

a) Patients were counted once only for each symptom AE

b) Events reflect the number of individual AE reported

c) Two AEs were grade 4 events (raised ALT – patient 7 and hypophosphataemia – patient 16)

Table 2: Treatment Emergent Adverse Event Related to Study Drug in All Patients (Grade 3/4)

The MTD was therefore identified as 96mg/m^2/day of AEG35156/GEM640 under the seven day continuous infusion regimen.

2.5.3.2 Efficacy

	Response	48 mg/m^2/day (N=1)	96 mg/m^2/day[a] (N=3)	125 mg/m^2/day[a,c,d] (N=12)	160 mg/m^2/day[a] (N=6)	Overall (N=22)
Target Lesions	PR	0	0	1	0	1
	SD	0	2	3	6	11
	PD	1	1	1	3	6
Non-Target Lesions[b]	NC	0	1	4	3	8
	PD	1	2	1	5	9
New Lesions	Yes	1	2	1[e]	5	9
	No	0	1	4	4	9
Overall Response	PR	0	0	0	0	0
	SD	0	1	3	4	8
	PD	1	2	2	5	10
	NE	0	0	2	1	3

PR – Partial Response, SD – Stable Disease, PD – Progressive Disease, NC – No Change, NE – Not Evaluable

a) Patients 3,5,6,7,9,11,12,14 completed only two cycles

b) Patients 11 and 13 were not assessed in terms of non-target lesions

c) Patients 20 and 24 only had baseline scans performed

d) Patients 17 and 19 were not evaluable for tumour response as no study treatment was commenced

e) Although a three month scan for patient 20 was not performed, a skin nodule was recorded as a new lesion

Table 3: Tumour Responses According to RECIST Criteria (Efficacy Population)

Overall, eight patients reported stable disease; ten patients reported progressive disease and three patients were non-evaluable. However, when comparing responses between the dose levels, there is a clear increase in the number of patients reporting stable disease as the dose levels rise (Table 3). The majority of stable diseases recorded were in dose levels 125mg/m^2/day and 160mg/m^2/day (three and four patients respectively).

The CT scan of the abdomen for a patient 10 with refractory stage 4 breast cancer is shown in Figure 5 where a response to AEG35156 in the liver lesions is clearly seen. Unfortunately this was not sustained and the disease progressed within 28 days. However treatment had been delayed over this 4 week period due to persistent abnormalities in the liver function tests.

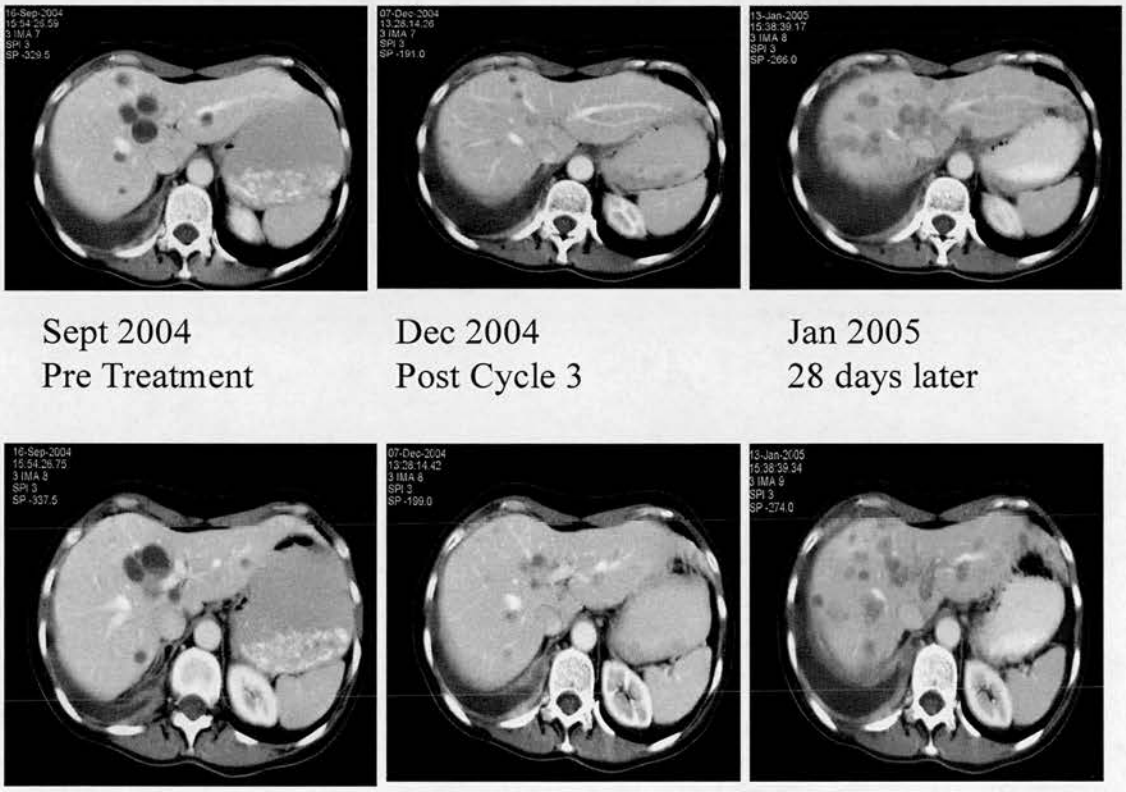

Figure 5: CT scan of the abdomen for Patient 10 with refractory Stage 4 breast cancer. The liver metastases exhibited a partial response of short duration.

In addition to patient 10, there were three patients that reported mixed responses, in terms of areas of tumour response combined with areas of progressive disease. One patient (Number 16) with refractory low grade non-Hodgkins lymphoma had repeated marked reductions in circulating lymphoma cells (Figure 6) implying a response to treatment with AEG35156.

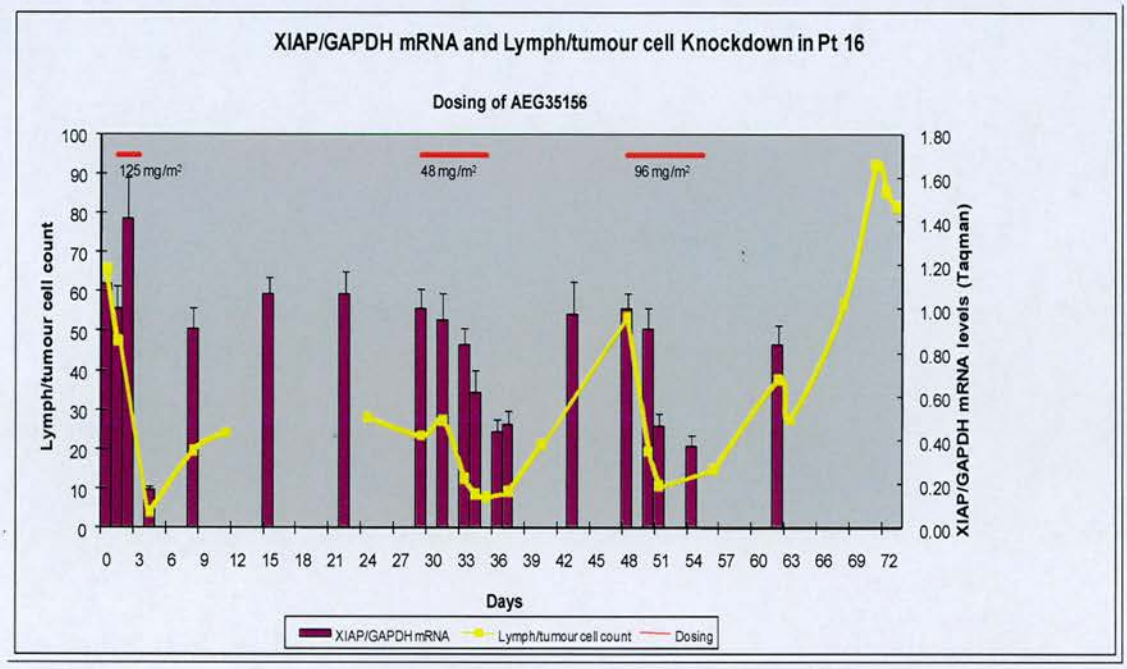

Figure 6: Circulating blast counts in Patient 16 with refractory low grade non-Hodgkins lymphoma and correlation with XIAP mRNA levels

One patient with colorectal cancer was included in the study and reported disease progression after 3 cycles of treatment.

2.5.3.3 Plasma Pharmacokinetics

Steady state plasma concentrations of AEG35156 were approximately dose proportional and were reached rapidly (within 6 hours) after the start of the infusion (Figure 7).

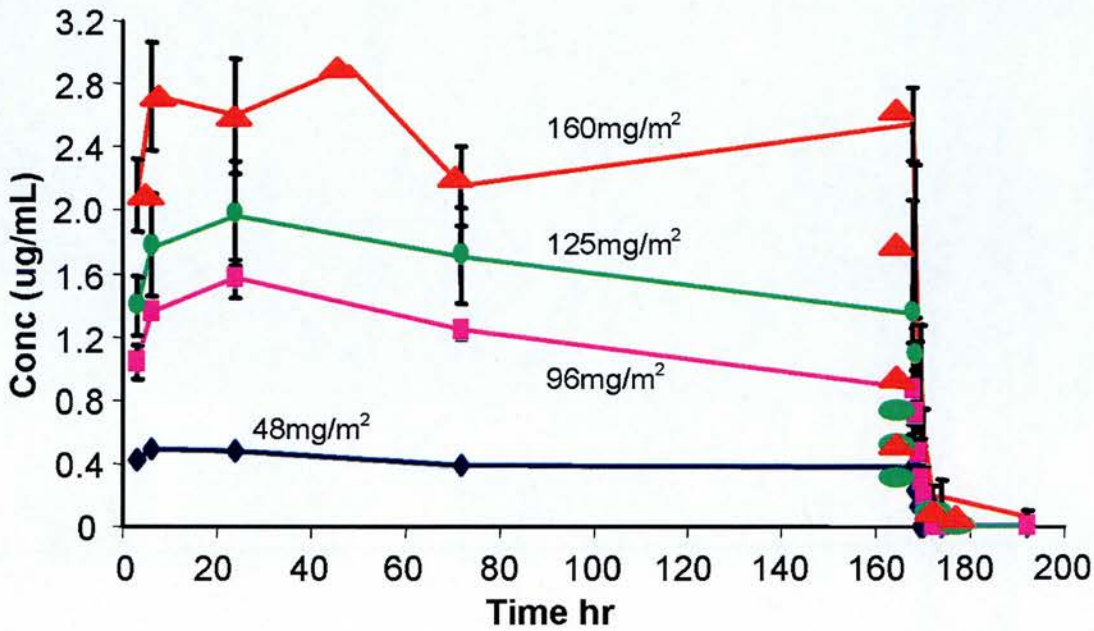

Figure 7: Plasma Concentrations of AEG35156 over time

2.5.3.4 Pharmacodynamic and Mechanistic Data

In this study the relationship between pharmacodynamic markers and AEG35156 was sought so that the optimal biological dose could be established for further studies. The aim was to evaluate XIAP inhibition and apoptosis in tumour biopsies or circulating tumour cells, and XIAP knockdown in peripheral blood mononuclear cells (PBMC). Also, M30/M65 cytokeratin 18 levels were used as a surrogate marker in plasma of patients with epithelial tumours (110).

XIAP mRNA knockdown of 82% at 125mg/m^2/day (Figure 6), was identified in patient 16 which coincides with the apparent clinical response to AEG35156. In the same patient cleaved poly ADP ribose polymerase (PARP) and active caspase 3 were associated with reduced XIAP levels in lymphocytes (Figure 8).

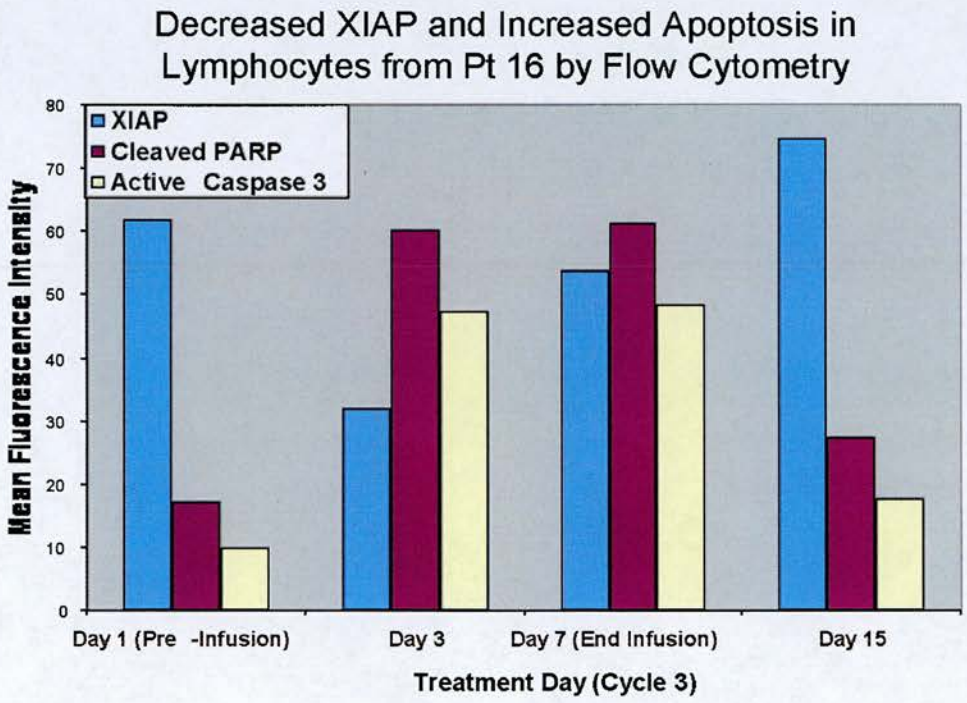

Figure 8: Levels of XIAP, cleaved PARP and active caspase 3 in patient 16 with refractory non-Hodgkins lymphoma during treatment with AEG35156

An immunohistochemistry assay was also developed during the study (Figure 9) which confirmed XIAP knockdown after treatment with AEG35156 in a patient with refractory breast cancer (Patient 20).

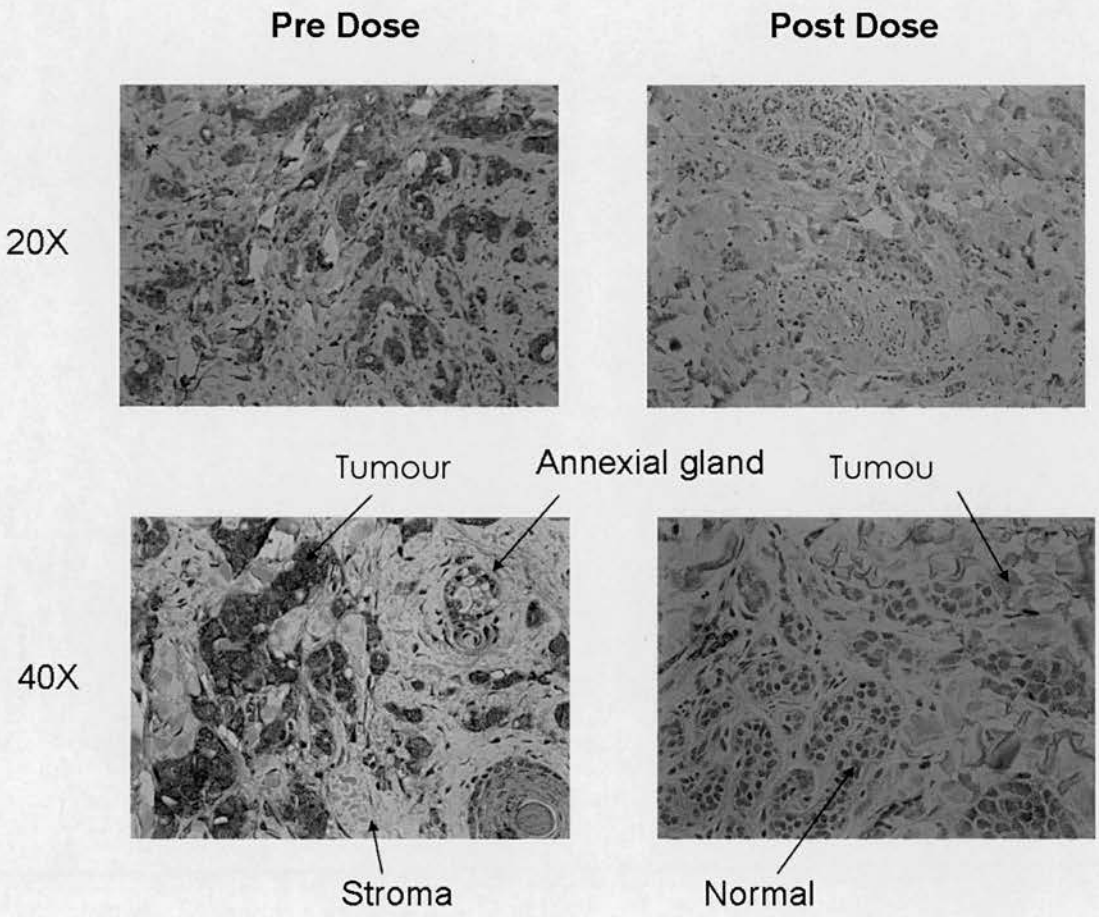

Figure 9: XIAP levels in tissue by immunohistochemistry before and after treatment with AEG35156 in a patient with breast cancer.

In some of the patients there was evidence of XIAP knockdown at the RNA and protein levels as shown in Figure 6 and Figure 9. The markers of apoptosis PARP cleavage and caspase activity were demonstrated (Figure 8) and these data correlate with clinical anti-tumour activity as shown in Figure 5 and Figure 6.

2.5.4 Discussion

This was a phase I, open-label study investigating the safety and tolerability of AEG35156/GEM640, administered over a seven day continuous infusion period in patients with advanced cancer.

Examination of the safety data revealed no major safety concerns associated with the seven day continuous infusion regimen of AEG35156. The most common study drug-related adverse events were liver function test abnormalities (ALT and AST) and were generally mild to moderate in severity. In common with the grade 3/4 toxicities, these events tended to occur at the higher dose levels (125mg/m^2/day and 160mg/m^2/day). Two patients withdrew from the study as a result of persistent raised ALT and transaminitis. Approximately 30% of patients reported serious adverse events (SAE), only two SAEs were considered to be study drug-related (pneumonia and transaminitis) and no deaths were attributed to the study drug.

Approximately 30% of patients (seven) reported DLTs, of whom 3 continued on treatment after dose reduction. DLTs occurred in the two higher dose levels (125mg/m^2/day and 160mg/m^2/day), however one patient (125mg/m^2/day) who was dose reduced to 48mg/m^2/day and re-escalated to 96mg/m^2/day did experience DLTs at these lower dose levels.

The dose limiting toxicity of liver transaminitis has been reported previously, as early as 1997, in rat toxicology studies (111) and in 2003 (112) in a Phase 1 clinical trial of antisense directed against Protein Kinase A. It is thought to be a class effect of the backbone of the drug, the mechanism of which remains unexplained but it occurs as a late effect due to tissue accumulation.

Tumour responses (defined as tumour stabilisation according to the RECIST criteria) were reported in 36% of the patients (eight patients). There was clear evidence that a

higher percentage of patients achieved tumour stabilisation with the 125mg/m^2/day and 160mg/m^2/day dose. There was also evidence of mixed responses in terms of areas of responding tumour and areas of progressive tumour.

Pharmacokinetic studies showed that the oligonucleotides reached steady state within 6 hours in the clinical trial which is consistent with the PK studies performed in primates (113). A Phase 1 trial of bcl-2 Antisense (G3139, Genta Inc) in Non-Hodgkin's Lymphoma also showed a linear correlation between plasma steady state concentration and dose (114) which is consistent with the data described here for AEG35156.

XIAP down regulation was demonstrated at the mRNA level by RT-PCR and protein level by flow cytometry and immunohistochemistry. That the mechanism of action was apoptosis was demonstrated by corresponding increases in cleaved PARP and active caspase 3. During the validation of RT-PCR technique, significant baseline variability (Day -5 and Day -7) in XIAP mRNA levels was noted in the pre-dose samples (115). This was thought to be due to day to day variation in the XIAP levels of PBMCs. Therefore although RT-PCR is a very accurate technique its usefulness as a biomarker is less obvious. It may be more useful to document a trend for each patient determined by frequent measurements during treatment rather than documenting an absolute percentage of XIAP knock down.

2.5.5 Conclusions

Administration of AEG35156 as a continuous intravenous infusion over seven days in patients with advanced cancer was found to be safe. All grade 3/4 adverse events were abnormal laboratory values; raised AST, ALT, GGT, alkaline phosphatase, thrombocytopenia, lymphopenia and hypophosphataemia. Grade 3/4 events were only reported at the higher dose levels (125mg/m^2/day and 160mg/m^2/day). The MTD for this study has been identified as 96mg/m^2/day, as a result of the DLTs observed at doses 125mg/m^2/day and 160mg/m^2/day. Both these dose levels caused DLTs in more than 30% of the patient population.

Evidence of anti tumour activity was observed in eight patients, who achieved stable disease. Ten patients were classified as progressive disease. There was evidence of mixed responses in terms of areas of tumour response (shrinking or stabilisation) combined with areas of progressive disease. There was a clear trend in terms of patients with stable disease at the two higher dose levels (125mg/m^2/day and 160mg/m^2/day). The MTD was defined as 96mg/m^2/day: below the dose levels where stable disease was identified. Therefore it would be important to assess whether this dose level was associated with PD effects before pursuing the dose level in either single agent or combination phase II studies. Data from the phase I three day continuous infusion regimen are awaited.

Further Phase 1 clinical trials of AEG35156 are ongoing in combination with docetaxel in solid tumours (NCIC) and idarubicin & cytarabine in AML (MD Anderson). In the UK, studies using a shorter (2 hour infusion) are also ongoing, similar to that being used in the US and Canadian studies.

Chapter 3

Materials and Methods

3 Materials and Methods

3.1 Chemicals and antibodies

All chemicals are from Sigma-Aldrich (Gillingham, UK) unless otherwise stated. Primary mouse monoclonal antibodies at the following dilutions were used; XIAP (AAM-050) Stressgen (Ann Arbor, Michigan, USA) 1:1000, MLH1 (554073) BD PharMingen (BD Europe, Belgium) 1:250, p53 (OP43) Calbiochem (San Diego, California, USA) 1:200. Membranes were also blotted against mouse β-actin antibody (CP01) Merck Biosciences (Nottingham, UK) at a 1:120000 dilution as loading control. Horseradish peroxidase-conjugated secondary antibodies are from Autogen Bioclear UK Ltd (anti-mouse) and Merck Biosciences Ltd (β-actin) respectively.

3.2 Therapeutic agents

Recombinant Human TRAIL/TNSF10 (R&D systems, Minneapolis, USA Cat no 375-TEC) was reconstituted in sterile PBS containing 0.1% bovine serum albumin to a stock concentration of 20μg/ml according to manufacturers instructions, aliquoted and stored at -20°C. The following therapeutic drugs were obtained from the manufacturers: Camptothecin (C9911), 5FU (F6627), Paclitaxel 6mg/ml (Taxol, Bristol-Myers Squibb, New York, USA), Docetaxel 10mg/ml stored in aliquots at -20°C (Taxotere, Sanofi-Aventis, Paris, France), Irinotecan 100mg/5ml (Campto, Sanofi-Aventis), Cisplatin 1mg/ml (Faulding Pharmaceuticals Plc, Leamington Spa, Warwickshire, UK), Oxaliplatin (Sanofi-Sythelabo Research, Great Valley, PA, USA), Doxorubicin 2mg/ml (Adriamycin, Pharmacia &Upjohn, Kalamazoo, MI, USA). AEG35156 (XIAP Antisense) and AEG35187 (Missense Control) were provided by Aegera Therapeutics (Montreal, Quebec, Canada) and were stored as a powder at -20°C and prior to use reconstituted with PBS (subsequently normal saline) to a stock concentration of 5mg/ml then stored at +5°C for less than 28 days.

3.3 Cell lines

HCT116, HT29, SW620, HCT15 and COLO205 cells were obtained from the American Type Culture Collection (Rockville, MD, USA) and grown in RPMI 1640 containing 2mM glutamine, 5% foetal calf serum and 1% penicillin G/streptomycin (Invitrogen, Paisley, UK). Cell cultures were incubated in the presence of 5% CO_2 at 37°C in a humidified atmosphere and split once a week using trypsin/EDTA (0.05%/0.02%). G418 (geneticin, Invitrogen) 50mg/ml was used to select and maintain the vector expressing cells at a 1 in 50 dilution.

3.4 Generation of stable XIAP shRNA HCT116 cells

The XIAP shRNA plasmid constructs were provided by Aegera Oncology according to the method described in (41) using a pCDNA3 vector containing a U6 promoter. 4 x 10^6 HCT116 cells were plated in 100mm plates overnight prior to a 24 hour transfection with 1μg of pCDNA_U6_luc (L prefix clones) or pCDNA_U6_shXIAP (X prefix clones) using Effectene (Qiagen, Crawley, UK) according to manufacturers protocol. The next day cells were trypsinised, a single cell suspension created and split 1:5 in 100mm Petri dishes. Geneticin was added to select vector containing colonies and media was changed after 3 days. After 10 days colonies were seen by eye, 24 of each X and L were picked, transferred to 24 well plates and allowed to proliferate in the presence of geneticin. Cells were passaged when nearing confluence and total RNA extracted to confirm XIAP knockdown at early passage (p4) and late passage (p8).

3.5 RNA extraction

Total RNA was extracted from cells in the exponential growth phase using Tri-Reagent according to manufacturer's instructions. All samples were DNase treated to avoid DNA contamination of samples for RT-PCR. Initial experiments used 20U of grade I DNase (Roche Applied Science, Indianapolis, USA) in the presence of 50U RNase inhibitor (Roche Applied Science) at 37°C for 60min. RNA was recovered

after phenol/chloroform and chloroform extractions followed by precipitation with 3M sodium acetate/absolute ethanol. Later experiments used TURBO DNase (Ambion, Applied Biosystems, Foster City, CA, USA) to avoid phenol/chloroform extractions and increase yield. RNA was dissolved in water and concentration determined by spectrometry at 260 and 280nm. For extraction from tissue, samples were removed from -80°C storage and quickly cut to weigh less than 100mg. 1ml TRI reagent was added, tissue was dismembrated for 1min at 1800rpm and extraction continued as above. The quality of RNA extracted from tissue was evaluated by electrophoretic analysis on a 2100 Agilent bioanalyser (Agilent Technologies, Santa Clara, CA, USA).

3.6 Primer Design

Primers for quantitative RT-PCR were designed with Primer 3 software (http://frodo.wi.mit.edu/cgi-bin/primer3/primer3_www.cgi/) using the mRNA sequence of the genes of interest deposited at the National Centre for Biotechnology Information (http:/www.ncbi.nlm.nih.gov/). The mRNA accession numbers were XIAP (BIRC4) NM_001167, cIAP1 (BIRC2) NM_001166, cIAP2 (BIRC3) NM_001165 and NM_182962, survivin (BIRC5) NM_001012270, NM_001012271 and NM_001168, XAF1 (BIRC4BP) NM_017523.2 and NM_199139.1, mouse XIAP NM_009688. Where more than one transcript was identified the primers were designed against a region of high homology using the Basic Local Alignment Tool (http://www.ncbi.nlm.nih.gov/blast/bl2seq/wblast2.cgi) to align sequences. Design criteria were the following: primer size of 18-22 bp, Tm between 57 and 63°C, GC content 45-55%, amplicon size 150-250 bp. Primer-dimer formation was minimised by setting the maximum 3' self complementarity to a value of 3. Primer specificity was checked using Blast search (http://www.ncbi.nlm.nih.gov/BLAST/Blast.cgi).

3.7 Quantitative RT-PCR

All transcripts were detected using QuantiTect SYBR Green RT-PCR kits (Qiagen). The reaction was carried out with 10ng total RNA per reaction and primers at a concentration of 20μM in a final volume of 15ul on a Rotor-Gene 3000 real-time DNA detection system (Corbett Research). Each standard and sample was performed in triplicate. Standard curves were built by serially diluting HCT116 RNA stock solution (200ng/ul) in water to a concentration of 0.5 – 50ng total RNA per reaction. For XAF1 expression, COLO205 was used as a standard as the gene levels were highly expressed (100ng for XAF1). Cycling conditions were 50°C for 30min, 95°C for 15min, followed by 45 PCR cycles at 94°C for 15sec (denaturation), 55°C for 30sec (annealing) and 72°C for 45sec (extension). Fluorescence was recorded on the FAM channel (Ex=470nm, Em=510nm) at the end of extension. Results were expressed as normalised fluorescence and data analysed using Rotorgene 6 software. A dynamic tube normalisation was used for each sample and the amplification reaction considered an exponential process. POLR2A (RNA polymerase II subunit A, RPII) was selected as the housekeeping gene for normalisation of the qRT-PCR data as minimal variation was seen across cell lines (116). For experiments where comparisons are made with microarray data, results are expressed per ng of total RNA relative to the HCT116 parental cell line.

3.8 Detection of protein by Immunoblotting

4 x 10^6 cells from *in vitro* studies were washed with PBS and suspended in lysis buffer (62.5mM Tris pH 6.8, 6M urea, 10% glycerol, 2% SDS) prior to sonication on ice. Protein quantitation was performed using the bicinchoninic acid (BCA) assay. 25μg protein was incubated with denaturing buffer (0.3M Tris pH 6.8, 10% 2-mercaptoethanol, 40% glycerol, 20% SDS, 0.02% bromophenol blue) for 5 min at 95°C. Samples were loaded onto a 10% SDS-polyacrylamide gel for electrophoresis at 60mA for 30mins then 35mA for 3-4 hours, full range rainbow molecular weight marker was also loaded (GE Healthcare, Bucks, UK). Proteins were transferred at 28V overnight at 4°C onto polyvinylidene fluoride membranes (Hybond-P, GE

Healthcare, Bucks, UK) and Ponceau stain performed to visualise proteins. Membranes were blocked in 5% non-fat milk TBS-Tween for 1 hour at room temperature and incubated overnight at 4°C in a primary antibody diluted in 2.5% non-fat milk. Membranes were then washed in TBS-Tween, and horseradish peroxidase-conjugated secondary antibodies incubated for 1 hour at room temperature and washed again. Immunoreactivity was detected using the Enhanced ChemiLuminescence Plus detection reagent (GE Healthcare) visualised on the Storm 840 Scanner (Amersham Biosciences). Protein quantification was performed with Image Quant version 5.2 software.

3.9 Microarray

RNA from the parental cell line HCT116 (in duplicate) and vector expressing cell lines X6, X10, X16, X23 (X) and L8, L15, L23, L24 (L) at an early passage (p4) and later passage (p8) were analysed by microarray. Total RNA was DNase treated to remove genomic DNA as described above and cleaned using the RNeasy mini kit (Qiagen) to remove organic solvents. RNA integrity was checked by Agilent bioanalyser and confirmed to be good quality. 5μg total RNA (minimum concentration 0.6μg/ul) was sent to the Patterson Institute for Cancer Research for microarray analysis.

The methods below are taken from the Paterson Institute for Cancer Research Website and URL and are included where appropriate. Samples were labelled using the Affymetrix One Cycle Target labelling Kit. All experiments were performed using Affymetrix HG_U133 plus 2.0 oligonucleotide arrays, as described at http://www.affymetrix.com/products/arrays/specific/hgu133plus.affx. Total RNA from each sample was used to prepare biotinylated target RNA, with minor modifications from the manufacturer's recommendations (http://www.affymetrix.com/support/technical/manual/expression_manual.affx).
Briefly, 10 μg of mRNA was used to generate first-strand cDNA by using a T7-linked oligo (dT) primer. After second-strand synthesis, in vitro transcription was

performed with biotinylated UTP and CTP (Enzo Diagnostics), resulting in approximately 100-fold amplification of RNA. A complete description of procedures is available at http://bioinf.picr.man.ac.uk/mbcf/downloads/ GeneChip_Target_ Prep_Protocol_CRUK_v_2.pdf. The target cDNA generated from each sample was processed as per manufacturer's recommendation using an Affymetrix GeneChip Instrument System (http://www.affymetrix.com/support/technical/manual/ expression_manual.affx). Briefly, spike controls were added to 10 μg fragmented cDNA before overnight hybridisation. Arrays were then washed and stained with streptavidin-phycoerythrin, before being scanned on an Affymetrix GeneChip scanner. A complete description of these procedures is available at http://bioinf.picr.man.ac.uk/mbcf/downloads/GeneChip_Hyb_Wash_Scan_Protocol_ v_2_web.pdf. Quality and amount of starting RNA was re-confirmed using an Agilent Bioanalyser. After scanning, array images were assessed by eye to confirm scanner alignment and the absence of significant bubbles or scratches on the chip surface. For further discussion on the principles of microarray see Chapter 7.

3.10 Microarray data analysis

Data were analysed by Richard Mitter, CRUK Bioinformatics and Biostatistics Group, London using Bioconductor 1.8 (117) running on R 2.3.0 (118). Expression measures were calculated using the 'Affy' package's Robust Multichip Average (RMA) default method (119). Differential gene expression was assessed between X and L cell lines for early (p4) and late (p8) passage cells using an empirical Bayes' t-test as implemented in the 'limma' package (120) (121) (122). Subsequent p-values were subjected to multiple testing correction using Benjamini and Hochberg's method for controlling the false discovery rate (123). Probe sets were called differentially expressed if their adjusted p-values were below a cut-off of 0.05. 'simpleAffy' (124) and 'hgu133plus2' (125) packages were used to link Affymetrix probe set ids to functional annotation.

3.11 Cell growth

Cells were seeded in 96-well plates at increasing densities (500 to 5000 cells per well) in 200µl media. Every 24 hours the number of cells present were estimated by SRB assay (see below for more detail) (126). The growth curve for each cell line was then constructed. The optimal cell density is defined as the cell density that gives an optical density of >1.5 when the cells are allowed to grow for three doubling times. A graph is drawn of log cell number against time, the equation parameters for exponential growth are $y=No.e^{kt}$. The doubling time is calculated according to the equation $t^2=\ln 2/k$. The plating efficiency is the ratio between the number of cells present after 24 hours when the media has been aspirated compared to no removal of media.

3.12 Cell Characteristics

The floating cell fraction was determined by counting (Becker Coulter Counter) an aliquot of the media from the tissue culture flask after the cells had been growing for 7 days. The adherent cells were then trypsinised and an aliquot counted. The floating cell fraction was expressed as a percentage of the total adherent and floating cells and the experiment repeated three times.

For morphological examination the media was changed immediately prior to examination and cells visualised under a phase contrast microscope. Spot Insight FireWire camera and software version 4.1 were used.

3.13 Annexin V-PI assay by flow cytometry

Apoptotic cells were detected by flow cytometric analysis using TACS Annexin V-FITC kit (TA4638/TA5532 R&D systems, Abington, UK) according to manufacturer's instructions. Exponentially growing cells, both floating and adherent fractions, were collected using Cell Dissociation Solution to avoid membrane

disruption and a single cell suspension formed. $1x10^6$ cells were washed once with cold PBS and resuspended in 100µl reagent, incubated in the dark for 15 minutes at room temperature. 400µl of 1X binding buffer was added and cells analysed by flow cytometry on the FACSCalibur (Becton Dickinson, San Jose, CA, USA) as described in (127). FITC and PI emissions were detected in the FL-1 (Ex=488 nm, Em=530 nm, band width 30 nm) and FL-2 (Ex=488 nm, Em=575 nm, band width 42 nm) channels, respectively. Cells were first analysed for the forward scatter *vs.* side scatter distributions. Cell debris characterised by low FSC/SSC were excluded from the analysis. The viable cells were then analysed on the FL-1 *vs.* FL-2 plot. HCT116 cells stained with PI or annexin V only were used to set up the compensation value between the two channels. HCT116 cells (low PI and AV) stained with both PI and AV were processed to define the 4 quadrants of interest: PI−/AV−, PI+/AV−, PI−/AV+. The samples (10,000 cells) were then analysed using the same settings to measure the distribution of the cells in the different quadrants: impermeable to both PI and AV (PI−/AV−), permeable to PI but not AV (PI+/AV−), permeable to AV but not PI (PI−/AV+), and permeable to both PI and AV (PI+/AV+). Data analysis was performed with Cell Quest software.

3.14 DR5 expression by flow cytometry

For these studies Cell Dissociation Solution was used to remove cells from the tissue culture flask to avoid potential disruption of the cell surface receptors with trypsin. A DR5 primary antibody conjugated to phycoerythrin (Abcam ab18365, Cambridge, UK) was optimised to assess the cell surface receptor expression. Jurkat cells were included as a control. 1 x 10^6 cells were washed with PBS, incubated for 30 minutes in the dark with antibody or 3% BSA control. Cells were then washed three times with PBS and analysed by flow cytometry. The procedure was optimised as described for AV-PI staining.

3.15 In vitro cytotoxicity using the SRB assay

Cytotoxicity *in vitro* was assessed using a cell death assay based on detection of cells by sulforhodamine B (SRB), a stain specific for proteins (126). Each cell line was plated in 96-well plates according to the optimal seeding density (2000 – 5000 cells per well) in 150µl media. To achieve log phase cell growth at the start of treatment cells were allowed to attach and grow for 72 hours. Drugs were added over a concentration range in 50µl media and incubated for 72 hours (for rhTRAIL experiments shorter time points were necessary). The cells were fixed with trichloroacetic acid (TCA), 10% final concentration, and the plates were incubated for 1 h at 4°C. Wells were washed gently under running water and allowed to air dry. SRB 50µl was then added to each well and the plates incubated 30 min at room temperature. The excess SRB was then removed with 4 washes of 1% acetic acid and the plates allowed to completely air dry. Tris-HCl, pH 10.5, 150µl was then added to each well and the plates incubated for 1 hour at room temperature on a mixing platform. Absorbance was read at 540nm on a Biohit BP800 microplate reader (Bio-Hit, Helsinki, Finland). For radiotherapy studies, cells were seeded in 96-well plates in triplicate at the optimal seeding density and left to attach for 24 hours. Gamma radiation was applied over a dose range 0 – 16 Gy adhering to local safety guidelines. Cells were then incubated at 37°C for 120 hours prior to SRB assay. Three independent experiments were performed.

3.16 In vitro cytotoxicity using the MTT assay

Cells were plated in triplicate according to the optimal seeding density as described above and allowed to adhere for 24 hours prior to cytotoxic treatment. Cells were incubated with 0.2mg/ml MTT for 3 hours in the dark at 37°C (128). Medium was then removed and formazan crystals solubilised in 200µl DMSO. The optical density was measured at 570nm using a Biohit BP800 microplate reader. Experiments were performed three times and the results expressed as a percentage of viable cells compared to untreated controls using GraphPad Prism 3 software.

3.17 Caspase 3/7 activity

Caspase 3/7 activity was estimated by cleavage of fluorescence peptide substrate in the ApoOne caspase 3/7 assay (Promega) according to manufacturer's instructions. Briefly, an equal volume of homogeneous caspase 3/7 reagent (Z-DEVD-Rhodamine 110 and lysis buffer ratio 1:100) was incubated with cells in a white-walled 96 well plate at room temperature on a plate mixer for 21 hours. The fluorescence was detected by excitation 485nm and emission at 538nm on a Fluoroskan Ascent FL platereader (Thermo Labsystems, Waltham, MA, USA) using Ascent software version 2.4.1. Experiments were performed three times and results expressed as the difference between treated and untreated cells or relative to the parental cell line.

3.18 In vivo xenograft establishment

Animal experiments were carried out under a project licence issued by the UK Home Office and UKCCCR guidelines (129) were followed rigorously. Studies were performed in C57/Bl6 Nu/Nu mice 6-weeks old bearing bilateral xenografts, five animals per group (10 xenografts). 10 million cells per flank were implanted subcutaneously in a final volume of 200 µl RPMI and two dimensional volume measurements taken three times per week with electronic callipers. Tumour volumes were calculated using the formula $V = [L \times (W^2/2)]$. Xenografts were collected on day 26, dissected to remove surrounding mouse tissue and blood vessels, and snap frozen in liquid nitrogen. For therapeutic studies, treatment started 7 days after implantation when tumour size reached 50-100 mm^3.

3.19 Statistical analysis

Growth inhibition curves were plotted as percentage of control cells and IC50 values were determined by GraphPad Prism 3 Software (San Diego, CA, USA). Other data are expressed as mean values ± standard deviation and an unpaired two-tailed t-test was used to detect significance. A value of $p<0.05$ was considered to be statistically significant.

Chapter 4

Characterisation of Colorectal Cell Lines

4 Characterisation of Colorectal Cells Lines

4.1 Introduction

A panel of five colorectal cell lines will be characterised and the results described in this chapter. The cell lines were investigated for their MLH1 and p53 protein status as these two features are known to be of clinical importance in colorectal cancer. The response to chemotherapeutic agents may vary depending on the expression of p53 and MLH1; Magrini *et al* investigated the effects of these two proteins in response to CPT11 treatment in isogenic derivatives of the HCT116 cell line and found that the mechanism of cytotoxicity varied (47). CPT11 was found to induce long term G2/M arrest in p53+ cells and short term growth arrest followed by apoptosis in p53- cells. In addition lack of the MLH1 protein enhances apoptosis in CPT11 treated HCT116 cells. Meyers *et al* were able to demonstrate that MLH1 deficient cells were more resistant to 5FU compared to mismatch proficient HCT116 cells (130). Therefore it is important to characterise the colorectal lines as their response to clinically important chemotherapeutic agents may differ.

It is also necessary to establish XIAP mRNA and protein levels in the panel of colon cancer cell lines prior to further investigation in order to identify an appropriate model for further study. Publicly available data on NCI/NIH Developmental therapeutics website (http://dtp.nci.nih.gov/mtweb/search.jsp) was accessed to directly compare the results of this study at the mRNA level. The levels of XIAP across the NCI panel of cell lines has previously been described in the literature (82, 86) and, although this data cannot be directly compared, it provides confidence in the methods used. The mRNA levels of three other members of the IAP family (CIAP1, CIAP2 and Survivin) are also presented with comparison to NCI data in addition to the negative regulator of XIAP, XAF1.

XIAP protein levels were investigated in an isogenic system to assess whether differences occur according to p53 or MLH1 status. The HCT116 cell line represents the parental wild type, HCT116 p53- is a p53 null cell line, HCT116 Chr3 has had Chromosome 3 replaced to provide a functional mismatch repair (MMR) system, HCT116 Chr3/M2 is a derivative of the previous cell line which serves as a control for the addition of an extra chromosome but with deficient MMR system.

4.2 Results

4.2.1 XIAP mRNA Levels

Total RNA was extracted from a panel of cell lines using the method described in Chapter 3. Figure 10 shows the comparison between results from this study and data published from the NCI/NIH Developmental therapeutics program. The qRT-PCR results correlate well with the NCI data for 4 out of 5 of the colorectal cancer cell lines, the exception being Colo205. Up regulation of XIAP mRNA is seen in all 5 colon cancer cell lines in comparison to normal adult human liver by qRT-PCR; the NCI data has no normal tissue comparison.

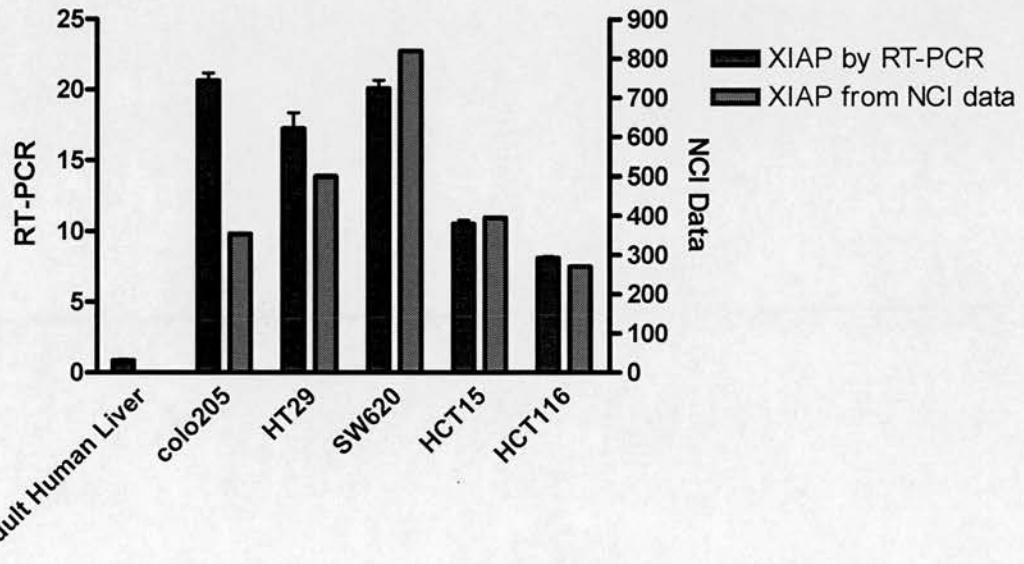

Figure 10: Left axis displays XIAP mRNA levels in 10ng total RNA by RT-PCR for a panel of colorectal cell lines, relative to human adult liver. Error bars show standard error of mean for triplicate reactions in the Rotorgene run. Right axis shows data from the NCI database (no normal tissue comparison).

Figure 11 shows the variability of the NCI data for XIAP levels by RT-PCR relative to HCT116. The cell line colo205 shows a large inter-experiment variability which may explain the difference in XIAP levels for this cell line seen in Figure 10.

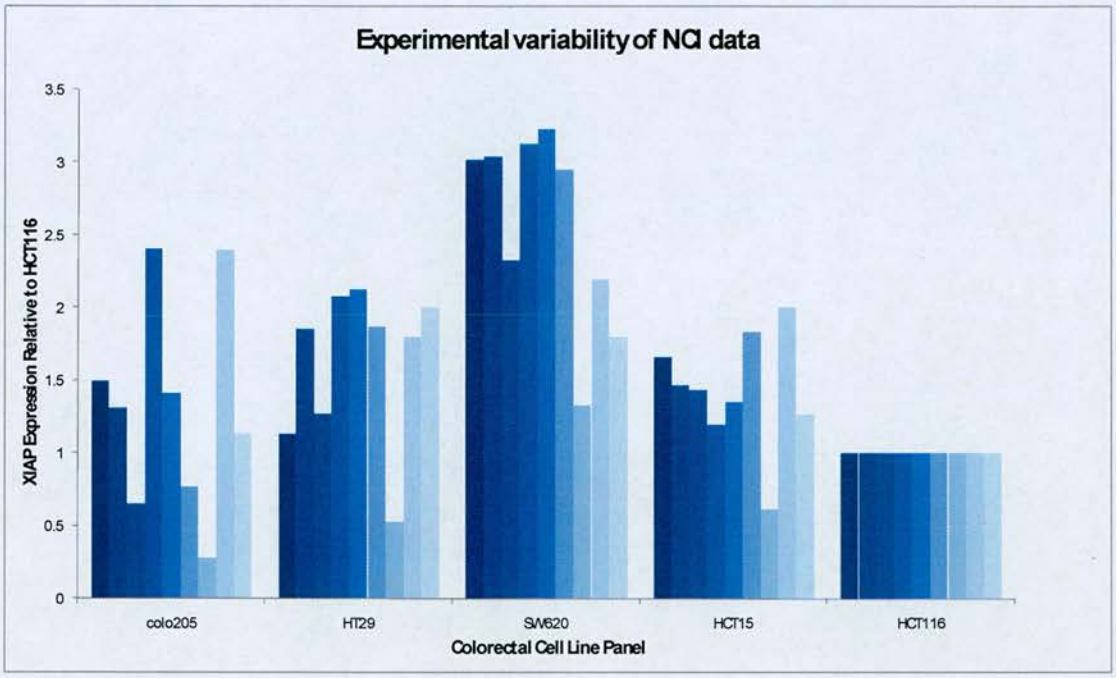

Figure 11: Experimental variability of NCI data. XIAP levels by RT-PCR from nine experiments from NCI for each of the five cell lines relative to HCT116

4.2.2 Characterisation of protein levels by Immunoblot

XIAP protein levels across the panel of colorectal cancer cell lines are shown in Figure 12. All of the cell lines express XIAP; HCT15 has the lowest levels and SW620 the highest. For SW620 a double band is seen; further optimisation of the experimental conditions may be required for this cell line.

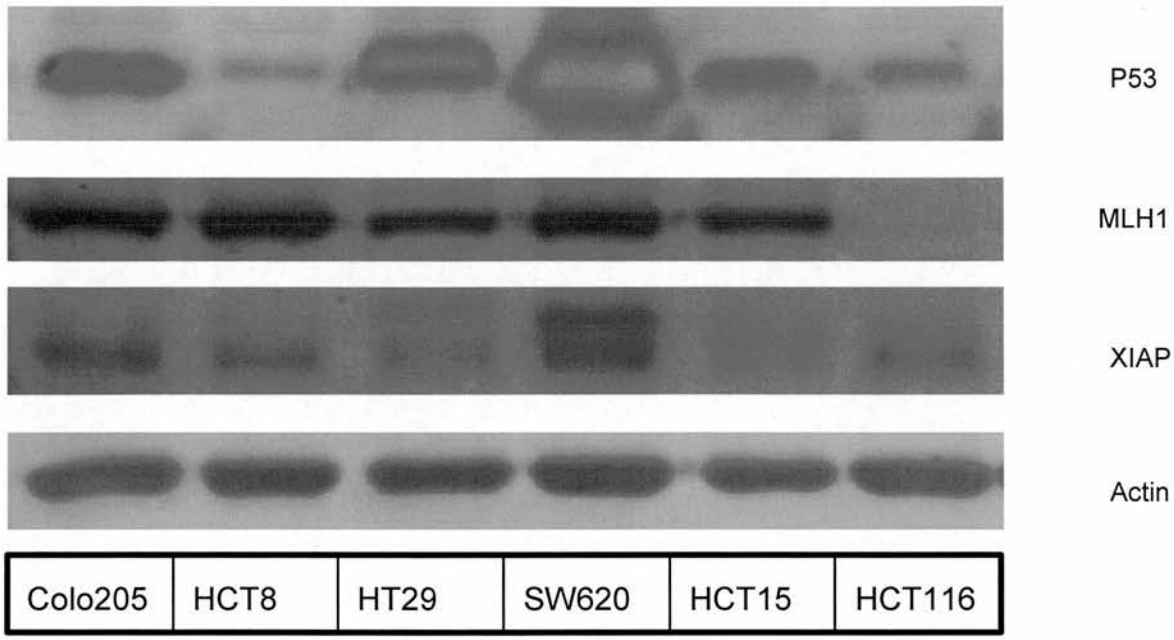

Figure 12: Western Immunoblot comparing protein levels of P53, MLH1 and XIAP across a panel of colorectal cell lines.

The p53 and MLH1 status across the colorectal cell line panel is shown in Figure 12 with publicly available data shown in Table 4 for comparison. The HCT8 cell line was included in this gel, but not in other studies and the data is shown to avoid cutting the gel. HCT116 is the only MLH1 deficient cell line in the panel studied which is consistent with NCI data (http://discover.nci.nih.gov/ cellminer/loadDownload.do). p53 levels correlate with mutation status when compared to data from the Sanger institute (http://www.sanger.ac.uk/ genetics/CGP/cosmic/) with the exception of HCT15 where p53 was mutated in their data.

	Colo205	HT29	SW620	HCT15	HCT116
P53	mut	mut	mut	mut	WT
MLH1	+	+	+	+	-

Table 4: P53 (Cosmic, Sanger Institute), MLH1 (CellMiner, National Cancer Institute) status for comparison with Figure 12.

4.2.3 XIAP in an isogenic HCT116 system

XIAP protein levels in HCT116 derivatives with variations in their p53 and MLH1 status are described in Figure 13. The results shown confirm the p53 and MLH1 status of these isogenic cell lines. The XIAP levels do not appear to vary across derivatives of HCT116 indicating that alterations in p53 or MLH1 protein levels do not affect the expression of XIAP in a quantitative manner.

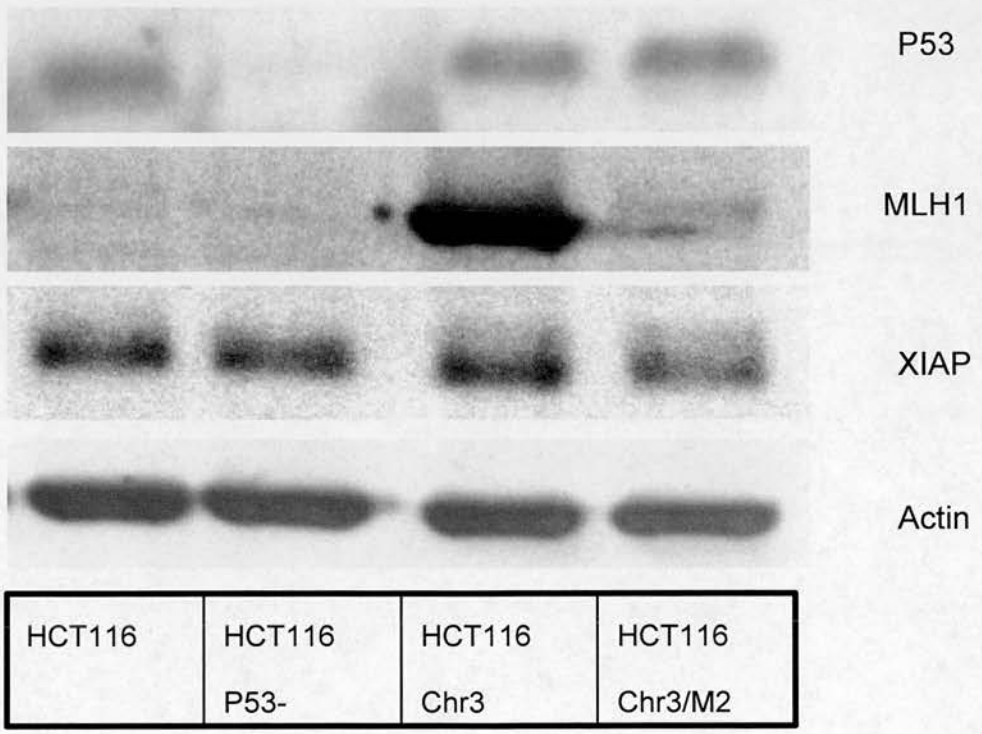

Figure 13: p53, MLH1 and XIAP levels by Western Immunoblot in isogenic HCT116 colorectal cell lines.

4.2.4 mRNA expression of other IAPs and XAF1

The levels of other IAP family members cIAP1, cIAP2 and survivin (Figure 14) were also quantified. These were found to be elevated by qRT-PCR in comparison to normal human liver although the correlation of expression in cancer cell lines with NCI data was inconsistent. This could be due to inter-experiment variability as described with XIAP in Figure 11 above or differences in the stage of cell cycle as the cells were not synchronised prior to RNA extraction.

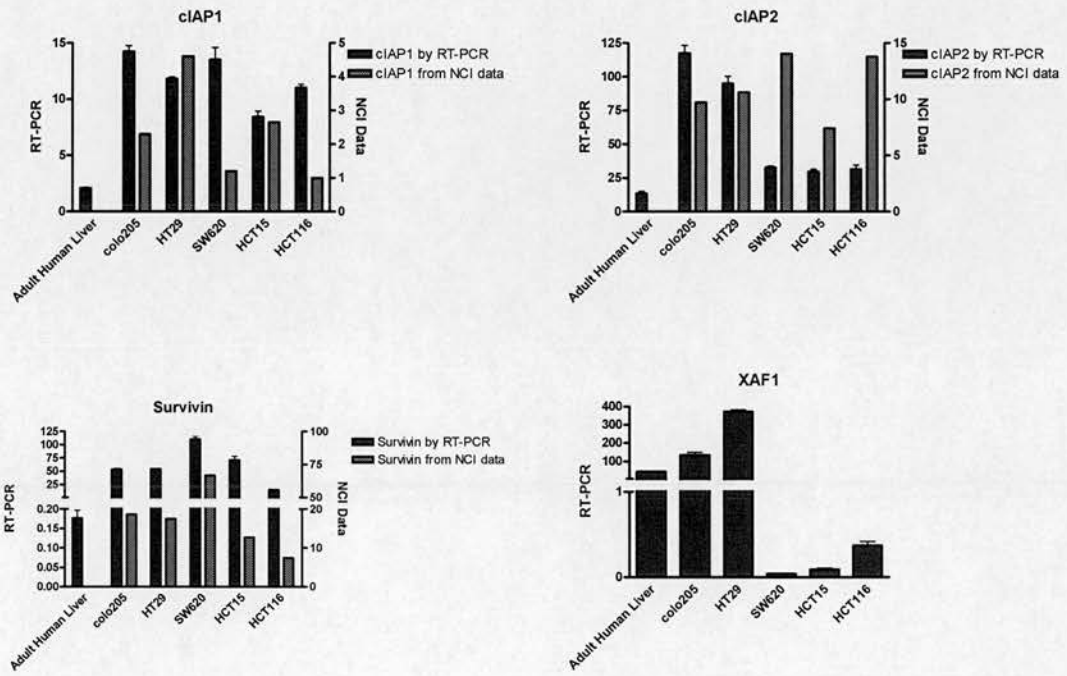

Figure 14: mRNA expression of IAP family members cIAP1, cIAP2 and survivin across the panel of colorectal cancer cell lines with normal human liver by qRT-PCR compared to the data from NCI. XAF1 mRNA expression across the panel of cell lines by qRT-PCR. Error bars show standard error of the mean for triplicate reactions in the Rotorgene run.

XAF1 levels are low in 3 out of 5 of the cancer cell lines compared with normal human liver (Figure 14). Two of the cell lines (HT29 and Colo205) have much higher levels (2 orders of magnitude) than those seen in normal tissue. No correlation between XIAP and XAF1 levels was seen.

4.3 Discussion

There is good correlation between XIAP qRT-PCR data generated in these studies and the publicly available results with the exception of the Colo205 cell line. The Colo205 cell line shows the most inter-experimental variability in the NCI data and it was therefore excluded as a candidate for further study. These data validate the primers which were designed (see methods) and the accuracy of qRT-PCR as a technique in the quantification of XIAP mRNA levels. Levels of XIAP, CIAP1 and CIAP2 have been described in the literature (82, 86) although it is difficult to compare these results as different experimental techniques and analysis were used. Of the 5 cell lines examined, HCT116 has the least (10 times) up regulation of XIAP compared to adult human liver. Takeuchi *et al* describe similar levels of XIAP up regulation (one order of magnitude) when comparing human colon adenomas to liver metastases by qRT-PCR (92) hence this model is relevant in the clinical setting.

The HCT116 cell line is deficient in MLH1 which is consistent with previous reports (47, 130). The results shown here describe no variation in XIAP depending on the MLH1 or p53 status. Krajewska *et al* (88) studied the protein expression in human colorectal tissue of several apoptosis biomarkers. They found that microsatellite unstable tumours revealed significant differences for p53, CIAP1 and CIAP2 immunostaining but no difference for XIAP, survivin, smac or BCL2 family members. Therefore we may assume that the MLH1 protein expression of the cell line does not affect XIAP expression. It is well documented that there are genetic differences between tumours which are microsatellite stable and unstable in terms of their p53 status. Cummins *et al* developed a XIAP knockout model by gene deletion (131) using two colorectal cancer cell lines which differed in their p53 status and found a consistent phenotype. This implies that XIAP expression is independent of p53 status; our data confirm such findings.

There are no data available from the NCI for expression of the negative regulator of XIAP, XAF1. However, Fong et al (82) describe low XAF1 expression in cancer cell

lines of the NCI60 panel by RT-PCR with the exception of Colo205 where the levels were higher than average, consistent with our study. They describe very low XAF1 levels in the HT29 cell line which is inconsistent with the data presented here; our experiment may need to be repeated under different cell growth conditions. Generally levels of XAF1 are lower in cancer cells when compared to normal cells, leading to its identification as a possible tumour suppressor gene. To date no specific mutations of XAF1 have been identified although the gene is located within an area of loss of heterozygosity at 17p 13 (82). More recently hypermethylation of the promoter region of the XAF1 gene has been described resulting in repression of transcription (132) which would explain the low levels of XAF1 in tumour cells.

The HCT116 cell line is mismatch repair deficient (MLH1-) but has a normal functioning p53. It expresses XIAP at levels similar to the other members of the colon cell line panel and is up regulated compared to normal tissue. HCT116 is a well characterised cell line which is easy to grow *in vitro,* readily modifiable and all the isogenic lines grow well as xenografts, making a good candidate for further study.

Chapter 5

In Vitro Studies with AEG35156 (XIAP Antisense)

5 *In Vitro* Studies with AEG35156

5.1 Introduction

In vitro studies with AEG35156 (XIAP Antisense) in the HCT116 colorectal cancer cell line will be described in this chapter. Transient transfection of antisense is a well established *in vitro* method of target down regulation. Delivery of antisense requires the use of transfection reagents such as Lipofectamine™ 2000 (LFA™2000) which intermittently disrupts the cell membrane allowing the oligonucleotide to enter the cell. The use of any transfection reagent may bias experimental results and therefore appropriate controls are necessary. In the following experiments there are 3 controls (Opti-MEM®, Phosphate Buffered Saline (PBS) and AEG35187 missense (MS)) and one experimental (AEG35156 XIAP antisense (AS)). The "Opti-MEM®" group represents the addition of serum free media with no LFA™2000 thus when compared to the "PBS" group (phosphate buffered saline plus LFA™2000) assesses the effect of the transfection reagent. When "MS" is compared to "PBS" the effect of the backbone structure of the drug may be delineated. The specific effect of XIAP down regulation is therefore only seen when comparing "AS" to "MS". In most experiments the targeted oligonucleotide does not cause toxicity to the cell but here it has the potential to do so as it is mounted on a phosphorothioate backbone hence the need for a backbone (missense) control.

For clinical development of the compound the backbone is essential to prevent breakdown of the targeted structure by enzymes after intravenous (IV) injection. Therefore the effect of this structure should also be assessed *in vitro*. The aim was to assess the cytotoxicity of this oligonucleotide with a view to combination studies with recognised cytotoxic agents and further *in vivo* studies. First the pharmacodynamic effect of the new compound was confirmed by quantification of the XIAP mRNA levels in a cell; this required optimisation of the transient transfection method. Second the dose range of the new compound was identified in order to balance the drug toxicity with the pharmacodynamic effect.

5.2 Method Optimisation

Two methods for transfection of antisense oligonucleotides were evaluated:

5.2.1 One day transfection

The day prior to transfection HCT116 cells were plated in 6-well tissue culture plates in triplicate at a seeding density of 1 x 10^6 cells per well (no antibiotics were added to media) and incubated overnight. Antisense (AS), missense (MS) or phosphate buffered saline (PBS) were added to the cells with Lipofectamine™ 2000 (LFA™2000) according to manufacturer's recommendations. A control using Opti-MEM® only without LFA™2000 was also included to assess the effect of the transfection reagent. Oligonucletide dilutions and complexes were made in Opti-MEM® (Invitrogen) reduced serum medium at a final concentration of 400nM or 1200nM. After 6 hours the medium was replaced and the cells were incubated for 24 hours prior to RNA extraction and XIAP level analysis by qRT-PCR. This method using AEG35156 has previously been described (133) in the non-small cell lung cancer cell line H460. For cytotoxicity assays (SRB, MTT and caspase 3/7 activity) the above protocol differed only in that 96 well tissue culture plates were used; the reagents were scaled according to the manufacturers recommendations keeping the drug concentrations accurate.

5.2.2 Two day transfection

The protocol above was followed and the cells transfected on the first day as above. After 6 hours incubation the medium containing complexes was removed and replaced for overnight incubation. The next day a further 6 hour transfection was performed. XIAP mRNA levels were quantified by qRT-PCR and cytotoxicity studies performed as described in Chapter 3. Increasing OGN concentrations were investigated and at the 100nM and 400nM doses, RNA was extracted to assess the extent of XIAP knockdown. The 400nM dose allows comparison with the one-day transfection protocol described above and the 100nM dose was chosen from the IC_{50} value of the SRB cytotoxicity assay (see Figure 20 below).

5.3 Results

5.3.1 One day transfection protocol

5.3.1.1 XIAP down regulation

The results of the one day transfection protocol at 400nM and 1200M are shown in Figure 15. Two sets of controls were investigated – PBS transfected and Opti-MEM® media only. No difference in the XIAP levels between the two controls was seen at either dose level (data not shown). Results are therefore shown relative to the PBS control as this is the solvent used for the AS and MS drugs. At the dose of 400nM a down regulation of 33 ± 8% ($p<0.02$, t-test) was seen in the AS treated cells relative to the PBS control with no change seen in the MS. At a dose of 1200nM a down regulation of 67 ± 9% ($p<0.001$, t-test) was seen with the AS. However the MS caused a 35 ± 13% ($p<0.02$, t-test) decrease in XIAP levels at this concentration.

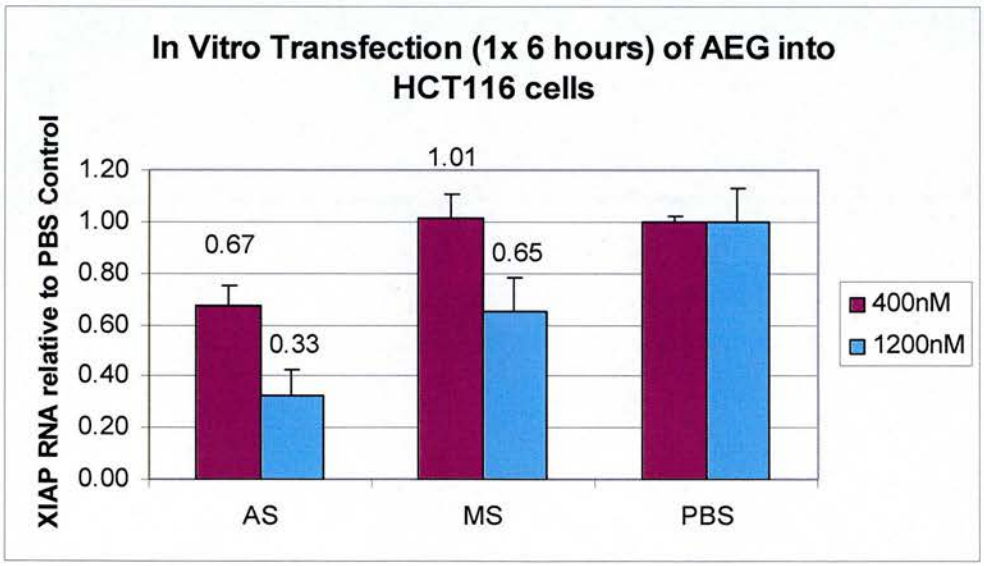

Figure 15: XIAP mRNA levels by qRT-PCR relative to the PBS transfected control at two concentrations (400nM and 1200nM) using the one day transfection protocol. Error bars represent standard deviation from the mean for three separate RNA extractions.

5.3.1.2 Cytotoxicity

To investigate whether this decrease in XIAP mRNA levels translated into cytotoxicity MTT and SRB assays were performed (Figure 16 and Figure 17)). There is no significant difference in either the ratio of cells fixed to the plate or the ratio of viable cells at increasing drug concentrations. In both assays there is cell death compared to the PBS transfected control in both the AS and MS treated groups. This implies that it is the phosphorothioate backbone which is present in both the AS and MS and not the down regulation of XIAP which is cytotoxic to the cells. In the MTT assay (Figure 16) maximal cytotoxicity is seen at a dose of 600nM whereas in the SRB assay (Figure 17) the maximum is seen at a dose of 400nM. This may potentially be explained by differences in the floating cell fraction. In the MTT method the active compound is added into the media of the tissue culture plate and all respiring cells produce formazan crystals which are then quantified. With the SRB assay the adherent cells are fixed onto the plate with trichloroacetic acid which precipitates proteins which are then stained for quantification. At a dose of 600nM there is a 20% difference in the ratio of cells (0.7 MTT and 0.5 SRB). Therefore it is possible that during these experiments detached cells are respiring. It is important to recognise that detached cells are not necessarily dead and in this case there is a fraction of 20% which are viable but not attached to the plate. If it is the toxicity of the phosphorothioate backbone which is causing the cells to detach, the floating cell fraction therefore needs to be assessed for XIAP status. The design of further experiments was therefore altered to avoid removal of detached cells.

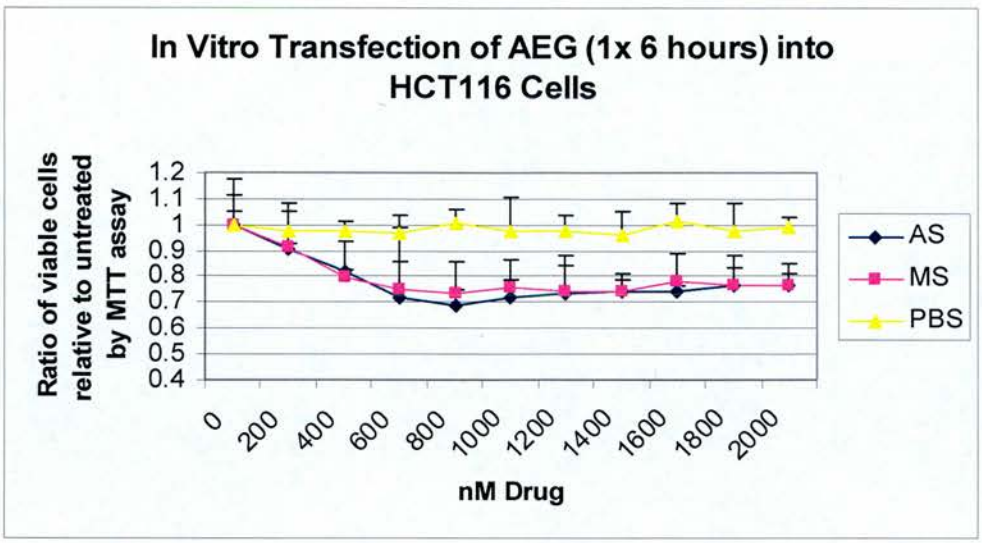

Figure 16: MTT cell viability assay at varying oligonucleotide concentrations using the one day transfection protocol. Error bars represent standard deviation from the mean for triplicate wells in the experiment.

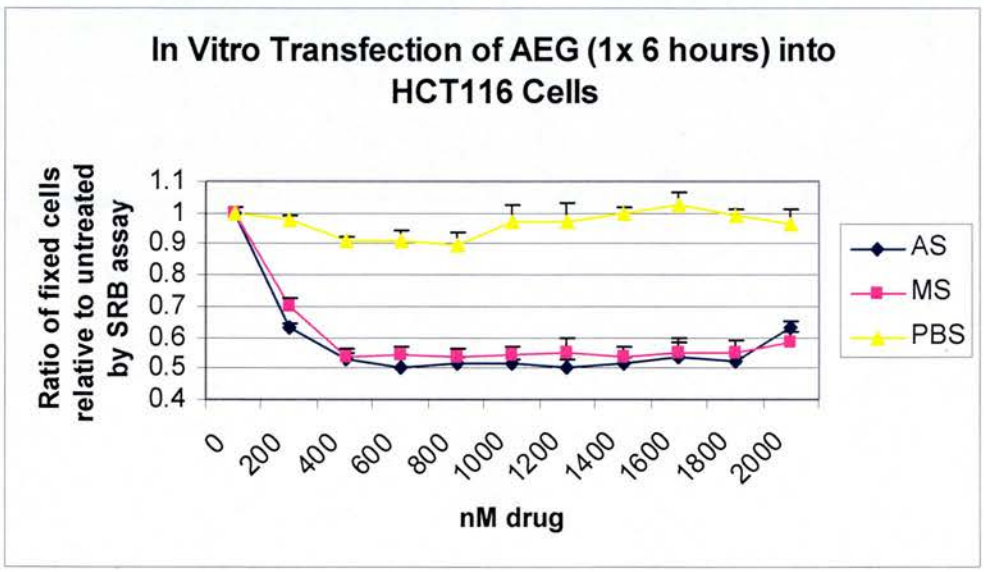

Figure 17: SRB cytotoxicity assay at varying oligonucleotide concentrations using the one day transfection protocol. Error bars represent standard deviation from the mean for triplicate wells in the experiment.

Cytotoxicity of the lower oligo doses (0 to 400nM) by SRB assay is shown in Figure 18. This was investigated as there was a suggestion that at lower doses (as seen in Figure 17 above) there may be a separation of the AS and MS lines. Two methods were employed – removing the media after 6 hours transfection then replacing with standard cell culture media (RPMI + 5% FCS) for 18 hours (dotted lines) or leaving the transfection mix in situ for 24 hours (solid lines). In both cases the media was removed after 24 hours in order to perform the SRB assay. When transfection was carried out for 24 hours, a dose-dependent cytotoxicity was observed, a maximal difference between MS and AS being obtained at the 200nM dose (survival fraction = 73 ± 4% for AS, $p<0.0002$ by t-test and 85 ± 3% for MS, $p<0.02$ by t-test). A shorter transfection (6 hours) led to a similar pattern of cytotoxicity: A maximal differential cytotoxicity between MS and AS was observed for a concentration of 200nM (survival fraction = 67 ± 4% for AS, $p<0.002$ by t-test and 81 ± 3% for MS, $p<0.05$ by t-test). Removal of the complexes at 6 hours compared to a 24 hour transfection does make a small difference in all 3 groups. The fact that the difference is most prominent in the PBS transfected group implies that long incubation of the transfection mix causes up to 10% increase in cytotoxicity to the cells and is not drug related. This method was therefore abandoned in favour of replacing the media after 6 hours.

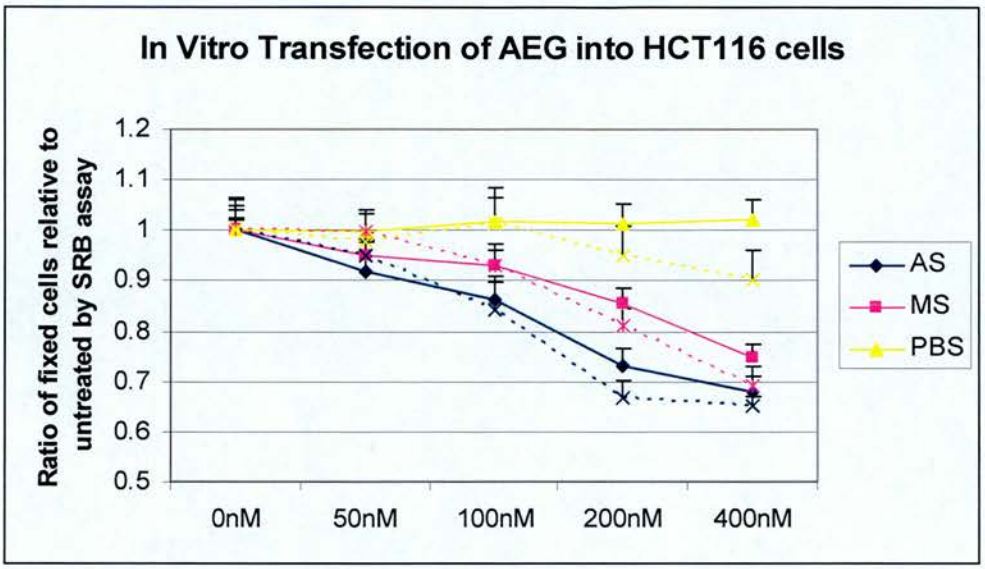

Figure 18: SRB cytotoxicity assay at varying oligonucleotide concentrations using the one day transfection protocol. Error bars represent standard deviation from the mean for triplicate wells in the experiment. Solid Lines represent transfection mix left on for 24 hours. Dotted Lines represent transfection mix removed after 6 hours and replaced with media.

5.3.2 Two Day Transfection Protocol

Using a single 6-hour transfection, a non-specific effect of the backbone of the oligonucleotide was observed at high doses (1200nM). At a lower oligo dose (400nM) this non-specific effect was not observed, however, the down regulation of XIAP was limited. Therefore, a second method was developed using a two day transfection protocol (two x 6 hours) after literature review (41).

5.3.2.1 XIAP down regulation

The pharmacodynamic effect of AEG35156 was assessed by qRT-PCR using the two day transfection protocol described above. At the 100nM concentration, relative to the PBS transfected control, a 72 ± 3% ($p<0.004$, t-test) down regulation of XIAP was seen for the antisense group and 44 ± 8% ($p<0.005$, t-test) for the missense group at the mRNA level (Figure 19). At the 400nM concentration an 81 ± 4% ($p<0.04$, t-test) down regulation of XIAP was seen for the antisense group and 69 ± 5% ($p<0.09$, t-test) for the missense group. These results imply that there is a significant non-specific effect of the missense for both doses using this transfection protocol. This protocol does achieve a level of XIAP down regulation consistent with the stable knockdown clones described in Chapter 7.

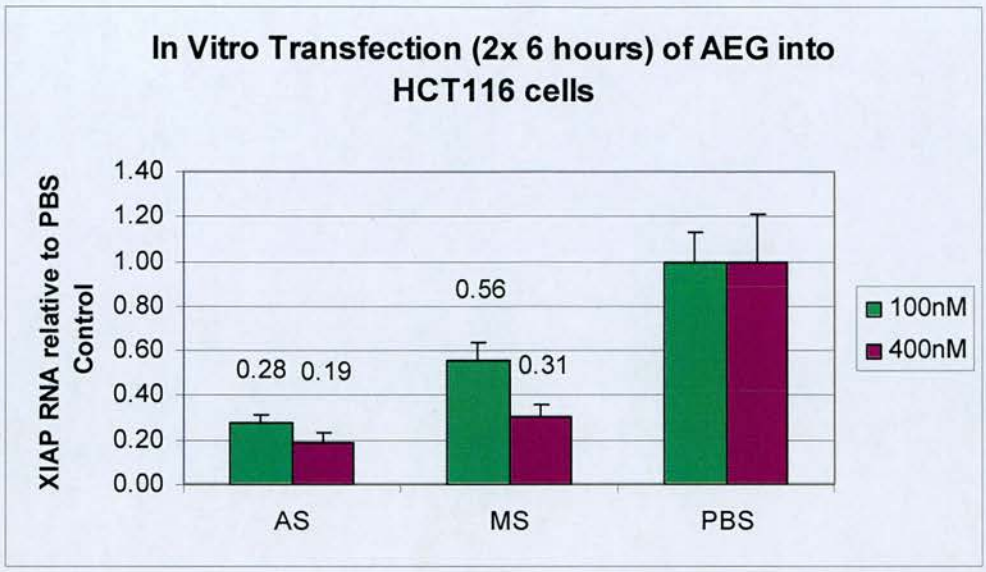

Figure 19: XIAP mRNA levels by qRT-PCR relative to the PBS transfected control at two doses (100nM and 400nM) using the two day transfection protocol. Error bars represent standard deviation from the mean for three separate RNA extractions.

5.3.2.2 Cytotoxicity

In order to ascertain whether this level of knockdown conferred cytotoxicity to colorectal cancer cells experiments were performed between 0 to 400nM of the AEG compounds (Figure 20). At a dose of 100nM 38 ± 7% of cells were alive in the AS group and 53 ± 7% in the MS group. At a dose of 400nM 15 ± 2% of cells were alive in the AS group and 24 ± 4% in the MS group. Therefore the transient transfection of AEG 35156 (XIAP antisense) does cause cell death in a dose dependent manner using this protocol however the missense control (AEG 35187) also results in a similar effect. This highlights the need for adequate controls when performing these experiments.

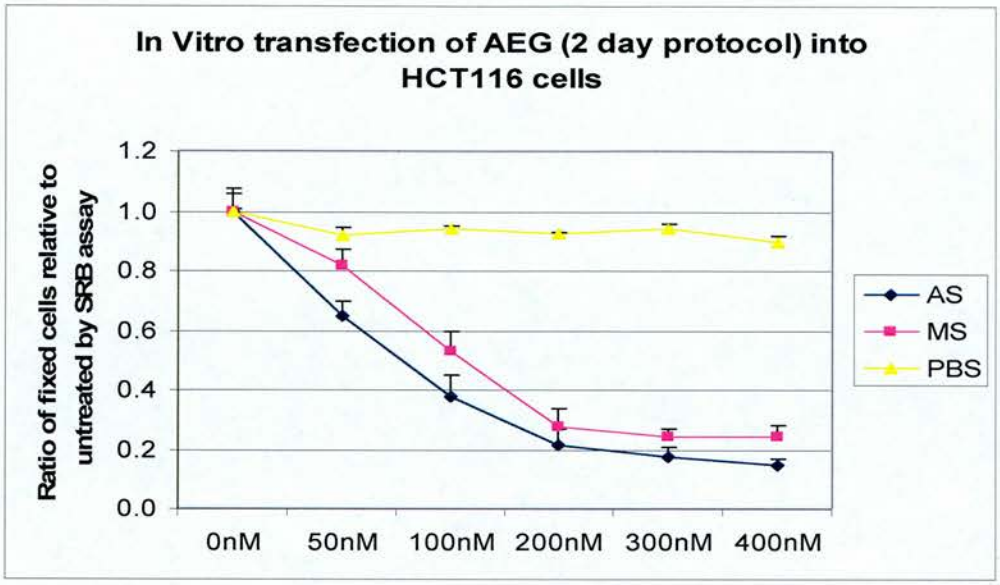

Figure 20: SRB cytotoxicity assay at varying concentrations using the two day transfection protocol. Error bars represent standard deviation from the mean for triplicate wells in the experiment. The IC50 dose of 100nM was chosen in order to maximise the effect between the MS and AS whilst still achieving XIAP down regulation.

5.3.2.3 Growth Curves

The growth pattern following XIAP down regulation is described in Figure 21 using a 100nM two day transfection. As described previously (Figure 19) 72% and 44% knock down were identified in the AS and MS groups, respectively. The adherent and floating cell fractions were harvested from 6 well plates and reseeded in 96 well trays prior to performing the SRB assay at daily time points. The AS and MS treated groups were unable to reattach to a tissue culture plate in contrast to the PBS transfected cells.

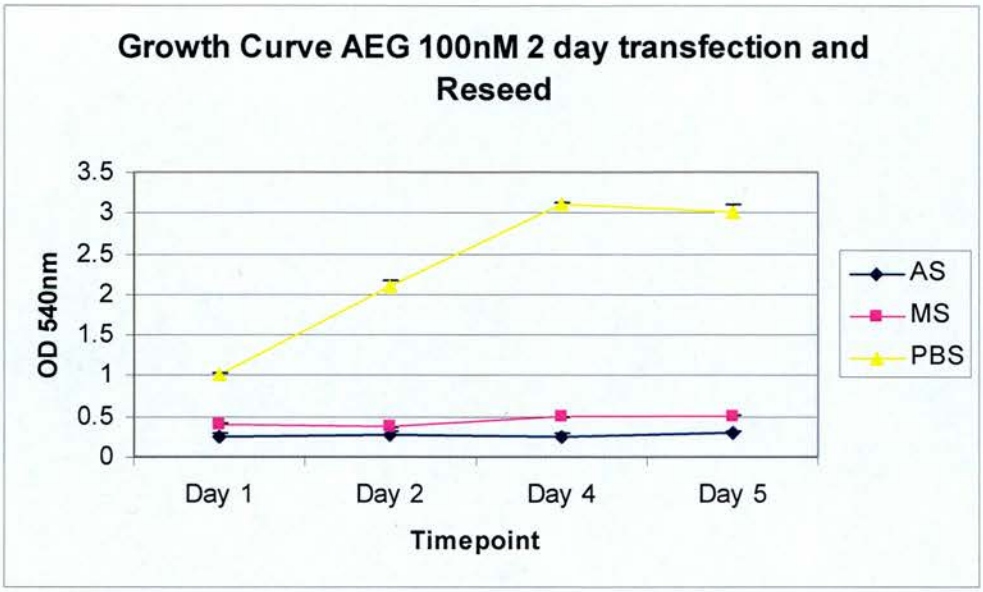

Figure 21: Growth curve by SRB assay for an identical number of cells re-seeded in a 96 well plate following the two day transfection protocol (concentration 100nM). Error bars represent standard deviation from the mean for triplicate wells in the experiment.

5.3.3 Comparison of two protocols

The results previously described in Figure 15 and Figure 19 are summarised in Figure 22 where the two transfection protocols are compared at the same dose of 400nM. The two day protocol achieves a higher XIAP knockdown (81% compared to 33%) with antisense but there is a substantial decrease in XIAP (69%) in the missense group with the two day protocol. The remainder of the experiments were therefore conducted using the one day protocol at the 400nM concentration in order to minimise the non-specific effect of the missense oligonucleotide. These conditions have shown cell cytotoxicity by SRB assay.

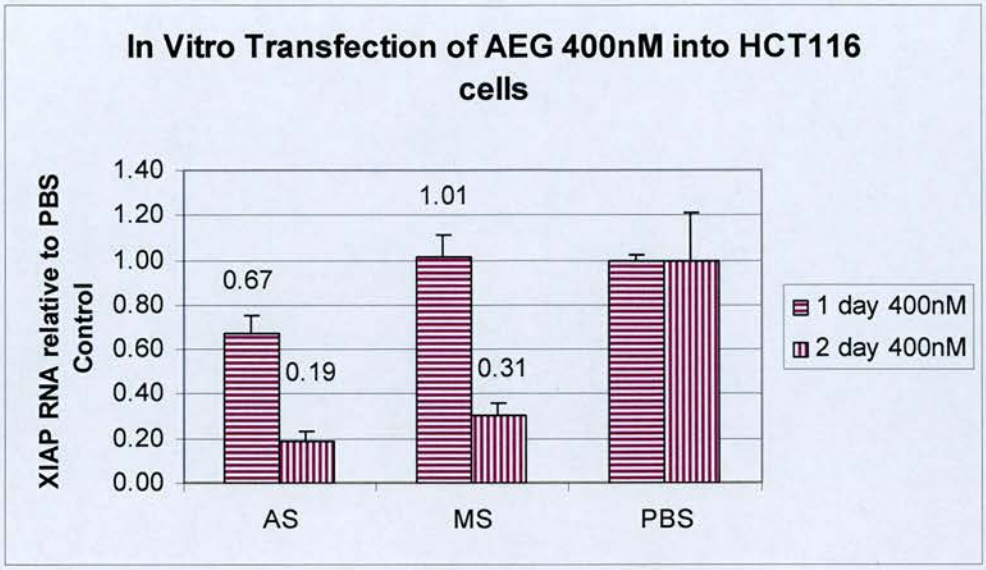

Figure 22: Comparison of XIAP mRNA levels by qRT-PCR relative to the PBS transfected control after one and two day transfection protocols at 400nM concentration. Error bars represent standard deviation from the mean for three separate RNA extractions.

5.3.4 TRAIL Treatment

The next series of experiments focussed on caspase 3 activity as a marker of activation of the apoptotic pathway. TRAIL was added to stimulate the pathway and to assess whether XIAP knockdown sensitised to this known cytotoxic agent. The caspase 3 assay relies on cells which are fixed to the plate and, as shown above (Figure 17), both the AS and MS treated groups detach from the cell surface therefore an SRB assay was performed simultaneously and the results expressed per unit OD value.

Comparison of the caspase activity in Figure 23 in the transfection only group (blue bars) shows a doubling of activity between the control (PBS 460 +/- 60) and both the AS and MS treated cells (AS 980 +/- 120, MS 900 +/- 70). It should be noted that there is 33% down regulation of XIAP in the antisense group only using this

protocol. These data add weight to the argument that it is non-specific backbone effect of the drug which is causing death, and here we confirm that the mechanism of that cell death is by apoptosis.

Figure 23 also shows the caspase 3/7 activity per cell after TRAIL treatment to directly stimulate the extrinsic apoptotic pathway following transfection of AEG compounds (yellow bars). Although the antisense + TRAIL had a 3 fold increase in caspase activity when compared to PBS (1620 ± 70 for PBS + TRAIL and 5270 ± 740 for AS + TRAIL, respectively), the missense + TRAIL showed a 2.5 fold increase (4120 ± 470), suggesting that the presence of an oligonucleotide rather than down regulation of XIAP was responsible for this effect. The effect of TRAIL alone (red bars) was similar across the 3 groups (PBS 1670 ± 70, AS 1660 ± 50, MS 1590 ± 100) which confirmed robust experimental technique.

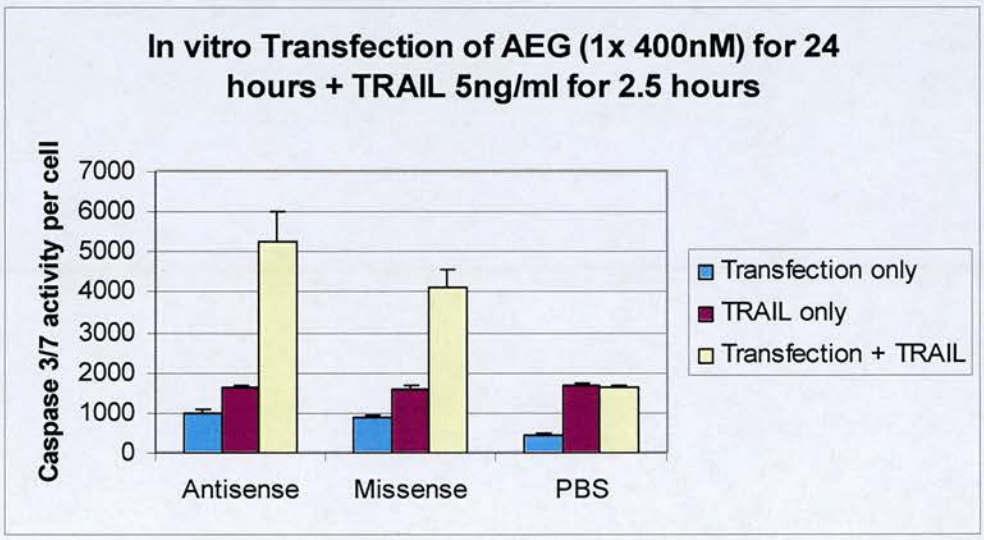

Figure 23: SRB and Caspase 3/7 assays performed in tandem to allow expression of caspase 3/7 activity per cell present. One day transfection protocol using 400nM concentration, the cells were then treated with 5ng/ml TRAIL and assays performed. Error bars represent standard deviation from the mean for triplicate wells in the experiment.

5.4 Discussion

Hu *et al* (133) describe a method of a single 6 hour transfection with assessment of pharmacodynamic effect at 24 hours at the protein level, this gives a maximum reduction in XIAP levels of 62% at a dose of 1200nM. This study focused on a library of first generation chemistry antisense oligonucleotides and subsequently second generation technology has led to the design of a phosphorothioate backbone (107). The second generation chemistry of the AEG compounds has improved *in vivo* pharmacokinetics and therefore the two cannot be directly compared and may explain the differences in results. These experiments were performed in a different cancer cell line and therefore the technique is likely to require some modification for use in a colorectal cancer model but it does provide a valuable starting point. The results presented here assess pharmacodynamic effect at the mRNA level but this is likely to be greater than that achieved at the protein level and therefore we have not been able to achieve an adequate degree of down regulation in the antisense group without significant non specific effects seen with the missense group.

McManus *et al* (41) describe a two day transfection technique in pancreatic cancer cells using the same second generation antisense AEG35156 as in the experiments described here. A 72% down regulation is seen in our studies at the mRNA level in the colorectal cell line compared to a 70% reduction seen by McManus *et al* at the protein level. The correlation between RNA and protein is similar to that seen in the stable shRNA expressing knockdown clones generated in Chapter 7 (87% and 67% for the X23 cell line). The concentration of 100nM of oligonucleotide used here was identical to the studies by McManus although reductions of XIAP protein were not seen in the missense group. Again, this was a different cell line but the non-specific effect was seen at the RNA level.

McManus *et al* were also able to identify sensitisation to TRAIL after down regulation of XIAP. From their data the approximate TRAIL doses required for 50% survival of Panc-1 cells were 0.1ng/ml for AEG35156 and 10ng/ml for AEG35187 transfected cells. This data was not replicated in the colorectal HCT116 cell line, where only 2-fold sensitisation was seen, due to non-specific sensitisation with the MS.

5.5 Conclusion

In conclusion a transient transfection method was developed which achieved 81% down regulation of XIAP mRNA using the AEG35156 compound. However, if this method was used, down regulation of XIAP mRNA was also seen with the missense AEG35187 compound. In order to achieve specific down regulation of XIAP only with the antisense (and not missense) a one day transfection at 400nM should be performed however the knockdown seen in this case is only 33%.

Cytotoxicity experiments show no significant therapeutic benefit of antisense over missense; both show a maximal cytotoxic effect of approximately 50% above doses of 400nM (one day protocol) and approximately 80% at doses above 200nM (two day protocol). Investigation of stimulation of the extrinsic apoptotic pathway with TRAIL following 33% XIAP down regulation does not confer a significant increase in apoptosis when compared to the missense control.

Combination studies with other recognised cytotoxics are unlikely to be effective with this level of selective down regulation of XIAP mRNA. Therefore a stable siRNA model of XIAP knockdown was developed and will be further described in Chapter 7.

Chapter 6

AEG35156 *In Vivo* Mouse Model

6 AEG35156 *In Vivo* Mouse Model

6.1 Introduction

The *in vitro* antisense studies described in Chapter 5 failed to show a specific effect of AEG35156 when compared to its missense control (AEG35187). However LaCasse *et al* have shown a 60% reduction in tumour volume *in vivo* for LS174T human colon xenografts treated with XIAP AS 25mg/kg/day when compared to a saline control. The antisense was also shown to be effective as a single agent *in vivo* in PC-3 prostate xenografts and in combination with docetaxel in H460 lung xenografts therefore the compound has been taken into Phase 1 clinical trial (40). In the same publication (40) dose dependent XIAP down regulation could not be demonstrated at the mRNA level when H460 and PC-3 cells were treated with XIAP AS *in vitro* compared to the nonsense control AEG35185; the data were not shown for LS174T *in vitro*.

Therefore, inconsistency exists between *in vitro* and *in vivo* data and a set of experiments were performed in an *in vivo* mouse model as an example of a physiological system. In this chapter two studies are described; first the anti-tumour effect and toxicity of the AEG compounds. Secondly, following demonstration of an anti-tumour effect a pharmacokinetic (PK) and pharmacodynamic (PD) study was undertaken to assess the extent of knockdown in the model system.

6.2 Methods

6.2.1 Anti- tumour effect

The study was performed by staff in the CRUK Biomedical Research Facility and supervised by Dr S Guichard. Her expertise is acknowledged and the results presented here with her permission. Animals were randomised into 3 groups: control, AEG35156 and AEG35187. Ten animals were used in the control group, 5 in each of the treated groups. Animals were treated by intraperitoneal injection of AEG35156 (XIAP AS) or AEG35187 (XIAP MS) at a dose of 25 mg/kg/d dx5 for 3 consecutive weeks, formulated in PBS. Control animals received vehicle (PBS) only. Tumour measurements and body weight were determined 3 times a week from start of treatment. Toxicity was assessed by body weight loss (weight measured 3 times per week) from the start of treatment to the recovery of the initial body weight. Efficacy was determined using the time to reach 5 times the initial tumour volume (Td5Vo). Statistical analysis was by comparison of Kaplan-Meier curves using a Log-Rank test.

6.2.2 Pharmacodynamic effect

This study was designed to incorporate pharmacokinetic and pharmacodynamic analyses. An HPLC based assay was being developed for another project in the PDDG relating to Bcl-xl AS and it was intended to adapt this assay for use with XIAP antisense. Unfortunately, difficulties related to the extraction of AS from biological matrices could not be overcome and therefore PD data alone will be presented here. The aim was to quantify the uptake of XIAP AS, the differential extent of XIAP knockdown and define the time course of both tissue retention and knockdown in mouse liver and human HCT116 xenograft tissue. The antisense oligonucleotide sequence remains under copyright and therefore has not been disclosed, but it should be noted that there is a 3 base pair mismatch between the mRNA sequence of mouse and human XIAP in the target region.

Data are presented for both the human tumour HCT116 xenografts and mouse liver XIAP mRNA levels. 24 hours after the completion of one, two or three weeks of treatment (days 6, 13 and 20 respectively) tissue was collected to establish whether the effect of XIAP antisense is cumulative. RNA was also extracted at 24, 72 and 168 hours (days 13, 15 and 19 respectively) after two weeks of treatment to assess the time point at which maximal XIAP down regulation occurs in order to aid schedule design of any potential combination studies with cytotoxic agents. The experiment was originally designed to extract the RNA at time points after a total of 3 weeks treatment but the xenografts were growing faster than anticipated and therefore the design was altered. This is discussed further below and the study plan is summarised in Figure 24.

The technique of RNA collection from *in vivo* samples was standardised to minimise the degradation of the RNA prior to qRTPCR analysis. From each animal the right flank tumour was trimmed to minimise any contaminating mouse tissue, snap frozen and stored at -70°C. The liver samples were immediately placed in RNAlater® solution to prevent degradation then stored at -70°C. RNA extraction was performed with TRI reagent® and all samples were DNase treated as described in Chapter 3.

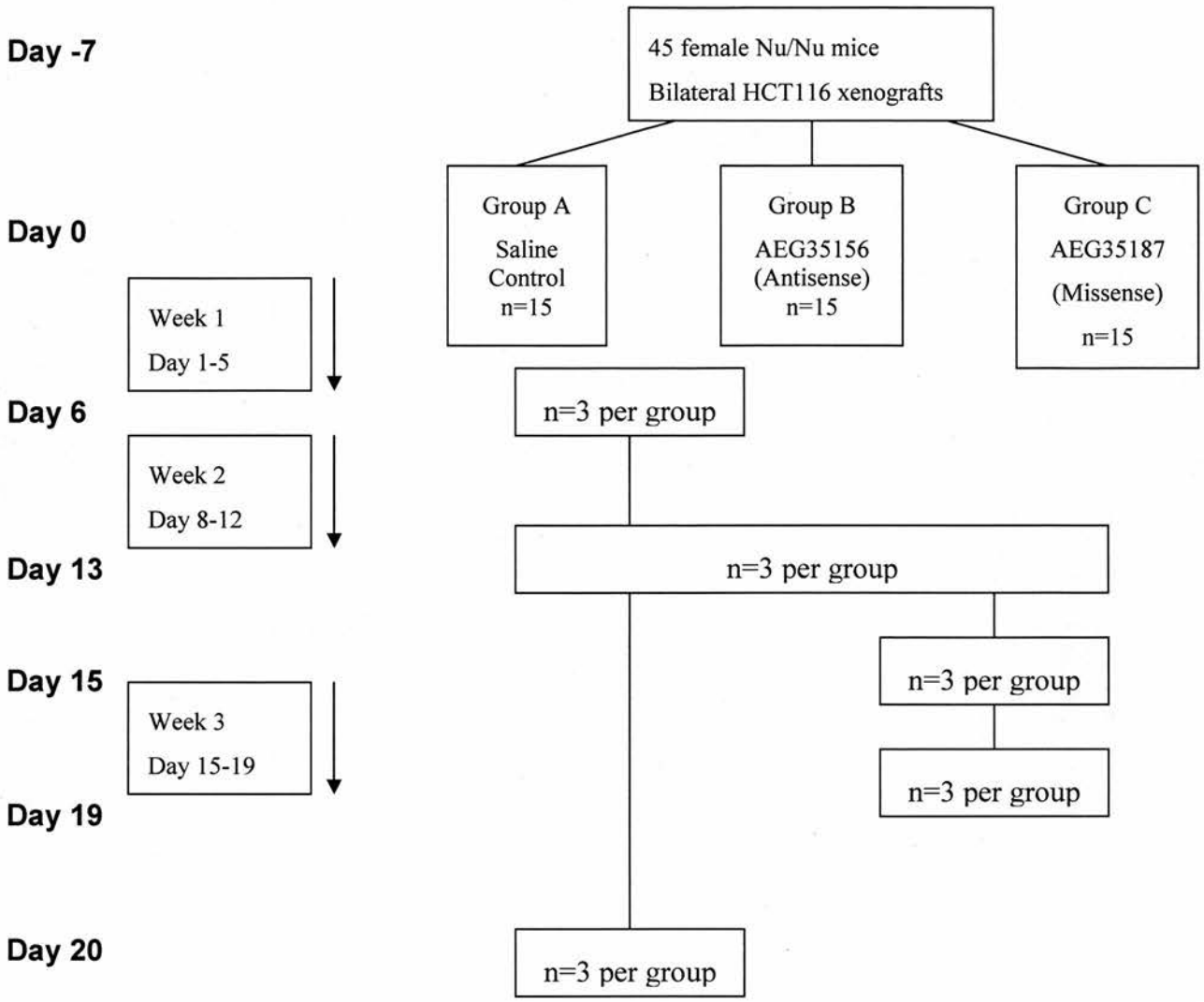

Figure 24: Schematic representation of the PK/PD study plan showing sample collection points and treatment times.

6.3 *Results*

6.3.1 Tumour growth before start of treatment

The tumour volumes for each group from 5 days before the start of treatment until the day of randomisation are presented in Figure 25. The average tumour volumes were consistent between each treatment group from day -5 to day 0.

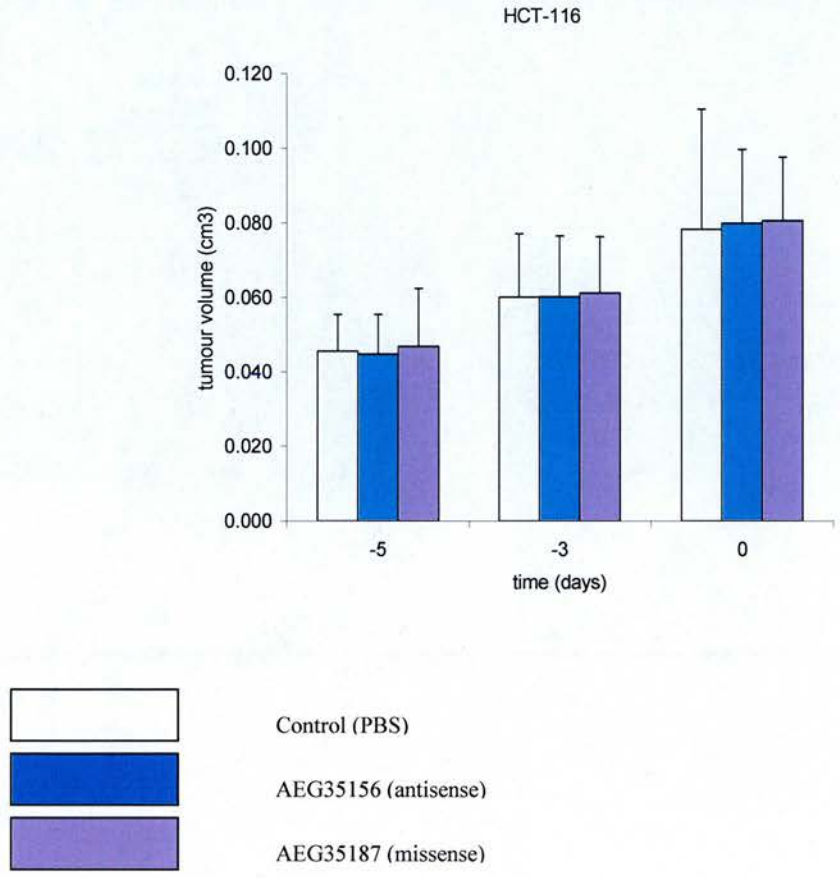

Figure 25: Tumour volumes from day –5 to day 0 before treatment. Tumour volumes are presented to show that on day 0 the randomisation did not generate any bias between groups.

The histogram of the tumour volumes for the HCT116 xenograft on day 0 is shown in Figure 26 which conforms to a gaussian distribution. Moreover, the tumour volumes all fell within the range specified for start of treatment: 50-150 mm^3. These parameters are important to assess prior to any *in vivo* study to prevent the introduction of bias when measuring xenograft growth response to drug treatments; if one group was larger to start with its growth rate would differ regardless of treatment given.

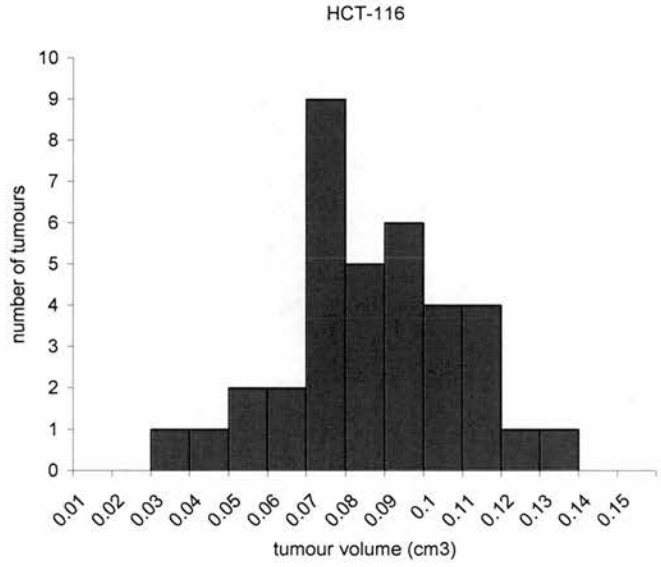

Figure 26: Histogram of tumour volumes on day 0 (randomisation) in the efficacy study.

6.3.2 Toxicity of AEG35156 and AEG35187

Toxicity was monitored by daily weighing of the animals and the mean percentage weight loss for the different groups of animals is presented in Figure 27. AEG35156 induced a significant weight loss at the dose of 25 mg/kg/d. This appears to be specific since no weight loss was observed in the animals treated with AEG35187 or the PBS treated control group.

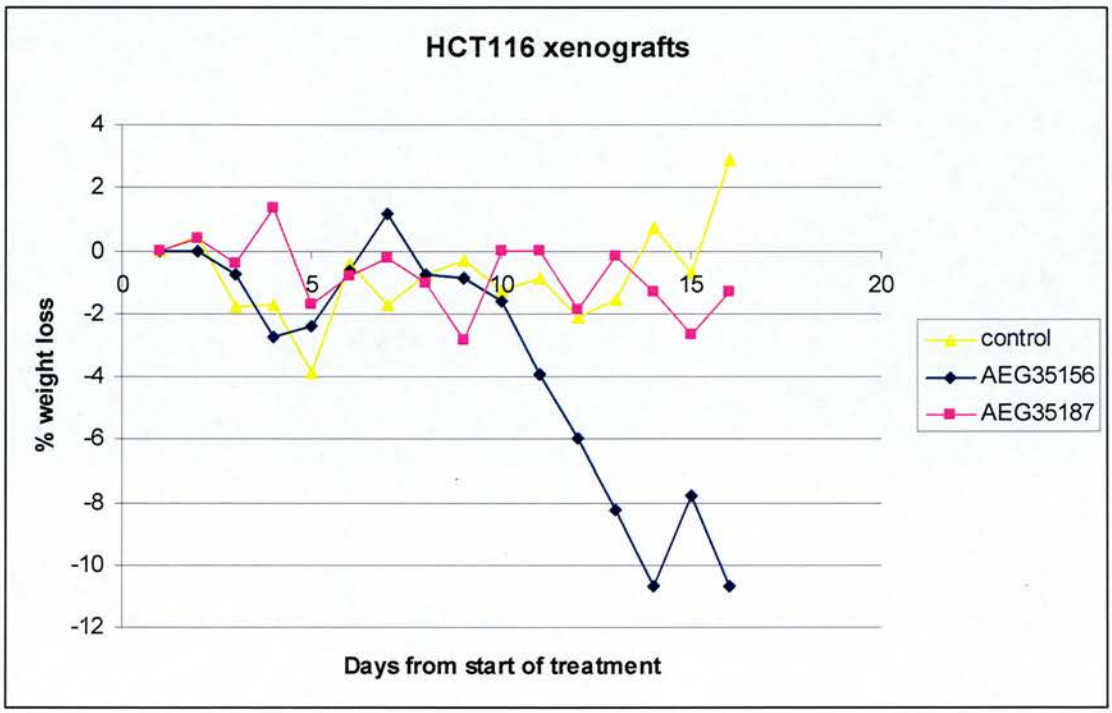

Figure 27: Body weight loss monitored from the first day of treatment to day 16 (treatment on day 0-4, 7-11, and 14-18). Data presented are average of 10 (control), and 5 animals (AEG35156 and AEG35187). As animals were culled due to tumour growth, the number of animals per group decreased to 3, 3, and 3 for control, AEG35156 and AEG35187, respectively.

When individual data were examined for each tumour, inter-individual variability was observed but the weight loss, when occurring, increased during treatment. Two cut-offs of 5 and 10% of body weight loss were used: Animals crossing these cut-offs at any one time during the experiment were considered positive. Table 5 summarises the data.

	> 5% BWL		>10% BWL	
	Control (PBS)	AEG35156	Control (PBS)	AEG35156
HCT116	3/10	5/5	1/10	3/5

Table 5: Body weight loss of animals bearing HCT116 xenografts when treated with AEG35156.

6.3.3 AEG35156 anti tumour effect

Tumour growth was recorded from start of treatment until tumours reached 5 times the initial volume ($5V_0$). Tumours were analysed individually despite being bilateral tumours in most cases. Results are presented as average tumour growth (Figure 28) or expressed as number of days to reach $5V_0$, presented in Figure 29 as Kaplan-Meier curves. Table 6 below summarises the average growth (V_t/V_0) for each xenograft.

Xenograft	Day	Group	Mean Growth on Day 11	SD	P value by t-test
HCT116	11	Control (PBS)	4.8	1.4	
		AEG35156	3.2	0.8	0.03
		AEG35187	4.6	0.6	0.8

Table 6: Mean growth of HCT116 xenografts following treatment with AEG compounds.

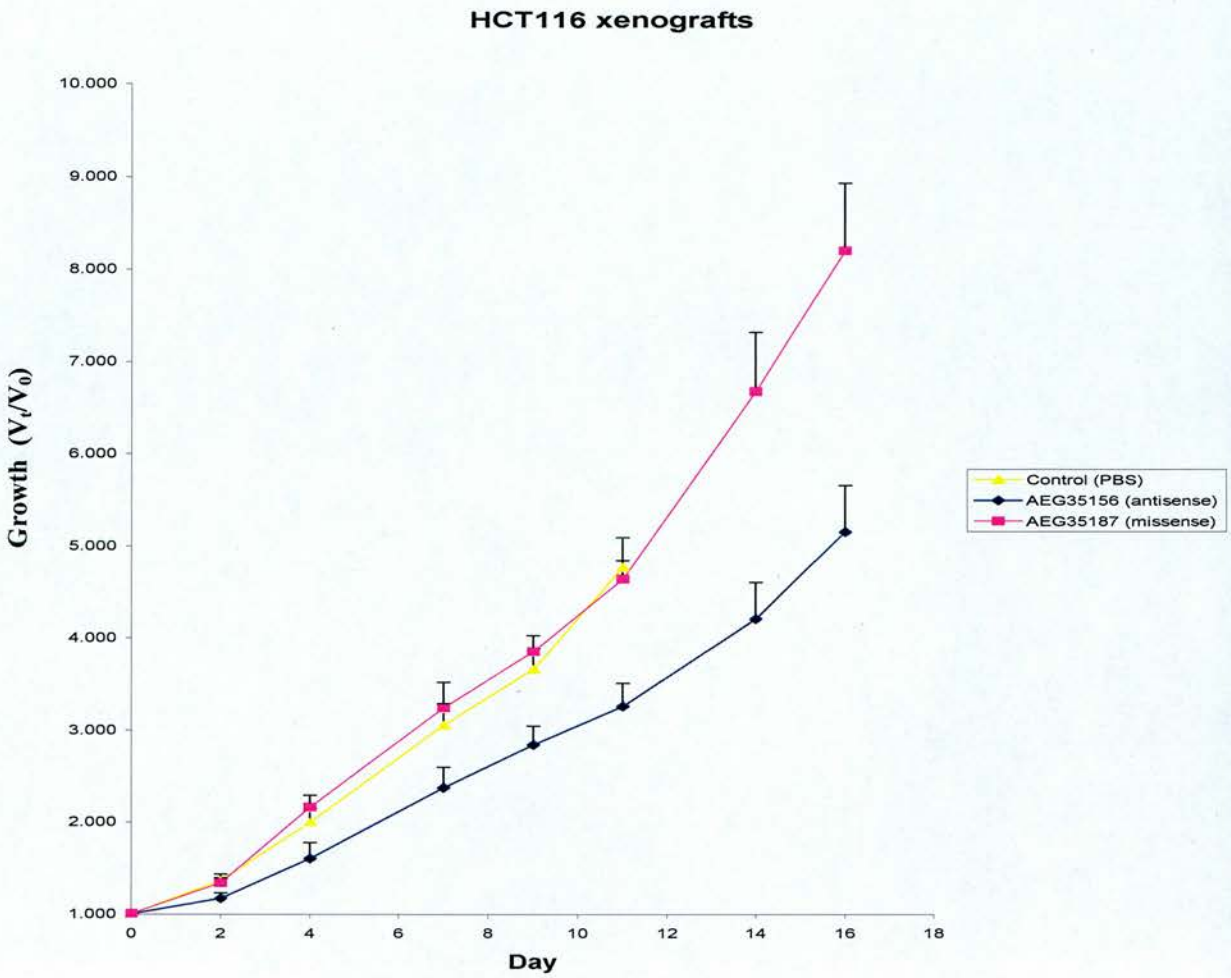

Figure 28: Growth of HCT116 xenografts after treatment with vehicle only, AEG35156 25mg/kg (dx5) x3 or AEG35187. Results presented are mean ± standard error of the mean.

Statistical analysis showed that AEG35156 induced a significant growth delay at day 11 in HCT116 xenografts as compared to control animals or animals treated with AEG35187 ($p=0.03$, t-test). The data were confirmed by Kaplan-Meier analysis (Figure 29) and clearly show a delay in tumour growth for HCT116 xenografts following treatment with AEG35156 ($p=0.02$, log rank test).

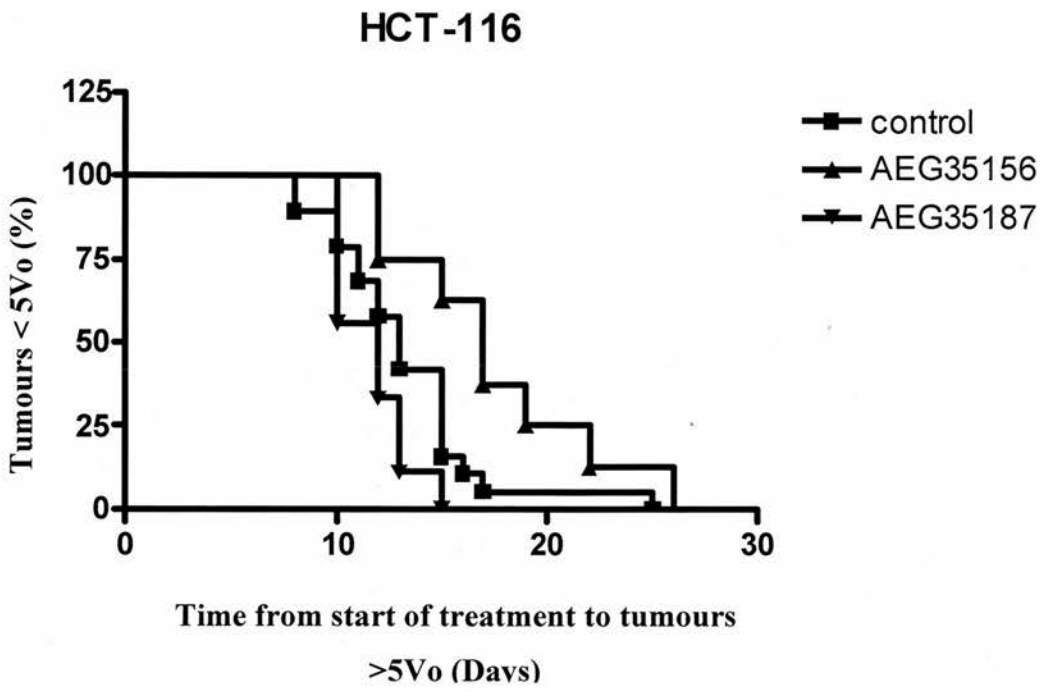

Figure 29: Antitumour effect of AEG35156 compared to control vehicle or missense oligonucleotide (AEG35187). Animals were treated with 25 mg/kg/day dx5 for 3 consecutive weeks.

6.3.4 Pharmacodynamic effect

The treatment times and sample collection points for the pharmacodynamic study are shown schematically in Figure 24. Using the technique described above, good quality RNA was obtained as confirmed by Agilent Bioanalyser 2100 and shown in Figure 30.

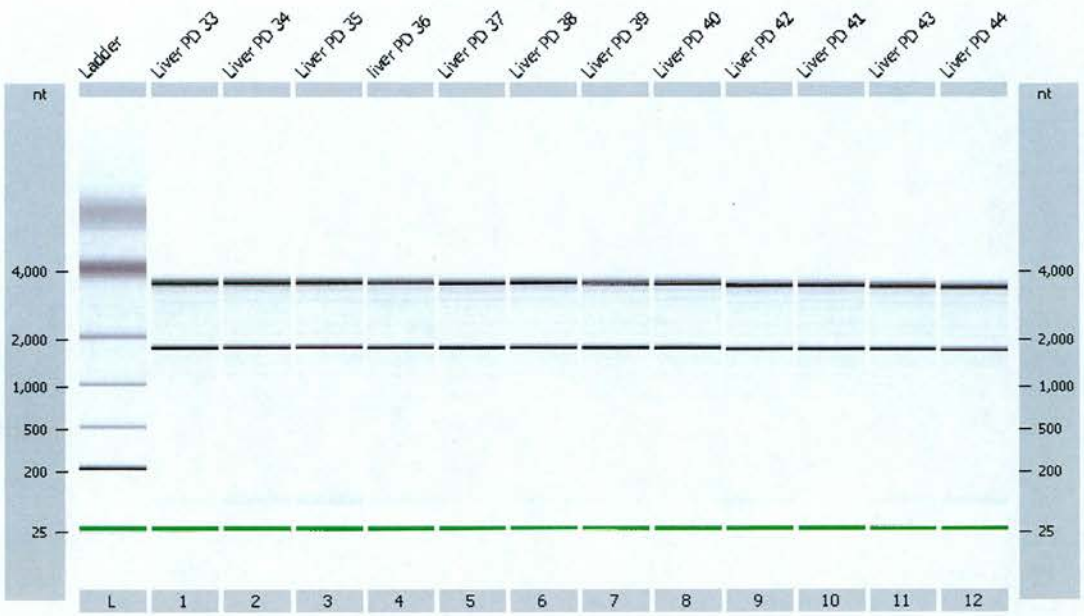

Figure 30: RNA extracted from mouse liver (PK/PD study) Agilent bioanalyser gel showing good quality RNA.

Although the primary aim of this study was to assess pharmacodynamic effect, the growth of the tumours was also recorded in an effort to confirm the results of the efficacy study described above. The tumour volumes prior to treatment in this study are shown in Figure 31 confirming no significant bias at randomisation of the groups of animals. However when the mean volume of tumours in the pharmacodynamic and efficacy studies were compared (Figure 25 and Figure 31), in the PD study the volumes were lower (0.044 – 0.051 compared to 0.078 – 0.081 cm^3).

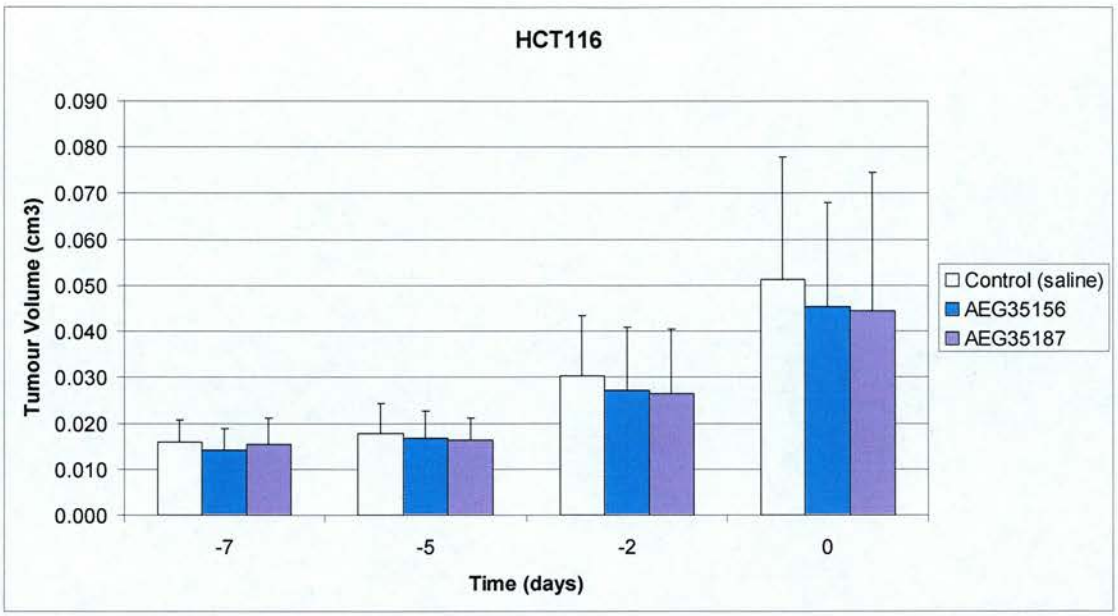

Figure 31: Tumour volume prior to treatment in PK/PD study. Error bars show standard deviation from the mean.

The mean growth of the HCT116 xenografts may be seen in Figure 32; there was no significant difference between the three groups. Differences in xenograft growth between the two studies may be noted (Figure 28 and Figure 32). For example, at day 9 in the control group, the V_t/V_0 was 3.7 in the efficacy study compared to 7.2 in the pharmacodynamic study. Therefore AEG35156 appears to be effective in the study with larger starting volumes and slower xenograft growth; further studies are necessary to confirm these data. In the efficacy study the control group was treated with phosphate buffered saline (PBS) whereas in the PK/PD study the control group was treated with saline as these were the respective vehicles used for the AEG compound dilution.

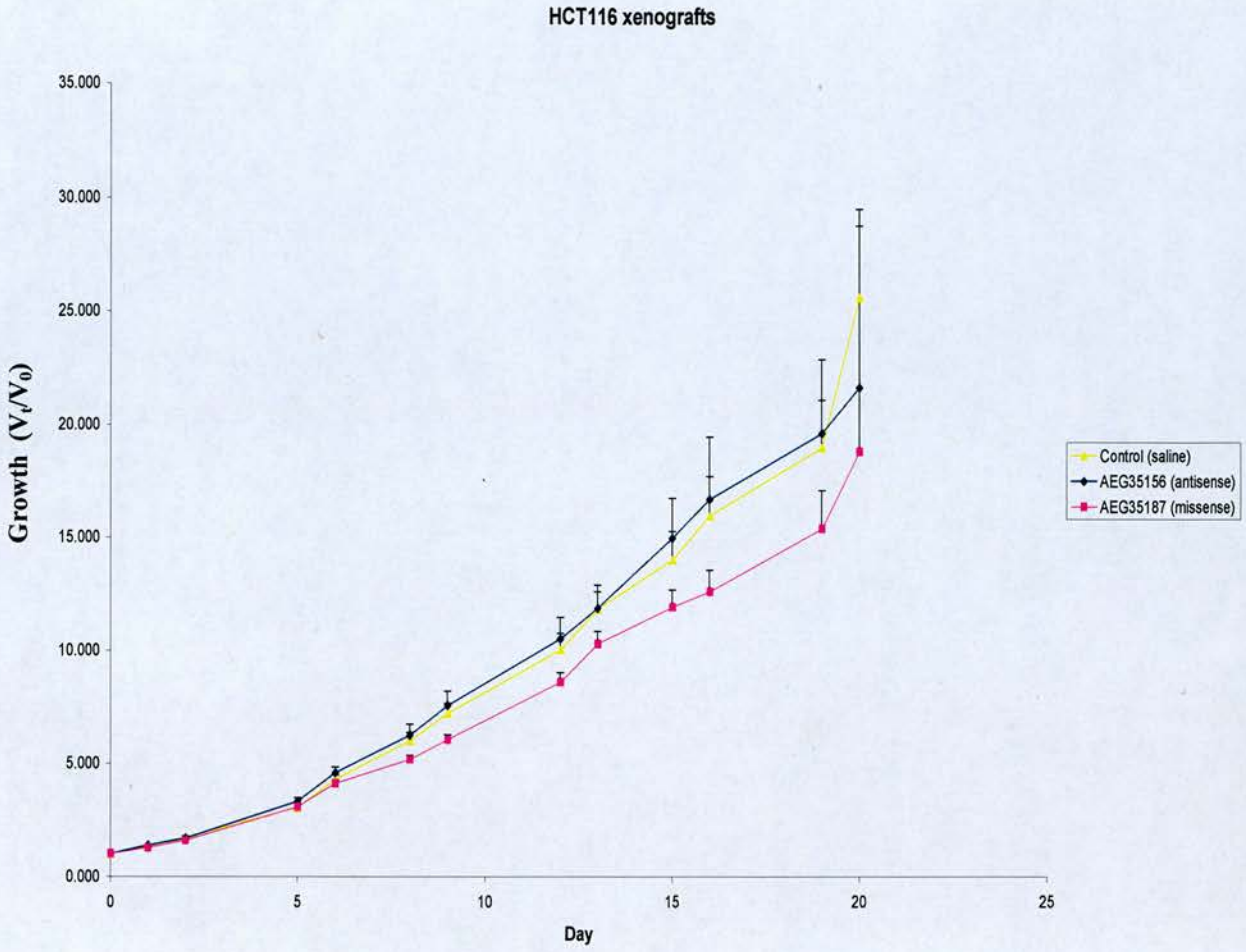

Figure 32: Growth of HCT116 xenografts in PK/PD study. Results show mean ± standard error of the mean.

HCT116 xenografts did not show significant XIAP mRNA knockdown at any time point at the dose 25mg/kg/dx5 in this model (Figure 33 and Figure 34). Also in this study AEG35156 did not slow tumour growth compared to the PBS and missense control groups. Establishing the drug levels in the tumour may have identified the cause for this, but as stated above, an assay was not available.

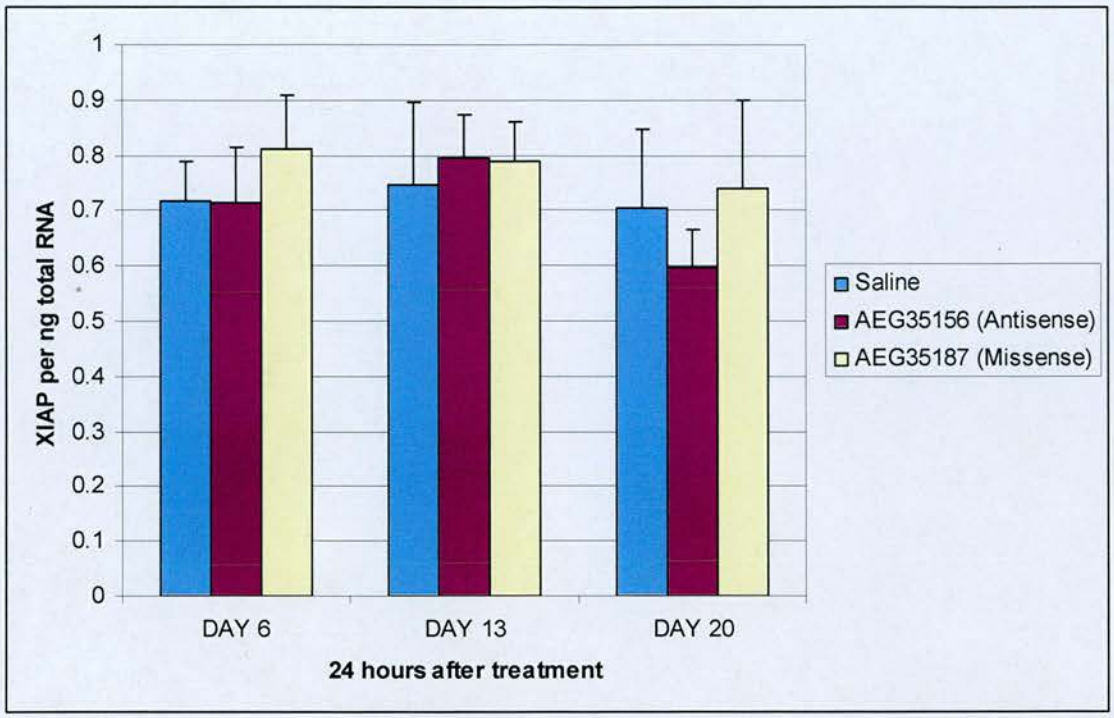

Figure 33: XIAP knockdown per ng of total RNA in xenograft. Error bars represent the standard deviation of the mean for 3 animals in the group.

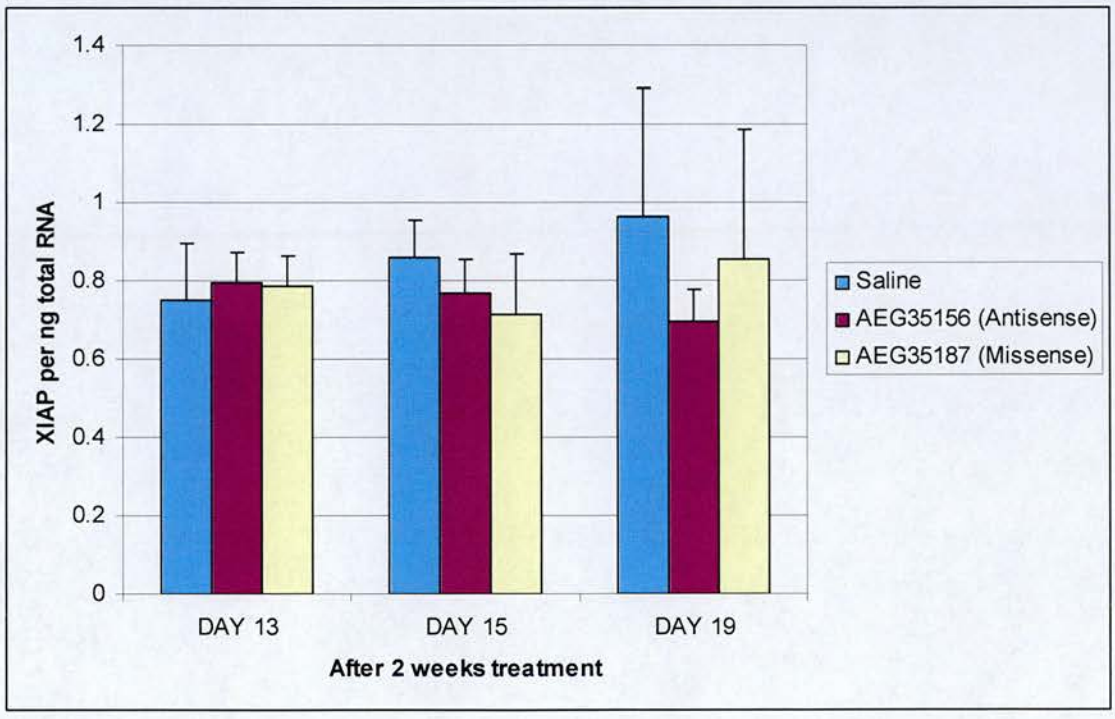

Figure 34: XIAP knockdown per ng of total RNA in xenograft. Error bars represent the standard deviation of the mean for 3 animals in the group.

The levels of XIAP in mouse liver 24 hours after the end of one, two or three weeks of treatment are shown in Figure 35. The percentage decrease in XIAP mRNA levels in the AS group compared to the MS group are Day 6 21%, Day 13 25% and Day 20 42%. At the day 20 time point (24hours after 3 weeks of dx5 treatment) this result reached statistical significance p=0.014 (t-test). These data suggest that the pharmacodynamic effect of AEG35156 was therefore cumulative over a period of three weeks. Previous experience suggests that AEG35156 has a long tissue half life of approximately 14 days (personal communication, Aegera Therapeutics Inc) which would be consistent with these results.

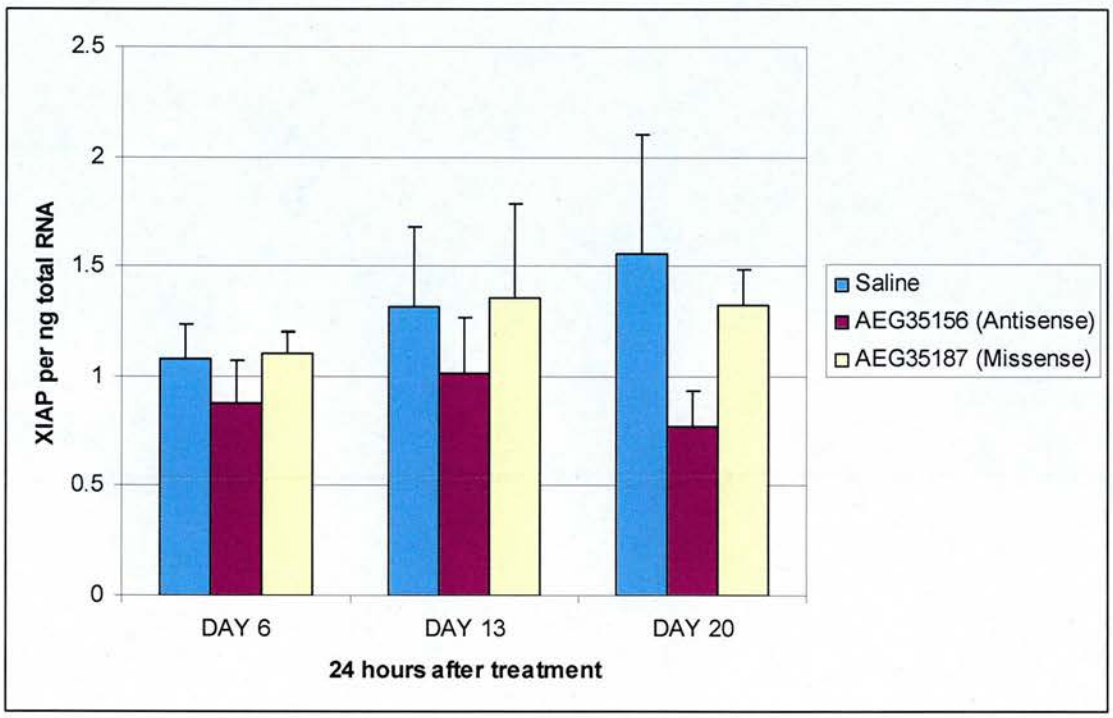

Figure 35: XIAP knockdown per ng of total RNA in mouse liver. Error bars represent the standard deviation of the mean for 3 animals in the group.

The levels of mouse liver XIAP mRNA 24, 72 and 168 hours after the end of two weeks treatment are presented in Figure 36. The percentage decrease in XIAP levels in the AS group compared to the MS group are Day 13 25%, Day 15 43% and Day 19 31%. At the day 15 time point (72 hours after 2 weeks of treatment) this result reaches statistical significance p=0.05 (t-test). Therefore the maximal XIAP mRNA down regulation occurred at 72 hours after treatment was completed.

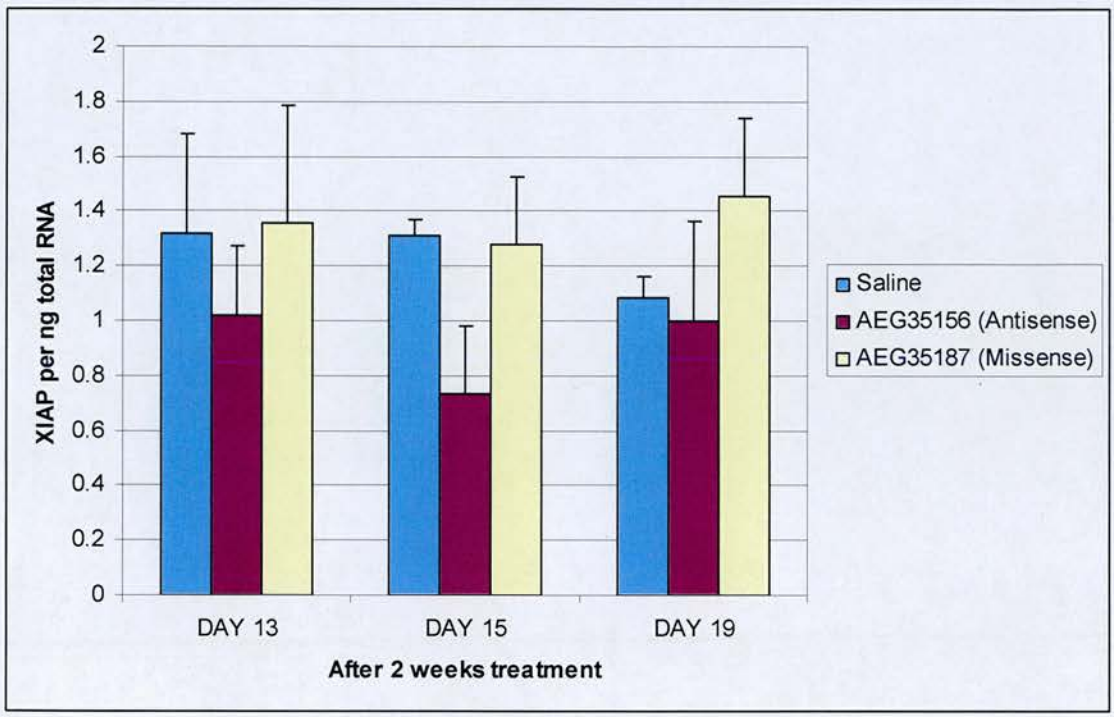

Figure 36: XIAP knockdown per ng of total RNA in mouse liver. Error bars represent the standard deviation of the mean for 3 animals in the group.

6.4 Discussion

The dose and schedule of the oligonucleotides (25mg/kg/day x5 for 3 weeks) by intraperitoneal injection was taken from the *in vivo* studies carried out in similar xenograft models; LaCasse *et al* described dose dependant efficacy of AEG35156 using this schedule in a LS174T colon cancer xenografts (40). Here we describe a reduction in mean V_t/V_0 from 4.6 ± 0.6 in the missense control group to 3.2 ± 0.8 in the antisense group. The efficacy study therefore provided encouraging data for XIAP antisense in an HCT116 colorectal cancer model and this schedule was repeated for the pharmacodynamic study.

The above results could not be confirmed in the pharmacodynamic study and the difference in starting volumes and growth rates between the two may explain some of the results. In this model, it may be necessary to start with larger volume tumours which have a slower growth rate in order for the AEG35156 to be effective. Alternatively further investigation of the optimal solvent for the AEG compounds – saline or PBS - may be helpful. The rationale for changing the protocol between the two studies was provided by the pre-clinical characterisation study (40) and the Phase 1 clinical trial (109) where saline was used as a vehicle for the oligonucleotides. The difficulty in reproducibility implies that further optimisation of this model is required. In retrospect during the initial efficacy study it would have been beneficial to extract RNA or protein from the xenografts to indicate whether XIAP down regulation had been achieved.

The toxicity of AEG35156 was assessed by monitoring the weight of the animals throughout the efficacy study and significant weight loss was seen. In this study it was found to be specific for AEG35156 whereas LaCasse *et al* describe weight loss in animals treated with AEG35191, an oligonucleotide with a four base mismatch, in addition to the antisense. The weight of the animals was seen to recover quickly on cessation of treatment (40).

In the pharmacodynamic study the choice of animal for cull at each time point was not random as the xenografts were growing too rapidly to complete treatment. Three weeks treatment was therefore given to the slowest growing xenografts. This will introduce bias into the results which should be interpreted with caution.

The tumour pharmacodynamic results were disappointing in that XIAP mRNA knock down was not demonstrated but perhaps not unexpected given the lack of efficacy in this experiment and may be a reflection of the model.

The pharmacodynamic results from liver samples extracted showed XIAP down regulation which was maximal 72 hours after the end of the infusion and is cumulative after 3 weeks of treatment. The maximal knock down seen was 43% in the liver which, although it is statistically significant, may not be clinically relevant as down regulation of 80% was seen in the clinical trial (109). It must be taken into account that AEG35156 is directed against human XIAP mRNA and there is a 3 base-pair mismatch with mouse XIAP (personal communication E. LaCasse). Despite this XIAP down regulation was seen in the antisense group relative to the missense group, suggesting particularly high concentrations in the liver. Supporting this, the preclinical toxicology studies with AEG35156 describe dose dependent accumulation of the oligonucleotides and its metabolites in the liver (113).

In the concurrent Phase 1 clinical trial (described in Chapter 2) the main toxicity observed was liver function abnormality (transaminitis) which was cumulative and reversible. Similar elevation of serum transaminases was the dose limiting toxicity in a Phase 1 trial of mixed backbone oligonucleotide targeting the regulatory subunit of protein kinase A (GEM231) (112). However, the exact nature of liver toxicity remains undefined. It is thought to be a class effect of antisense oligonucleotides which has been observed in other situations and was not related to the specific knockdown of the target (134).

Further investigation of the plasma liver function tests in our mouse studies would have assessed whether transaminitis was seen in these animals. Correlation with levels of XIAP knock down might then have provided further insight into the mechanism of hepatic dysfunction seen in the clinical trial. The development of a method of oligonucleotide quantitation in tissue by mass spectroscopy would also be useful to correlate with XIAP levels in both the antisense and missense groups and to assess the drug delivery to the xenograft.

6.5 Conclusion

AEG35156 (XIAP antisense) initially appeared to have a significant effect on tumour growth in HCT116 xenografts compared to the missense control AEG35187, however a subsequent study was unable to confirm this. Weight loss was observed in the antisense group which may correlate to toxicity in the animals.

Antisense directed against human XIAP caused target knock down in mouse liver despite a 3 base pair mismatch. Mouse liver XIAP down regulation of 43% appeared to be maximum 3 days after end of treatment and cumulative at 42%, 24 hours after 3 weeks of treatment.

Chapter 7

The Development of Stable XIAP Knock Down Cell Lines using shRNA

7 The Development of Stable XIAP Knock Down Cell Lines using shRNA

7.1 Introduction

The development of clonal derivatives of the HCT116 cell line which express either a short hairpin RNA against XIAP (X cell lines) or luciferase (L cell lines) is described in this Chapter. This approach was taken for two reasons; first to assess the longer term effects of stable down regulation of XIAP and second as an alternative method to complement the "antisense" approach which is currently in Phase I clinical trial. In addition, the difficulties of transient XIAP knockdown over a shorter time period as discussed in Chapter 5 and seen with siRNA (135) can be avoided, facilitating experiments with cytotoxic therapies over a period of 6 days. It is possible that down regulation of XIAP over an extended time period causes compensatory changes in a cell and therefore this was investigated further.

The genetic makeup of the clonal cell lines generated was compared at the RNA level using a microarray genechip. The four X cell lines (XIAP knockdown) were compared with the four L cell lines (luciferase expressing control) at 2 time points. HCT116 cell line RNA was also included in the microarray study in order to assess the changes between the parental cell line and luciferase expressing control (L lines) and validate the L lines as an acceptable control. Therefore three groups were studied; HCT116 (parental cell line), X (XIAP knockdown) and L (luciferase control). The early passage cells (p4) were investigated to assess the acute changes associated with XIAP down regulation and the late passage (p8) the sustained changes. Four genes were selected for validation by qRT-PCR to assess whether these data correlated with the changes seen on microarray, this would validate the techniques and preclude the need for multiple RT-PCR experiments.

With any new cell line it is necessary to characterise the growth pattern, plating characteristics and morphology to document any differences which need to be

anticipated in the experimental design. Experiments to document the activity of the apoptotic pathway are also relevant in this case to establish the effect of XIAP down regulation alone before combination with other cytotoxic agents are considered.

7.2 Genechip Microarray

7.2.1 Principles of Microarray

The principles of microarray are visually described in Figure 37 which is taken from the Affymetrix website (http://www.affymetrix.com). This technique is helpful in comparing the differences in gene expression between 2 sample groups. The sample RNA is labelled with a fluorescence emitting compound and gene expression can be quantified according to the intensity of the coloured light signal when complementary RNA (cRNA) binds to oligonucleotides on the genechip.

Synthetic DNA oligonucleotide probes of defined sequence interrogate the cRNA derived from the target sample. A number of probes are designed from unique regions at the 3' end of each transcript to give a set of probe pairs for each mRNA. The precise location of each probe is a feature, and millions of features can be contained on one array. By extracting and labelling nucleic acids from experimental samples, and then hybridizing those prepared samples to the array, the amount of label can be monitored at each feature.

Affymetrix GeneChipR Human Genome U133 Plus 2.0 Array analyses the expression of over 47,000 transcripts and variants including 38,500 human genes. There are 54,000 probe sets and 1,300,000 distinct oligonucleotides features.

A)

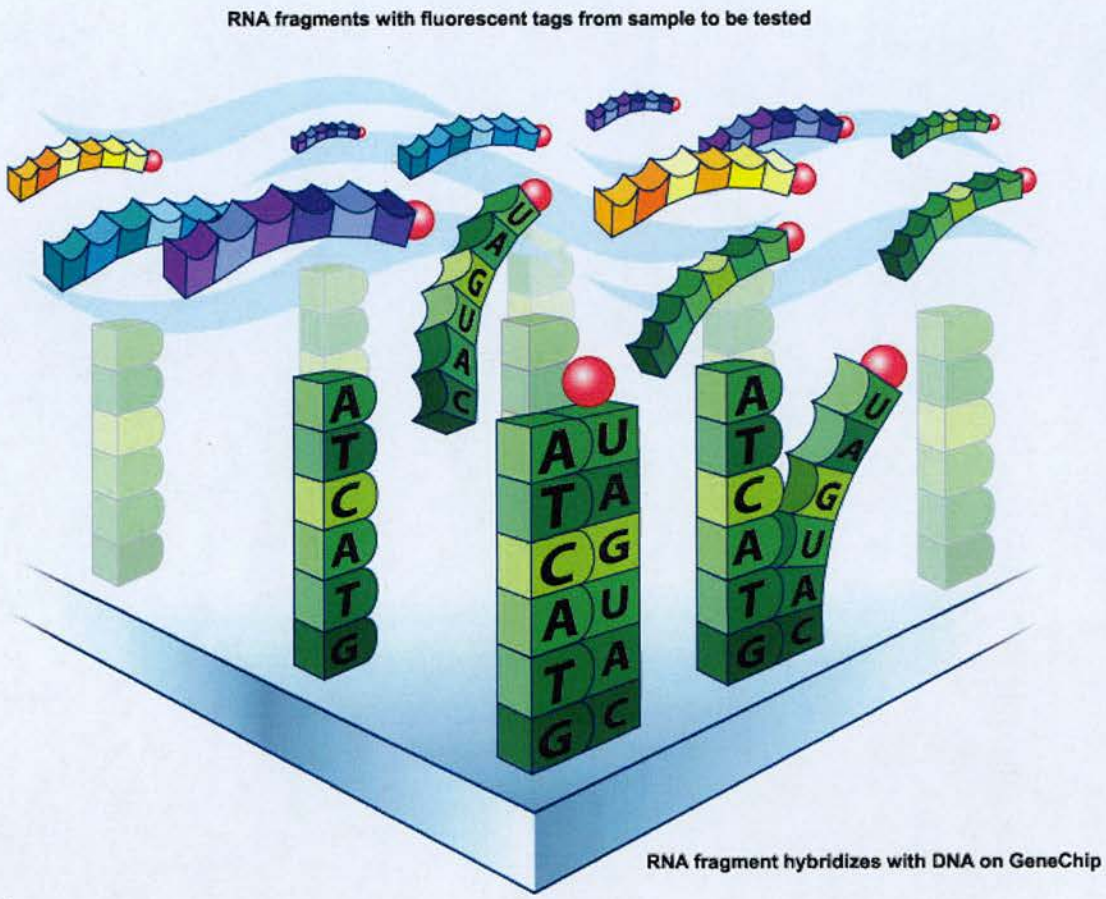

B)

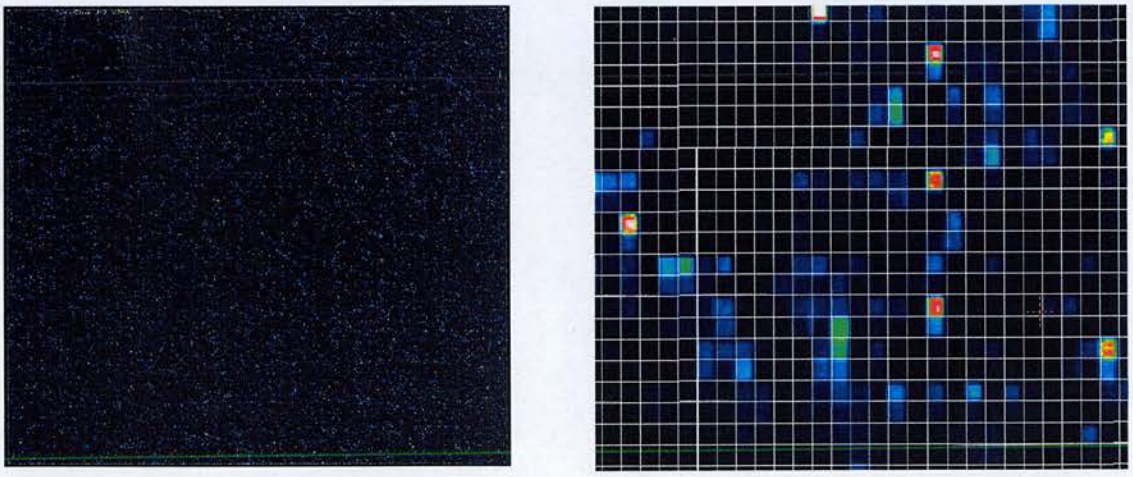

Figure 37: Pictures from Affymetrix website. A) Fluorescent labelled RNA from sample binds to complementary DNA fragment on GeneChip. B) Each feature (spot) is detected as red colour by the scanner when the RNA binds to it.

7.2.2 Probe Design

Oligonucleotide probes complementary to each corresponding sequence are synthesised in situ on the array. Eleven pairs of oligonucleotide probes are used to measure the level of transcription of each sequence represented on the GeneChip. The high density of microarrays affords the ability to use multiple probes for each expression measurement made. The use of multiple probes provides for high sensitivity and reproducibility. The probe set – a combination of twenty two 25mer probes – balances sensitivity and specificity, allowing for consistent discrimination between signal and background noise and accurate data sets.

Each probe pair consists of an oligonucleotide that is a perfect match (PM) and one that is a mismatch (MM) that has one base changed in the centre of the oligonucleotide sequence. This probe pairing strategy serves as a control for non-specific hybridisation allowing the software to calculate a signal intensity for each probe set and determine an absent, marginal or present result.

7.2.3 Quality Control

The scale factor is a value that the array intensity must be multiplied by to give the target intensity of 100. The signal intensity values of every probe set on the array are calculated, the highest and lowest 2% are removed and the remaining values are averaged to give the average array intensity. The scaling factor is then calculated as the value that adjusts the average array intensity to the set target intensity. This factor is then applied at the individual feature level not the average signal intensity level.

The background intensity, derived from the intensity values of the lowest 2% of cells on the chip, establishes an overall baseline intensity to be subtracted from all cells before gene expression levels are calculated. Noise is derived from the standard deviation of the background intensity measurement.

Spike controls are added to the total RNA sample in varying amounts. BioB is added at the lower limit of detection therefore, if there is too much noise present, low abundance transcripts and the BioB will not be detected. Hybridisation efficiency is only considered acceptable when the spike control genes are present in increasing intensity BioB<BioC<BioD<CreX.

7.2.4 Experimental Design

The microarray experimental design can be summarised in Figure 38 below.

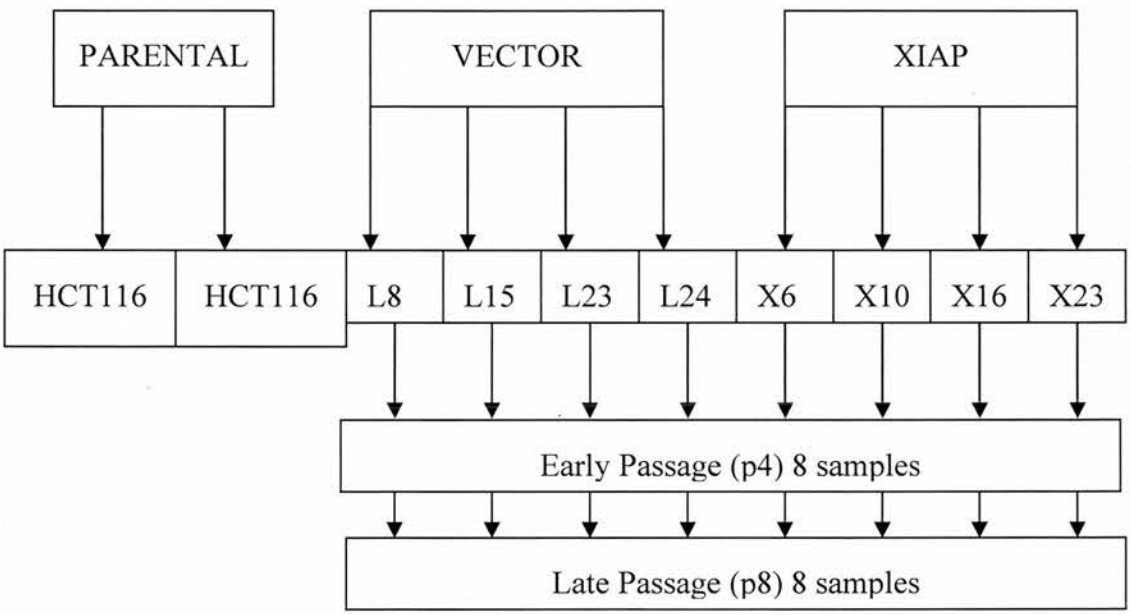

Figure 38: Schematic representation of the design of microarray experiment

7.3 Results

7.3.1 Isolation of the cell lines and confirmation of XIAP status

Twenty four geneticin-resistant clonal cell lines were isolated after transfection with shRNA expressing either XIAP (X clones) or luciferase (L clones). The levels of XIAP mRNA were determined by quantitative RT-PCR (Figure 39) and identified four X clones (X6, X10, X16 and X23) with low XIAP mRNA levels. Four L clones (L8, L15, L23 and L24) were selected with mean XIAP levels similar to the mean of the whole L group (11.6 ± 3.7). The mean XIAP mRNA level in the four selected vector control cell lines was 12.7 ± 1.1, and percentage knockdown was calculated relative to this. The knockdown clones show reductions of 93%, 82%, 83% and 87% in XIAP mRNA for X6, X10, X16 and X23 respectively relative to the mean of the XIAP levels in the four vector expressing L control group. The mean level of XIAP mRNA of four selected clones in the L group (12.7 ± 1.1) was not significantly different to the level in the parental cell line (15.3 ± 2.0, t-test p=0.07).

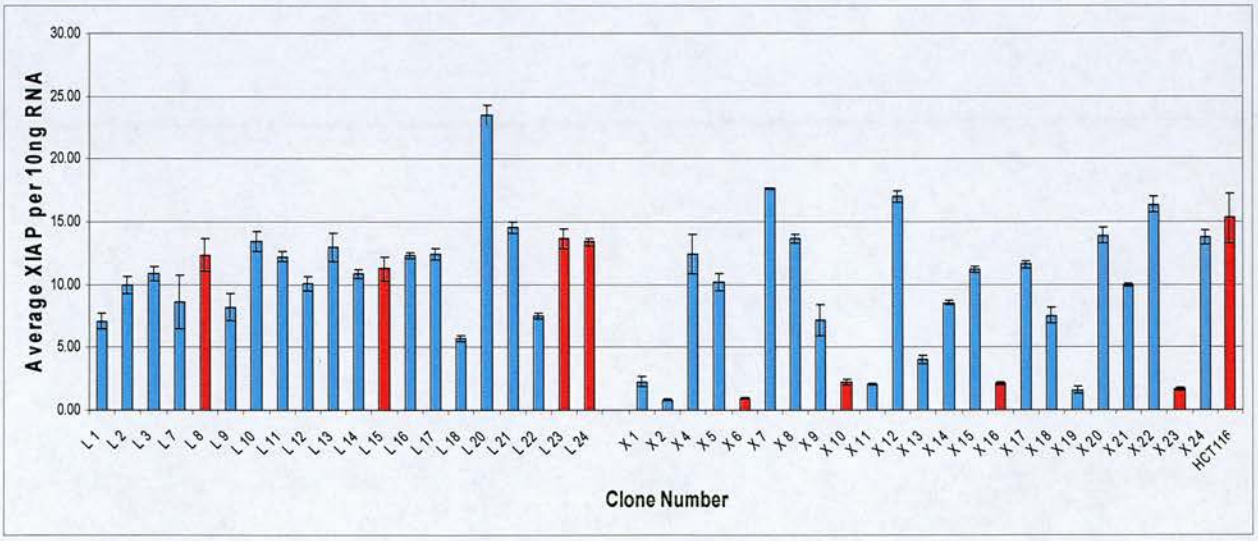

Figure 39: XIAP mRNA levels per 10ng total RNA by qRT-PCR. Parental cell line HCT116, luciferase expressing vector control (L prefix) and vector expressing short hairpin RNA to XIAP (X prefix). Error bars show standard deviation from the mean for triplicate samples in the experiment.

XIAP protein levels by Western immunoblot confirmed knock down in the X clones of 89%, 79%, 73% and 67% for X6, X10, X16 and X23 respectively relative to the mean level in four L clones (0.435 ± 0.08) (Figure 40).

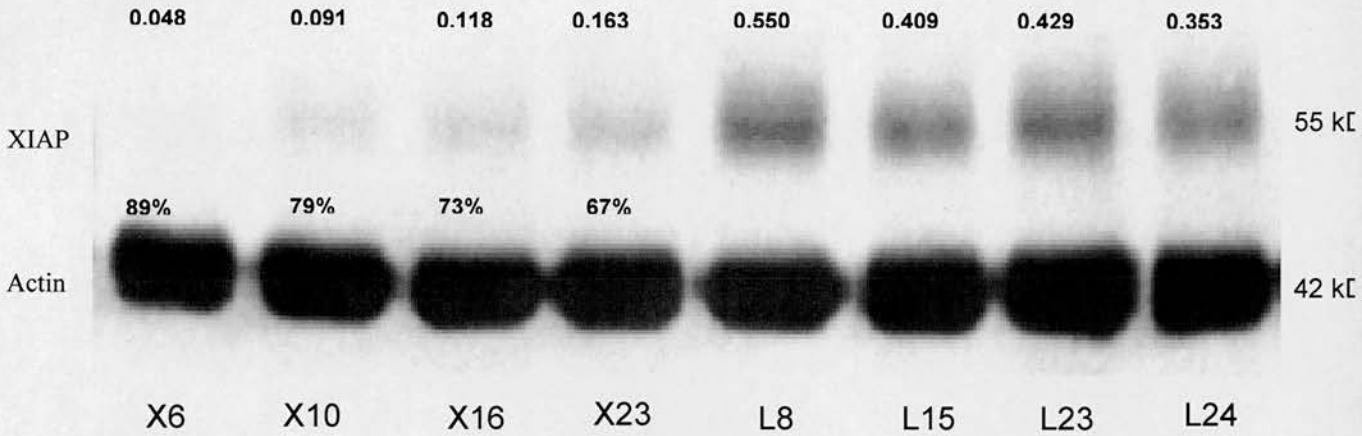

Figure 40: Western immunoblot using XIAP monoclonal mouse antibody (Stressgen). Quantification performed with Image Quant software and corrected protein ratio XIAP/Actin shown at early passage (p4). Percentage knockdown expressed relative to the mean level of XIAP in the four vector controls (0.435 +/-0.08).

7.3.2 Stability of knockdown with cell passage

Stable knockdown at the mRNA level was maintained at passage 8 (Figure 41) in X6 (85%), X16 (81%) and X23 (79%), however the mRNA levels in X10 had risen to only 59% knockdown.

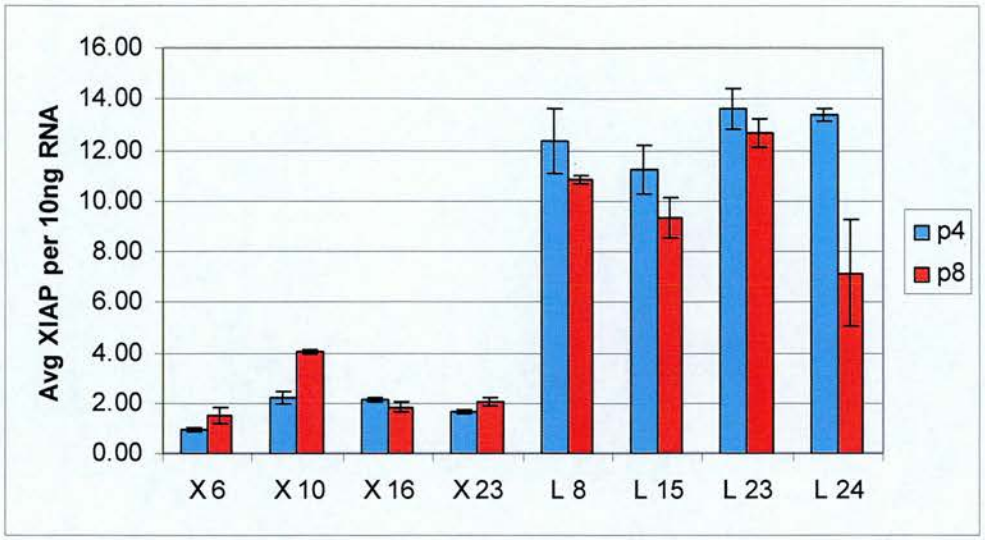

Figure 41: Average XIAP mRNA levels per 10ng total RNA by qRT-PCR comparing early (p4) and late (p8) passage of cells. Error bars show standard deviation from the mean for triplicate samples in the experiment. XIAP levels are consistently high for the four L clones at p4 and p8. XIAP levels are low at p4 and p8 for three of the X clones except for X10 where the XIAP levels have risen at p8.

Stable knockdown was confirmed by protein quantification at passage 8 (Figure 42); X6 90%, X16 72% and X23 63%. These results are consistent with the early passage data described above, however the protein levels in X10 had increased to 49% XIAP knockdown. Owing to the lack of long term stability of the construct in the X10 cell line at both the mRNA and protein levels, it was removed from cytotoxicity studies in later chapters. A summary of percentage XIAP down regulation at the RNA and protein levels at early and late passage is presented in Table 7.

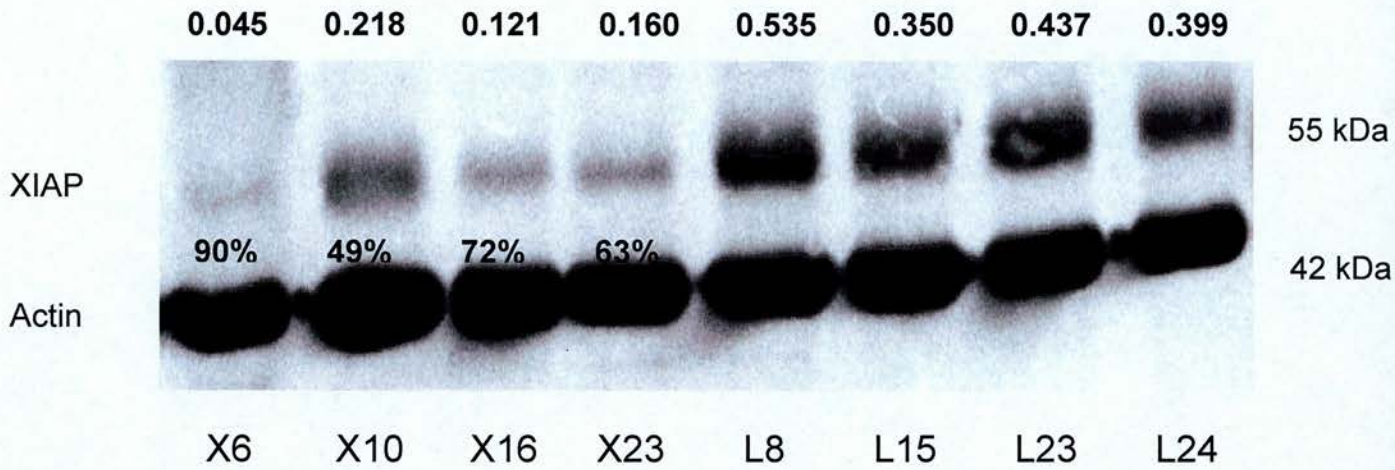

Figure 42: Western immunoblot using XIAP monoclonal mouse antibody (Stressgen). Quantitation performed with Image Quant software and corrected protein ratio XIAP/Actin shown at late passage (p8). Percentage knockdown expressed relative to the mean level of XIAP in the four vector controls (0.430 +/-0.08).

	mRNA p4	mRNA p8	Protein p4	Protein p8
X6	93%	85%	89%	90%
X10	82%	59%	79%	49%
X16	83%	81%	73%	72%
X23	87%	79%	67%	63%

Table 7: Summary of percentage knockdown in each of the X cell lines at the RNA and protein levels at early and late passage.

7.3.3 Microarray

The quality of the RNA extracted from the clonal cell lines by Agilent Bioanalyser is shown in Figure 43. Two distinct 18S and 28S rRNA bands are clearly seen. The Nanodrop spectrophotometer was used to quantify RNA before sending it for microarray analysis and the A260/280 ratio was found to be between 1.94 and 2.12 (acceptable range 1.9 – 2.1).

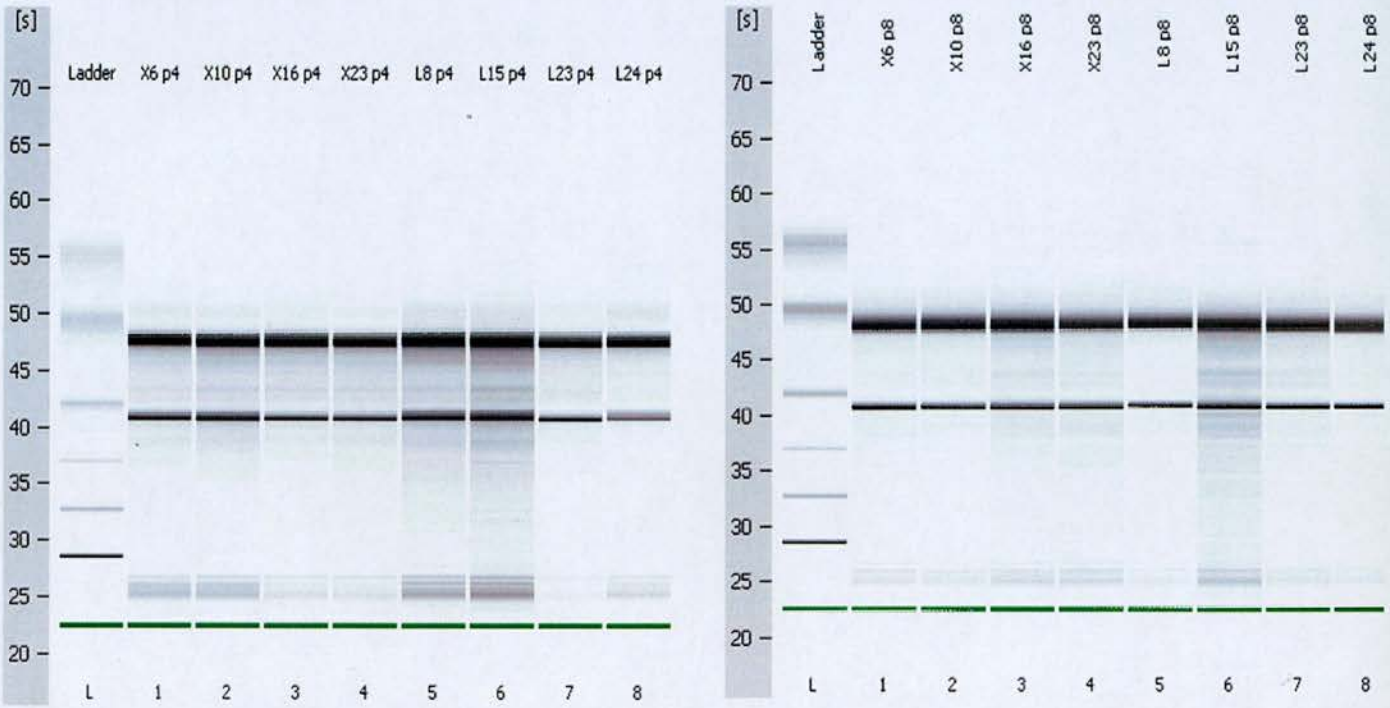

Figure 43: Agilent Bioanalyser RNA quality extracted from clonal cell lines at early (p4) and late (p8) passage. For these samples the RNA integrity number (RIN) was 7.6 – 9.7. The A260/280 ratio by Nanodrop spectrophotometer was 1.94 – 2.12.

Details of quality control measures can be seen in Table 8. 3'/5' ratios for GAPDH and beta-actin were 0.92 – 1.66 (target < 3). BioB spike controls were found to be present on all chips, with BioC, BioD and CreX also present in increasing intensity. When scaled to a target intensity of 100 (using Affymetrix MAS 5.0 array analysis software), scaling factors for all arrays were within the 3 fold acceptable limit (0.575 – 1.020), as were background and mean intensities.

Sample Name	Scale Factor	Background	Present	GAPDH 3'/5'	BActin 3'/5'
L8p4	0.575	45.74	0.445	0.95	1.25
L15p4	0.793	50.77	0.428	1	1.31
L23p4	0.727	47.78	0.442	0.95	1.17
L24p4	0.767	49.44	0.43	0.98	1.17
X6p4	0.893	45.25	0.427	1.04	1.08
X10p4	0.798	46.85	0.436	0.94	1.40
X16p4	0.859	48.56	0.440	0.93	1.14
X23p4	0.695	48.70	0.444	0.95	1.18
X6p8	0.843	46.42	0.436	1	1.54
X10p8	0.834	48.97	0.439	0.97	1.25
X16p8	0.884	52.68	0.431	1.05	1.31
X23p8	0.789	50.60	0.448	1.06	1.34
L8p8	0.824	46.74	0.447	0.98	1.20
L15p8	1.02	47.04	0.445	1.05	1.66
L23p8	0.732	43.43	0.459	1	1.35
L24p8	0.808	45.56	0.460	1	1.51
HCT116B	0.858	48.60	0.433	0.99	1.02
HCT116C	0.84	51.48	0.430	0.92	1.01

Table 8: Quality Control Data for 18 RNA samples on the Affymetrix HG U133 plus 2 GeneChip.

Several groups of genes were investigated according to literature review and potential relevance of known pathways, these are summarised in Table 9. Seven IAP family members (NIAP, cIAP1, cIAP2, XIAP, survivin, apollon, livin) were quantified; the eighth member of this family ILP2 was not represented on the Affymetrix chip. Members of the bcl-2 family, the extrinsic pathway members and other factors which have been reported as showing interactions with XIAP on literature review (MURR1 (75), akt2 (92), smac/Diablo (106), XAF1 (81), htra2/omi (136), apaf1 (88), GSPT1 (85) and NF-κB (71)) were also analysed.

IAP Family	BCL2 Family	Association with XIAP	Extrinsic Pathway
NAIP	BCL2	MURR1	TRAIL
CIAP1	BAX	AKT2	DR4
CIAP2	BAK1	smac/diablo	DR5
XIAP	BAD	XAF1	FAS
survivin	BCL2L1	htra2/omi	FADD
appollon	BCL2L2	APAF1	CASP3
livin	BID	GSPT1/Erf3	CASP7
		NF-κB1	CASP8
			CASP9

Table 9: The categories of gene analysed by microarray and the identified members of these groups. Colours correspond to Figure 44, Figure 45 and Figure 46 below. XIAP is represented in black.

For the purpose of considering which genes were differentially expressed, a twofold change was used i.e. -2 being a twofold down regulation of the gene and +2 being a twofold up regulation of the gene. In Figure 44, Figure 45 and Figure 46 the X axis represents $\log_2$ fold change, the two vertical lines represent ± 2 fold change in expression. The Y axis is a negative $\log_{10}$ transformation of the FDR (false discovery rate) adjusted p-value; points above this line pass a p-value cut-off of <0.05 which was considered significant. The genes of interest may therefore be found in the top right and top left of the volcano plots.

The results in Figure 44 show that none of the genes of interest were significantly changed when comparing the parental HCT116 cell line to the luciferase expressing controls. In fact only 3 genes on the whole chip are significantly changed using our criteria. This validates the L cell lines as a good reference for the XIAP knockdown clones and therefore the parental HCT116 cell line was excluded from further investigation.

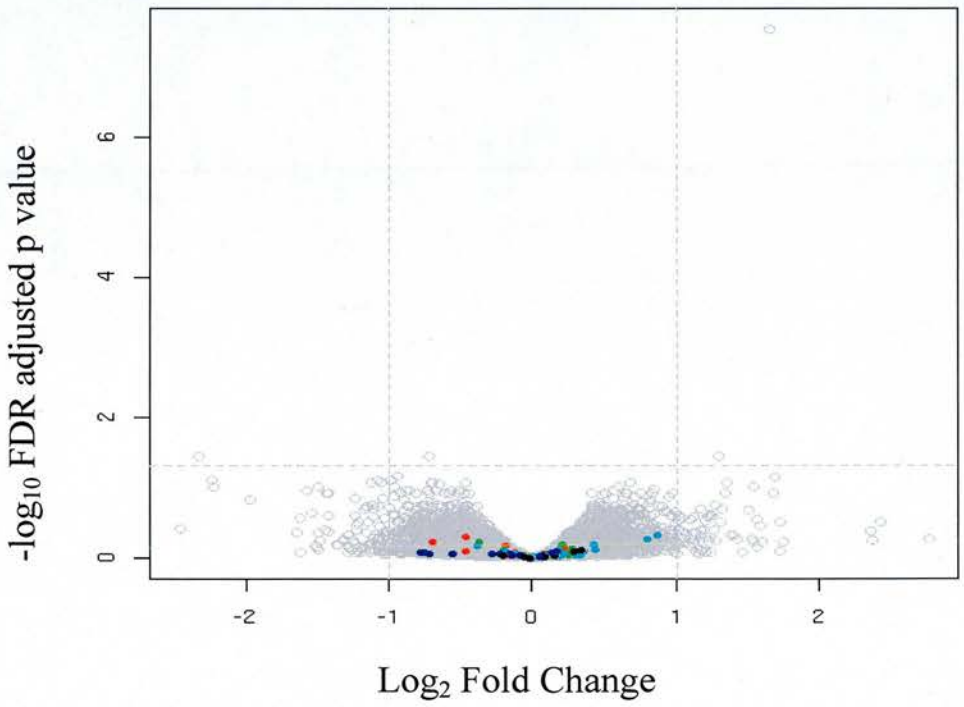

Figure 44: Comparison between HCT116 cell lines (duplicate) and luciferase expressing controls (four L cell lines) at early passage (p4).

The results in Figure 45 show significant down regulation at 6 (out of a total 7) XIAP probe sets (shown in dark blue) at early passage. There was no compensatory up regulation in other members of the IAP family also shown in dark blue. BCL2 family members, genes linked to the extrinsic pathway and other genes reported to be associated with XIAP were also not significantly changed when comparing X with L cell lines. There was one BCL2 family member (BCL2) which was up regulated (green dots) however this did not reach statistical significance and it was only one out of 8 BCL2 probe sets represented on the GeneChip. There are a number of other genes which are significantly changed (grey circles), 9 up and 2 down. Further study of these genes may provide insight into the regulation and function of XIAP but is beyond the scope of this project.

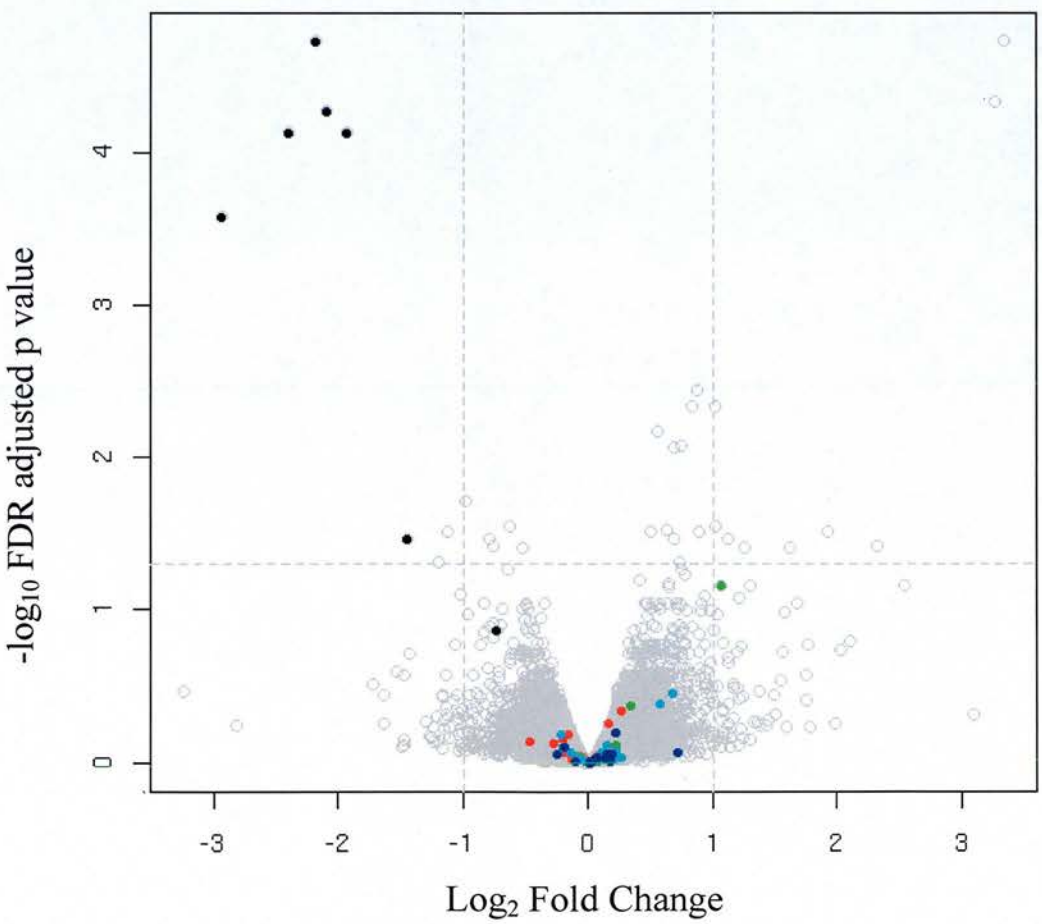

Figure 45: Comparison of the four X cell lines and four L cell lines at early passage (p4).

A significant down regulation of XIAP was seen in 3 out of 7 probe sets at later passage (p8) in Figure 46. Again, none of the other genes of interest were differentially expressed. Of the other genes on the GeneChip only 2 other (grey circles) were significantly up regulated, these 2 genes were also significantly increased at early passage.

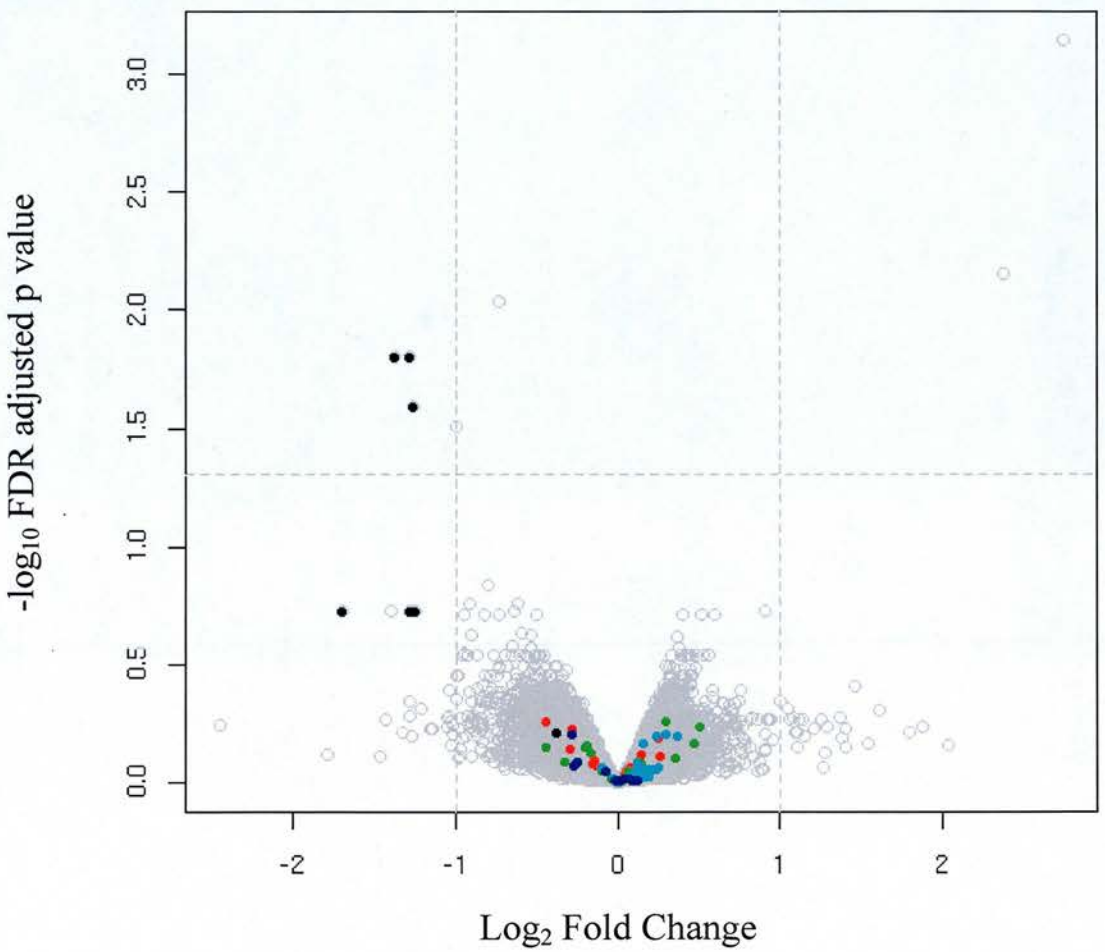

Figure 46: Comparison of the four X cell lines and four L cell lines at late passage (p8).

XIAP fold changes and level of significance at the seven probe sets by Accession Number on the Affymetrix GeneChip are compared in Table 10. The mean XIAP fold change is greater at the p4 time point 4.3 ± 1.9 when compared to the p8 time point 2.4 ± 0.6. One of the probes NM_001167 showed a fold change <2 which was not statistically significant at both time points. The XIAP fold change at p4 is comparable to the down regulation seen by qRT-PCR (described in Figure 39 and correlated Figure 49), these are different techniques but both assess changes at the mRNA level. There is a good correlation between the two techniques (Figure 49).

Accession Number	Fold Change p4	p value	Fold Change p8	p value
U32974	-2.73	0.03419	-2.45	0.18938
NM_001167	-1.66	0.13738	-1.29	0.61492
N30645	-4.25	0.00005	-2.60	0.01574
N30645	-5.24	0.00007	-2.39	0.18938
BF109251	-7.63	0.00027	-3.25	0.18938
AW675725	-4.51	0.00002	-2.45	0.01574
BE380045	-3.83	0.00007	-2.41	0.02554

Table 10: Microarray comparison by fold change and level of significance of XIAP levels of the 4X and 4L cell lines at seven probe sets (GenBank Accession Number shown) at early passage (p4) and late passage (p8).

7.3.4 Gene expression of IAP family members and related genes

Members of the IAP family cIAP1, cIAP2 and survivin were analysed by quantitative RT-PCR. There is large variation in cIAP2 (15 fold) and survivin (34 fold) levels throughout the cell lines (Figure 47); cIAP1 shows less variation (2 fold). In all cases there is no correlation of IAP family expression with XIAP status.

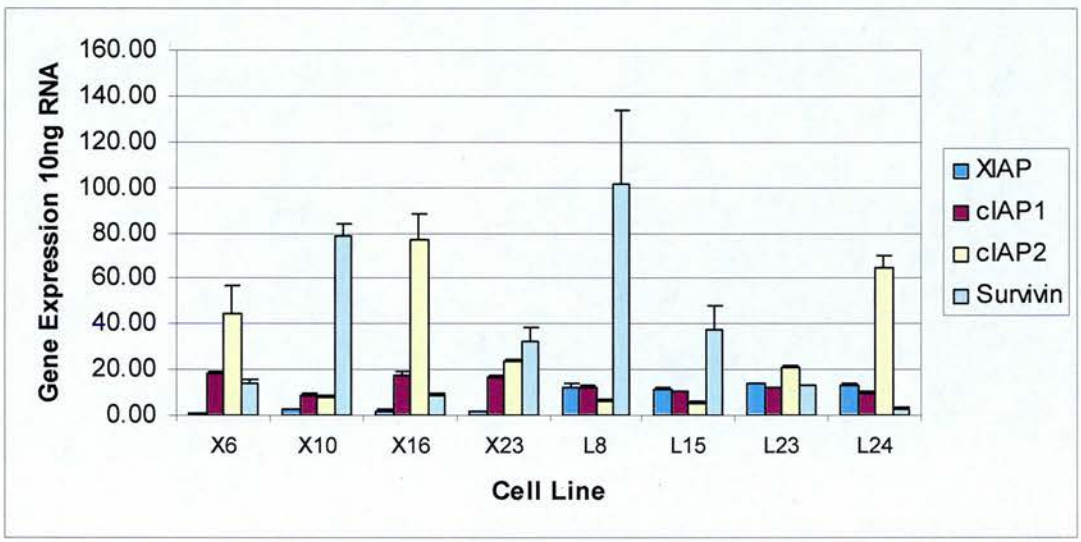

Figure 47: IAP family expression per 10ng total RNA in clonal cell lines at early passage by qRT-PCR. Error bars show the standard deviation from the mean.

XAF1 expression (Figure 48) ranged between 0.01 and 0.05 for most clonal cell line derivatives except L24 which, at 1.51, is beyond the scale of the graph. There is no correlation between XIAP and XAF1 levels in this model.

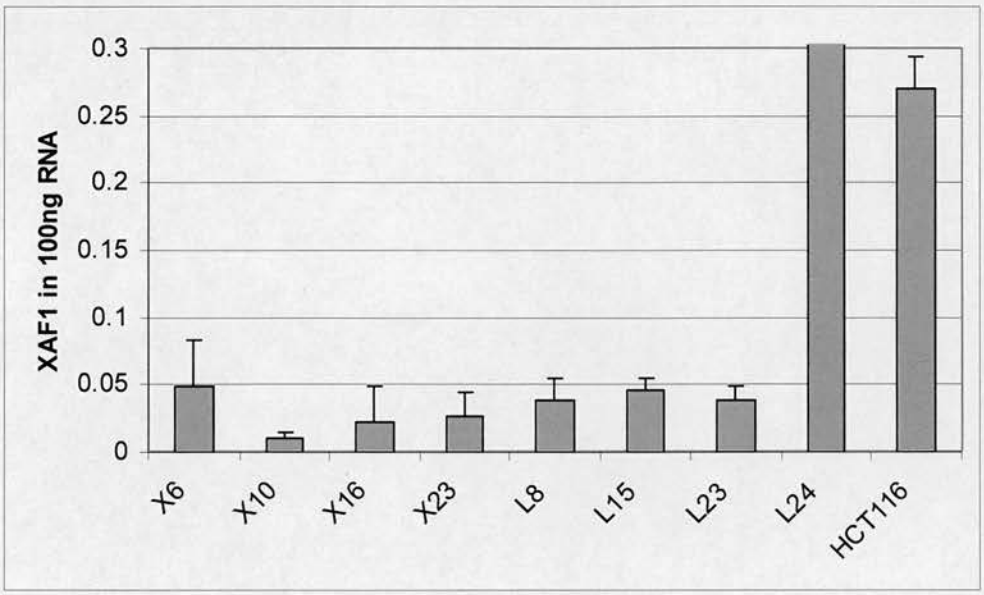

Figure 48: XAF1 expression by quantitative RT-PCR per 100ng total RNA in early passage clonal cell lines. Error bars show standard deviation from the mean. A Colo205 standard curve was used due to relatively low expression of XAF1 in HCT116, therefore these results cannot be directly compared with other qRT-PCR data.

The three other members of the IAP family cIAP1, cIAP2 and survivin were analysed by qRT-PCR (Figure 47) and the results compared with microarray data in order to validate the newer technique (Figure 49). The R^2 values for these correlations are XIAP 0.80 - 0.98, CIAP1 0.57, CIAP2 0.90 - 0.98, Survivin 0.90 – 0.94 (Table 11). There was good correlation between microarray and quantitative RT-PCR data for three out of the four members of the IAP family investigated.

CIAP1 shows a poorer correlation however there is only one probe set for this gene and perhaps this highlights the need for multiple probesets on the GeneChip.

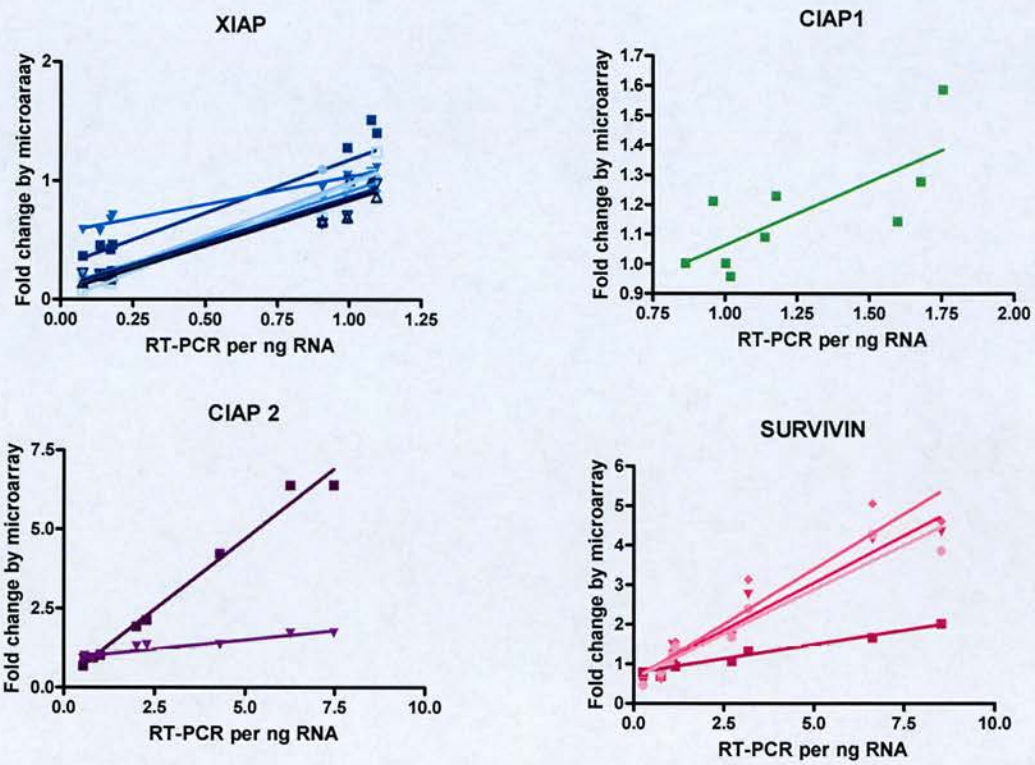

Figure 49: Correlation of RT-PCR and Microarray data for four IAP family members at early passage (p4). Each dot represents a cell line. Each line shows the correlation of the gene expression by RT-PCR with a probe set on the Affymetrix Genechip.

For RT-PCR data the results are expressed as a mean value of three reactions per ng total RNA then normalised to the parental HCT116 level. For Microarray data each probe set is shown normalised to the HCT116 parental value.

	XIAP		CIAP1		CIAP2		Survivin	
	R^2	p value	R^2	p value	R^2	p value	R^2	p value
M1	0.8031	0.0011	0.5661	0.0193	0.9843	< 0.0001	0.9366	< 0.0001
M2	0.9709	< 0.0001			0.9039	< 0.0001	0.9412	< 0.0001
M3	0.983	< 0.0001					0.9062	< 0.0001
M4	0.9652	< 0.0001					0.9214	< 0.0001
M5	0.9558	< 0.0001						
M6	0.9354	< 0.0001						
M7	0.9237	< 0.0001						

Table 11: R^2 correlation values for RT-PCR data with microarray data, p value for slope of line significantly non zero for Figure 49 above.

7.3.5 Cell Line Characteristics

7.3.5.1 Morphology

The morphology of the two cell lines L8 and X23 was compared by light microscopy (Figure 50) at the optimal seeding density for each cell line, at the same passage on the same day after seeding. The X23 cell line shows "spindle like" protrusions such that the cells appear elongated. Survivin, a member of the IAP family, has been shown to have role in mitotic cell division and spindle assembly (137) and it is possible that XIAP has similar but yet unidentified properties. Geisbrecht *et al* describe a role for dIAP1 (drosophila inhibitor of apoptosis) in cell migration and found that cells lacking this protein fail to migrate (138). In addition, smac, the negative regulator of XIAP, inhibits cell motility and random migration at low cell density (139).

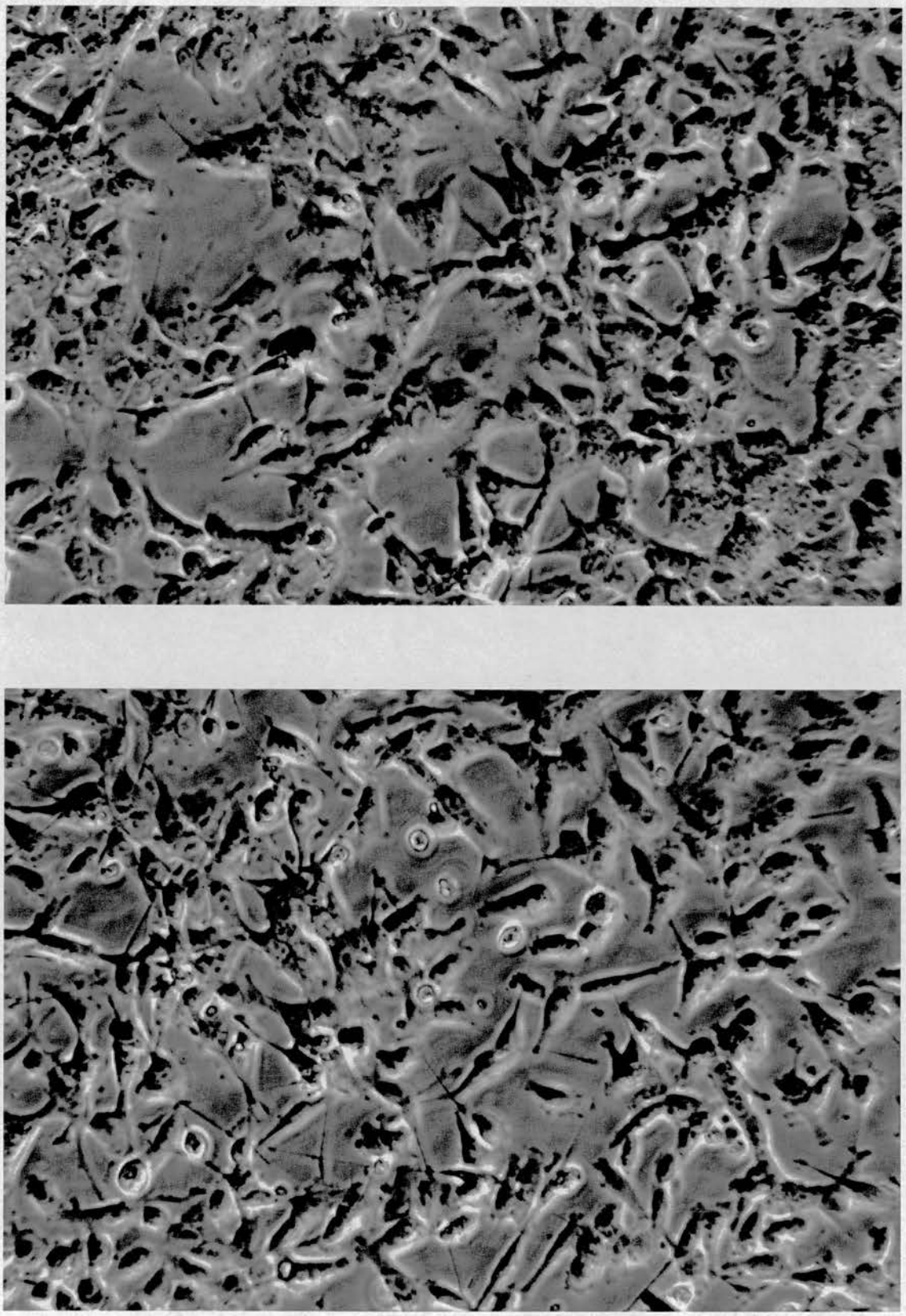

Figure 50: Morphology of the L8 (top) and X23 (bottom) cell lines at late passage x20 magnification.

7.3.5.2 Growth curves

The growth curves of the nine cell lines differed (Figure 51) with the X cell lines growing at a slower rate than the L cell lines. Thus to produce the superimposed growth curve necessary for cytotoxicity experiments the seeding density of each cell line in 96-well plates differed. A greater number of X cells per well were required; X6 4000, X10 3500, X16 5000, X23 5000 cells per well compared to L8 3500, L15 4000, L23 4000, L24 2500 L cells per well and HCT116 2000 cells per well. When these seeding densities are adhered to, similar doubling times are seen (mean 21.7 +/- 1.36 hours) as shown in Table 12. The growth curve for HCT116 differs in that there is a shorter lag phase before exponential growth. This could be explained by the differences in growth media; the HCT116 cell line is grown without geneticin which is an antibiotic required for the maintenance of the expression vector in cell lines.

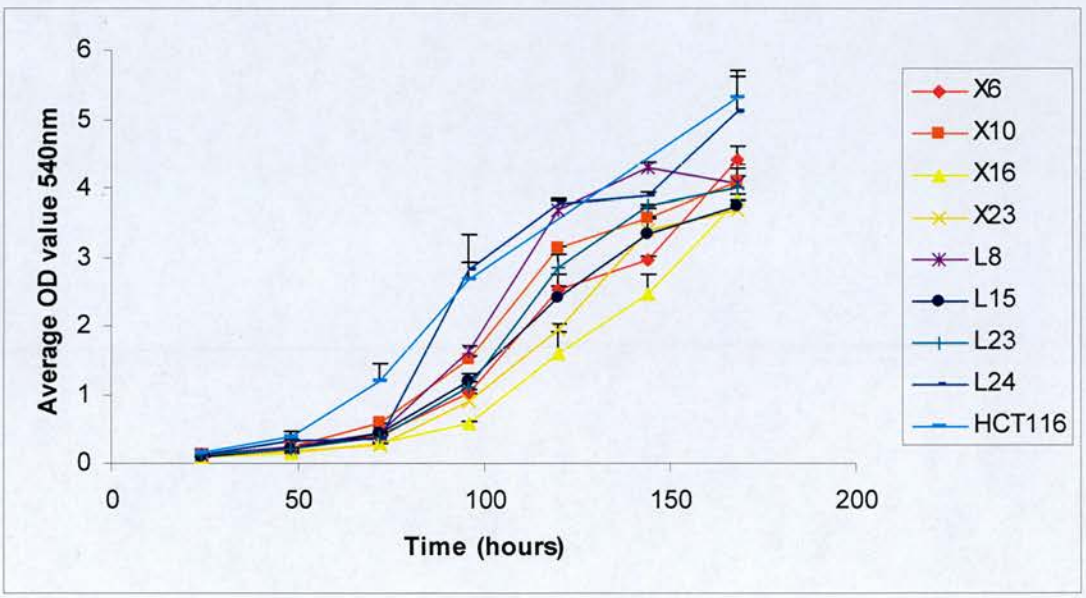

Figure 51: Growth curve by SRB assay at seeding density of 3500 cell per well. In order to achieve a similar growth curve and doubling time for comparison between cell lines the number of cells per well differs. Note the plating efficiency differs between cell lines.

Cell Line	Seeding Density (cells/well)	Doubling Time (hours)	Plating Efficiency (ratio)	Floating Cell Fraction (%)
X6	4000	22.9	0.72	2.22
X10	3500	22.2	0.60	1.11
X16	5000	23.3	0.81	3.42
X23	5000	21.6	0.52	3.3
L8	3500	21.5	0.73	0.98
L15	4000	20.6	0.61	1.27
L23	4000	23.2	0.62	0.9
L24	2500	19.3	0.40	0.28
HCT116	2000	20.5	0.69	

Table 12: Growth characteristics (Doubling time, Plating efficiency and Floating cell fraction) for each cell line at optimal seeding density.

7.3.5.3 Plating efficiency and Floating cell fraction

The plating efficiency varied across all cell lines examined (Table 12) therefore all experiments were designed in order to avoid removal of growth media and the resulting introduction of bias. The X cell lines have a higher floating cell fraction (1.11 - 3.42%) compared to the L cells lines (0.28 - 1.27%), Table 12.

7.3.5.4 Apoptosis

Annexin V – PI staining showed a higher percentage of early apoptotic cells in the X23 cell line 10.2% compared to 6.5% in the L8 cell line (Figure 52). However, the increased fraction of cells which stained positive for both annexin V and PI (10.4% vs 5.9%) indicates that there was also a higher proportion of cells which have cell membrane damage and therefore these results should be interpreted with caution.

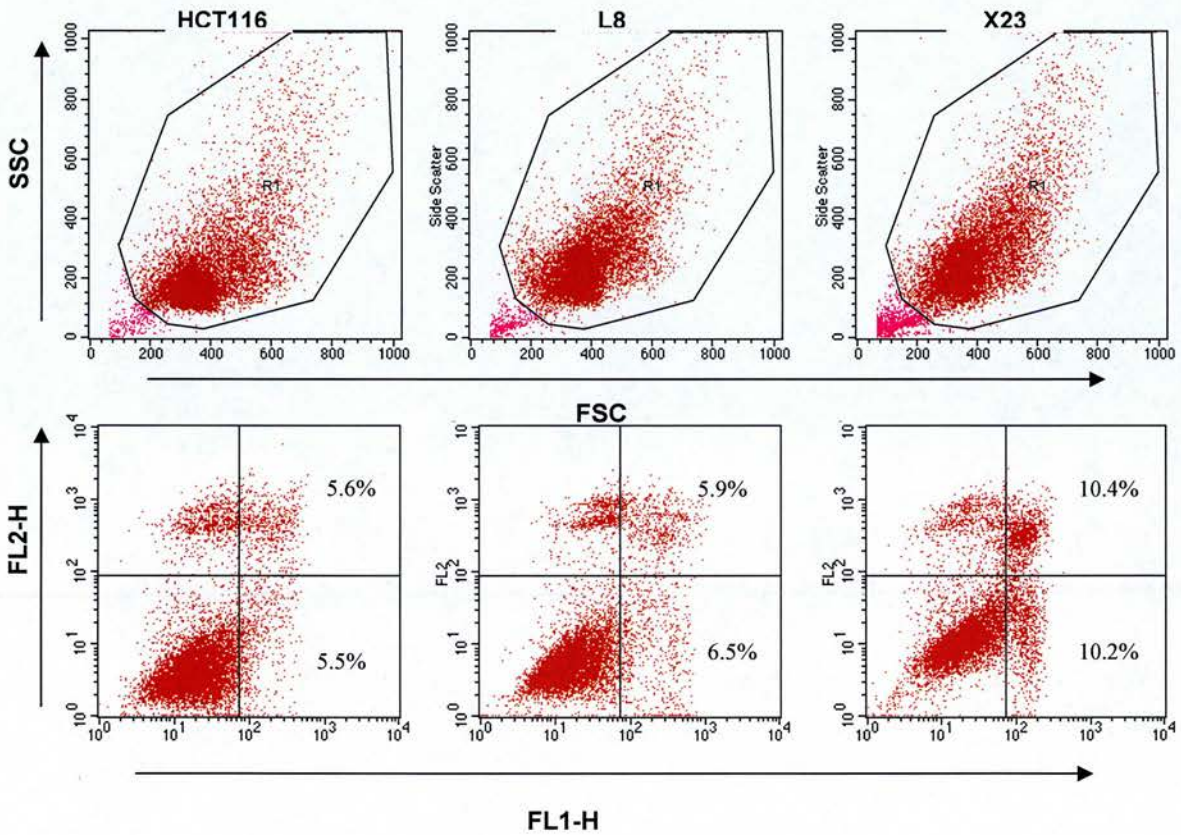

Figure 52: Annexin V – PI staining with FACS analysis. The X23 cell line has a higher percentage of early apoptotic cells which stain positive for annexin V (10.2% vs 6.5% in L8).

The level of caspase activity in the cell lines was determined to investigate whether stable XIAP knockdown leads to increased activation of the apoptotic pathway; a late event. The levels of activated caspase 3/7 by ApoOne assay were unchanged when comparing HCT116 (50 ± 11.6), L8 (57 ± 3.0) and X23 (46 ± 8.1), T-test p = 0.14 (Figure 53).

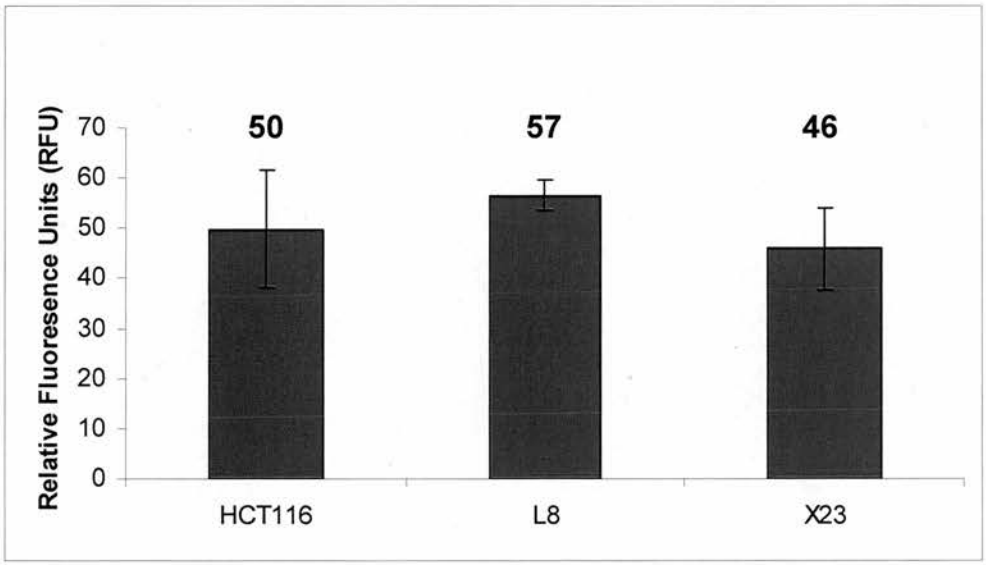

Figure 53: Caspase 3/7 activity minus background levels for untreated cells at the same seeding density. There was no difference in baseline ApoOne caspase 3/7 activity between the cell lines. Error bars represent standard deviation from the mean for three independent experiments.

The X23 cells could therefore be considered as "primed" to undergo apoptosis as the early annexin V results suggest but the caspases have not been activated as seen in the ApoOne assay.

7.3.5.5 DR5 membrane expression

The expression of TRAIL receptors (DR5) on the cell surface was quantified by flow cytometry prior to performing experiments with the agonist rhTRAIL (Figure 54). The results are compared to a leukaemia cell line (Jurkat) which is known to express DR5. The median fluorescence for Jurkat cells was 30, HCT116 75, L8 91, X23 89 confirming that the receptor expression between the control cell line L8 and XIAP knockdown cell line X23 was unchanged.

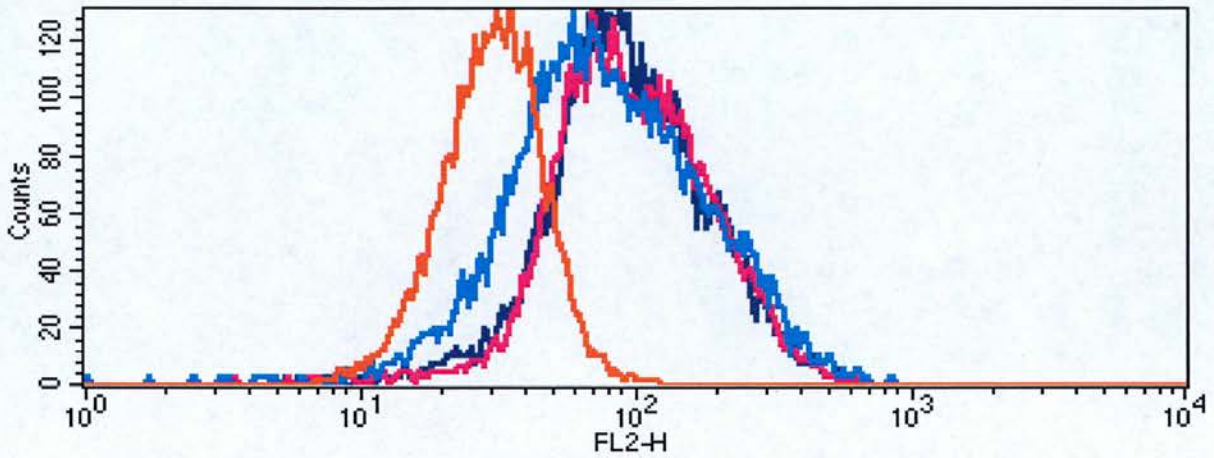

Figure 54: Cells stained with phycoerythrin conjugated DR5 antibody and analysed by flow cytometry (X23 purple, L8 pink, HCT116 blue). Jurkat cells (orange) used as positive control. There is similar DR5 expression in L8 and X23

7.4 Discussion

An isogenic model has been developed from derivatives of the HCT116 colorectal cell line where the only genetic difference between the cell lines is the XIAP expression. There is down regulation of 82-93% at the mRNA level which is generally stable (79-85%) over the course of four passages; 4 weeks of cell growth with the exception of the X10 clone which would appear to have lost the vector construct. When the same vector construct (provided by Aegera Therapeutics Inc) expressing shXIAP was used in the breast cell line MDA-MB-231, 85% reductions in the mRNA level and 85-95% reductions in the XIAP protein level were seen (41).

The X23 and L8 cell lines were selected for further study based on the results of *in vivo* xenograft growth studies which will be discussed further in Chapter 9. Quantification of protein levels will be less accurate as the technique relies on image analysis and is not referenced to a standard curve as in the qRT-PCR technique.

There are limitations to using a stable knockdown model; in this study investigation of XIAP levels was limited to 8 passages and therefore further experiments were only valid if performed within this timeframe. McManus *et al* (41) noted stable down regulation of XIAP over 24 passages of the knockdown cell lines. An alternative is transient siRNA transfection, one study (135) has shown 80-90% XIAP down regulation at the mRNA level in 3 canine tumour cell lines at 72 hours post transfection with lipofectamine. The disadvantage of transient models is the short lived dynamic effect and potential acute gene changes associated with the use of transfection reagents, as discussed in Chapter 5. A further alternative is an inducible "Tet-on" system in which the gene expression change may be switched on by adding tetracycline to the cell growth media. This technique has recently been developed in the HCT116 colorectal cell line (140) and has the advantage of a stable cell line in which to investigate the consequences of gene manipulation. However, these systems are technically difficult to establish.

The microarray study described here shows that a large number of transcripts may be quantified in a short period of time. It is essential that the RNA is good quality as the technique is very sensitive and the quality control measures must be adhered to. Here the expression of a relatively small number of genes has been assessed; however, a further analysis could be performed to identify potential new associations with XIAP which have not yet been reported.

With large volumes of data generated by microarray it is necessary to set a threshold above or below which a change in gene expression is considered significant. The fold change (+/-2) and the p value selected (<0.05) are arbitrary values based on experience in bioinformatics and statistics. It is entirely possible, however, that the expression of key genes involved in the cell survival apparatus need only small changes in expression to trigger dramatic changes owing to complex downstream pathways amplifying their effects. Such genes are in danger of being overlooked when using arbitrary thresholds to analyse the microarray data and it may be more important to consider genes which remain significantly changed at p4 and p8 regardless of the fold change. In this data set there are only 6 genes with significantly altered expression at both time points – three XIAP as mentioned above, two others which reached the fold change cut off and one whose fold change was -1.99 hence did not reach the original criteria. This gene may be worth considering as it could be argued that a sustained change (which is statistically significant) is as biologically significant as a magnitude change. This highlights a pitfall with interpreting microarray data: it would be easy to miss biological effect as one is only detecting gene expression change. Some genes may only require small magnitudes of change in order to produce functional change within the cell. Microarray should therefore be used as a large scale screening tool and functional characterisation studies remain important when assessing biological effect within a cell.

The results described above confirm specific and stable down regulation of XIAP with no impact on the related genes identified on literature review. In a breast cancer model of stable (41) XIAP knockdown using the same vector constructs no

compensation of other IAP family members was seen in concordance with our microarray and qRT-PCR data. The XIAP knockout mouse (76) shows compensatory up regulation in CIAP1 and CIAP2 at the protein level. As XIAP is the most potent caspase inhibitor in the family of IAPs, in a model where a small amount of XIAP remains, it is likely that this small amount is enough to carry out a functional role.

There was good correlation between microarray expression and qRT-PCR data therefore validating the newer microarray technique. The four XIAP knockdown cell lines developed here may therefore be confidently used for cytotoxicity studies *in vitro* over many weeks. *In vivo* xenograft establishment and XIAP mRNA levels are discussed in Chapter 9.

There have been concerns that down regulation of XIAP would be compensated by increases in other members of the IAP family implying redundancy of the target. In the XIAP deficient mouse (76) there were increases in cIAP1 and cIAP2 protein levels and this may be the case in a model with complete XIAP loss rather than 80% down regulation. In a breast cancer model of stable (41) XIAP knockdown no compensation of other IAP family members was seen; this is in concordance with the qRT-PCR data presented here.

Here we report differences in the growth pattern of shXIAP expressing cells. Our data show that the XIAP deficient cell lines grow at a slower rate than their luciferase expressing counterparts. The HCT116 grows in a different manner which may be due to the absence of geneticin in the media or that it does not carry the short hairpin expressing vector. For comparison of the effects of XIAP down regulation it is therefore more accurate to compare X with the L control rather than the parental HCT116 cell line data. The knockdown cells also detach from a cell culture plate more easily as seen by the higher floating cell fraction. It is possible that stable down regulation of XIAP causes subtle phenotypic changes which have yet to be identified. When the XIAP knockout mouse was developed (76) there were initially thought to

be no phenotypic changes but since then differences in copper metabolism (75), mammary gland development (141) and signal transduction cascades (54) have been documented. This is to be expected as it is now known that role of XIAP extends beyond caspase inhibition; there is evidence for effects on cell division, cell cycle progression and signal transduction (3).

The Death Receptor 5 (DR5) expression in these cell lines was unchanged which is important to document prior to conducting experiments with TRAIL. There have been reports of the death receptors being up regulated in certain situations such as radiation treatment (34) and the levels of DR4 and DR5 have also been noted to vary across colorectal cell lines (34). Low levels of DR4 expression were seen in the HCT116 though DR5 was highly expressed. However, there was no good correlation between expression of the DR5 receptor and cytotoxicity with the DR5 agonist monoclonal antibody (142).

AV-PI assay results showed an increased early apoptotic fraction in the X23 cell line suggesting that the cells have commenced the journey along the apoptotic pathway but the effectors of apoptosis are not yet activated as we report similar levels of caspase 3/7 activity across untreated X and L colorectal cell lines. Given that initial studies of XIAP described its ability to directly inhibit caspases (55) it is necessary to examine whether XIAP down regulation alone increases caspase activation. McManus *et al* (41) found no increase in caspase 3 or 9 activity in untreated stable XIAP knockdown breast cancer cells consistent with our data. There have been reports of XIAP down regulation alone inducing apoptosis (95); in transient XIAP inhibition with antisense there was an increase in apoptosis in a lung cancer model in vitro compared to a missense control. This suggests that the effect may be due to the acute short term nature of the knockdown.

Current clinical methods for down regulation of XIAP – by antisense – are given as an infusion over seven days (as described in Chapter 2). The tissue half life of the

drug is known to be long (many days) though the plasma half life is only a few hours. The model developed here therefore draws more parallels with the clinical situation where the goal is to cause XIAP tissue levels to decrease for a significant period of time as compared to transient transfection in cell line models which may cause cellular changes related to the transfection agents used.

7.5 Conclusion

A colorectal cancer HCT116 cell line model has been developed using short hairpin RNA targeting XIAP stably expressed in the HCT116 cell line model. XIAP was down regulated at the mRNA and protein levels and this knockdown was maintained over at least 4 weeks. The 80% down regulation was similar to levels which may be achieved clinically with antisense targeted to XIAP. There was no compensatory up regulation of other members of the IAP family (cIAP1, cIAP2 and survivin) or XAF1, the negative regulator of XIAP.

The microarray technique was a powerful tool for identifying gene changes in this model of XIAP down regulation. The results confirm down regulation of XIAP at early and late passage although some of the fold change effect was lost over time. The data correlates well with the RT-PCR data therefore validating the newer technique. There were no compensatory changes in genes currently documented to have an association with XIAP function. Therefore a colorectal cancer model has been developed using isogenic cell lines which differ only in the XIAP status at clinically relevant levels.

The *in vitro* characterisation of these cell lines show differences in cell growth, plating efficiency and morphology in the XIAP deficient cell line. The functional caspase 3/7 activity levels and the DR5 receptor expression were similar when comparing X23 and L8 cell lines.

Further studies will investigate the isogenic cell line developed *in vitro* and in an *in vivo* mouse model. This model may be used to study the role of XIAP down regulation in combination with classical cytotoxic agents to identify useful potential clinical combination therapies.

Chapter 8

In Vitro Cytotoxicity in stable XIAP knock down cells

8 In Vitro Cytotoxicity in stable XIAP knock down cells

8.1 Introduction

The clonal cell lines developed in Chapter 7 were investigated *in vitro* for cytotoxic response to chemotherapeutic agents and the results are described here. Classical agents used in the treatment of colorectal cancer; camptothecin, 5-FU, oxaliplatin and γ radiation were used in the stable XIAP knock down model in an attempt to identify potential combination strategies for further development.

In order to identify whether XIAP plays a role in resistance mechanisms to drugs not usually used in the treatment of colorectal cancer, treatment with paclitaxel and docetaxel were investigated. These agents have shown efficacy combined with XIAP down regulation in lung, prostate and breast cancer models (40, 41) and therefore the mechanism may be related to a class effect of the taxanes rather than a feature of colorectal cancer.

rhTRAIL (recombinant human TNF-related apoptosis-inducing ligand) is known to stimulate apoptosis by directly activating the extrinsic apoptotic pathway (see Figure 1, Chapter 1). This allows a targeted approach to the XIAP mechanism of resistance without the potential complications of other less specific chemotherapeutic agents.

8.2 Results

8.2.1 Response to rhTRAIL

As a preliminary study all clonal cell lines were exposed to rhTRAIL over a concentration range for 24, 48 and 72 hours to investigate the optimal dose and time point for further experiments (Figure 55). For the X10 and L24 cell lines the IC50 is >100ng/ml. Given the variation in cytotoxicity over time throughout the cell lines it was prudent to select a pair which had similar characteristics. The IC_{50} was constant over time for the X23 and L8 cell lines and therefore these were selected for further studies using rhTRAIL. McManus *et al* (41) assessed cell viability at the 20 hour time-point after TRAIL treatment in a breast and lung cancer model and it was therefore decided to perform cytotoxicity assays at the 24 hour time-point in subsequent studies. The selection of L8 and X23 was also based on the *in vivo* growth curves which were performed simultaneously (see Chapter 9) in order to allow translation to an animal model.

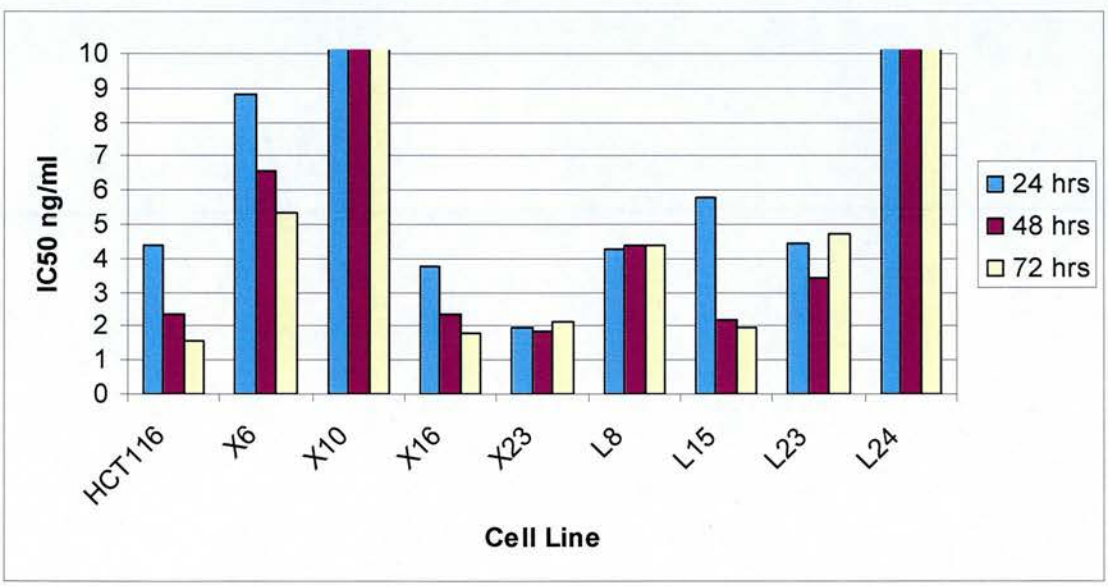

Figure 55: Clonal HCT116 cell lines treated with rhTRAIL over a concentration range (0.01 – 100 ng/ml). Cell viability assessed by MTT assay at three time points (24, 48, 72 hours). For the X10 and L24 cell lines the IC50 is >100ng/ml.

The cytotoxicity curve for a representative experiment is shown in Figure 56. The cells were seeded at the optimal seeding density, treated with a range of rhTRAIL concentrations (0.01 – 100ng) and cell viability estimated by the MTT assay. The mean IC_{50} of three experiments for X23 was 0.39 ng/ml (SD 0.16) compared to mean IC_{50} for L8 1.31ng/ml (SD 0.42). The X23 cell line shows a statistically significant ($p<0.05$ by t-test) 3-fold increase in cytotoxicity when compared to the L8 cell line.

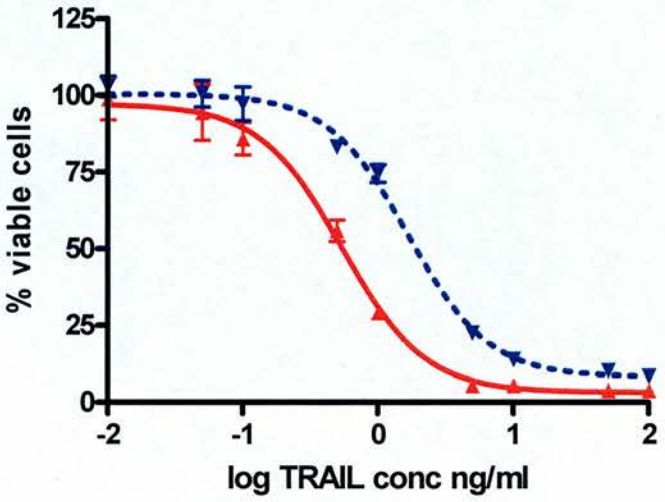

	IC50 ng/ml (mean of 3 experiments)	Standard Deviation
X23	0.39 *	0.16
L8	1.31	0.42

Figure 56: Cells treated with range of rhTRAIL (0.01 – 100ng) concentrations for 24 hours. Viable cells calculated relative to control by MTT assay. Graph shows representative experiment, error bars show standard deviation of the mean.

To confirm that loss of cell viability was due to the activation of the extrinsic apoptotic pathway caspase 3/7 activity was estimated with the ApoOne assay. Cells were seeded at the optimal seeding density for 24 hours prior to treatment with rhTRAIL at 5ng/ml for 2.5 hours. There is a two fold increase in caspase 3/7 activity in the XIAP knockdown cell line (Figure 57); X23 186 RFU (SD 20.2) compared to L8 87 RFU (SD 19.7), $p<0.004$ by t-test.

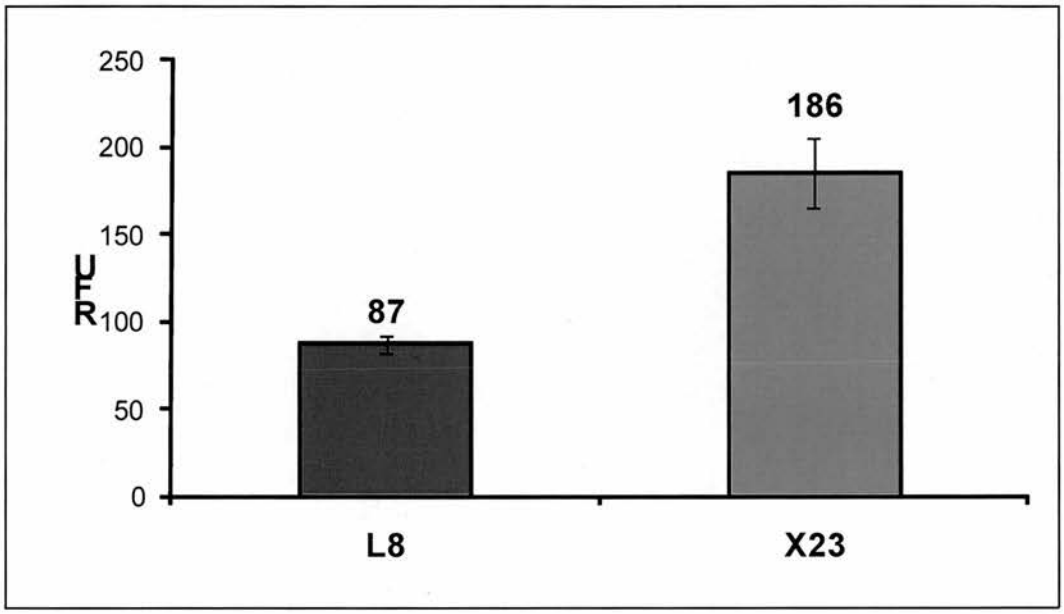

Figure 57: Cells treated with rhTRAIL 5ng/ml for 2.5hrs. Difference (treated – untreated) in caspase 3/7 activity by ApoOne assay across cell lines. Error bars show standard deviation from the mean for three independent experiments.

8.2.2 Response to radiotherapy

As colorectal cancer is commonly treated clinically with radiotherapy we investigated the effect of this treatment modality in our XIAP knockdown model. The cells were seeded at the optimal seeding density and allowed to attach overnight prior to treatment with a single fraction of γ radiation over the dose range 0-16 Gy. The cells were incubated for 120 hours (5 days) prior to estimation of cell number by SRB assay. The radiotherapy dose for 50% survival of the 3 X clones was X6 9.7, X16 11.5, X23 10.2 Gy compared to L8 12.2, L15 14.3, L23 13.4, L24 13.7 Gy for the 4 L clones (Figure 58). Mean 50% survival value for X clones is 10.5Gy (SD 0.93) and L clones is 13.4 Gy (SD 0.88), $p < 0.02$ by t-test. Radiotherapy studies showed approximately 20% increase in sensitivity for the X cell lines compared to the L cell lines.

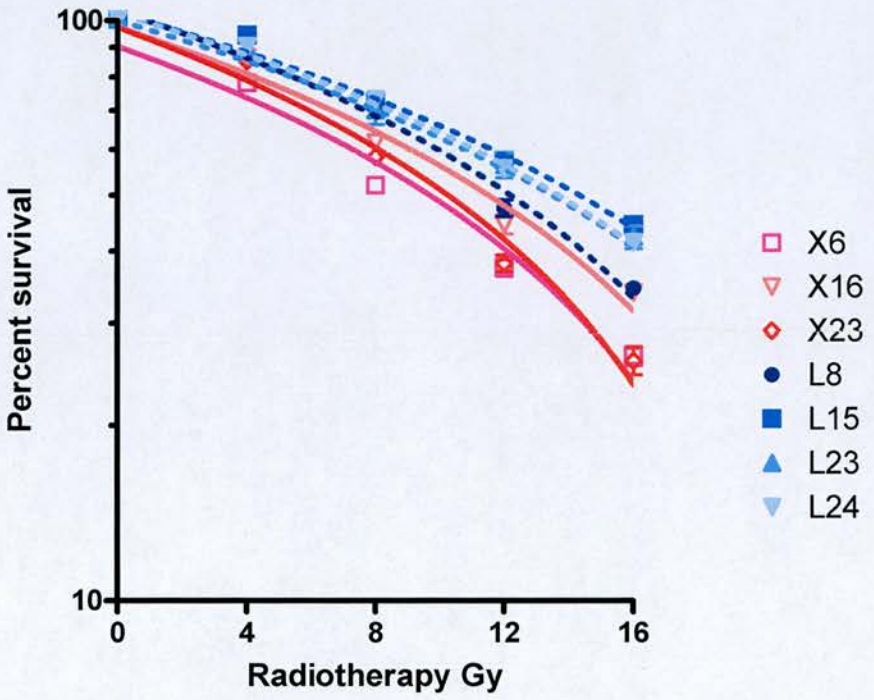

	Dose for 50% survival (Gy)
X6	9.7
X16	11.5
X23	10.2
Mean	**10.5 (+/-0.93)**
L8	12.2
L15	14.3
L23	13.4
L24	13.7
Mean	**13.4 (+/-0.88)**

Figure 58: Effect of radiotherapy over a dose range of 0-16 Gy for cell lines by SRB assay. Error bars show standard error of the mean for 3 individual experiments. There is a significant increase in sensitivity to radiotherapy (t-test p<0.02).

8.2.3 Response to cytotoxic agents

Due to the relatively long drug exposure described by McManus et al (41) (72 hrs, three doubling times) a lower cell number was plated in order to be within the validated range for the SRB assay. However, in order for these cells to be growing exponentially, a 72 hour incubation was required prior to treatment (see growth curves Chapter 7).

Preliminary data from cytotoxicity experiments with 5FU and oxaliplatin where cells were treated at the IC_{50} dose are shown in Table 13. These data showed no benefit of XIAP down regulation across the X and L cell lines and therefore full cytotoxicity studies were not pursued.

% cells	X6	X16	X23	L8	L15	L23	L24
5FU 5μM	46.0	53.2	51.3	65.2	66.0	43.9	63.6
Oxaliplatin 1μM	44.7	78.0	57.7	68.7	81.7	53.4	68.3

Table 13: Clonal cell lines treated with 5FU and oxaliplatin at the IC50. Percentage cells by SRB assay.

Cytotoxicity studies with camptothecin (Figure 59) showed no consistent difference in the IC_{50} of the X cell lines compared to the luciferase controls, the two groups overlapped in terms of IC_{50} giving a mean of 62.2nM (SD 43.3) for three X cell lines compared to a mean of 76.9nM (SD 35.0) for four L cell lines which is not statistically significant.

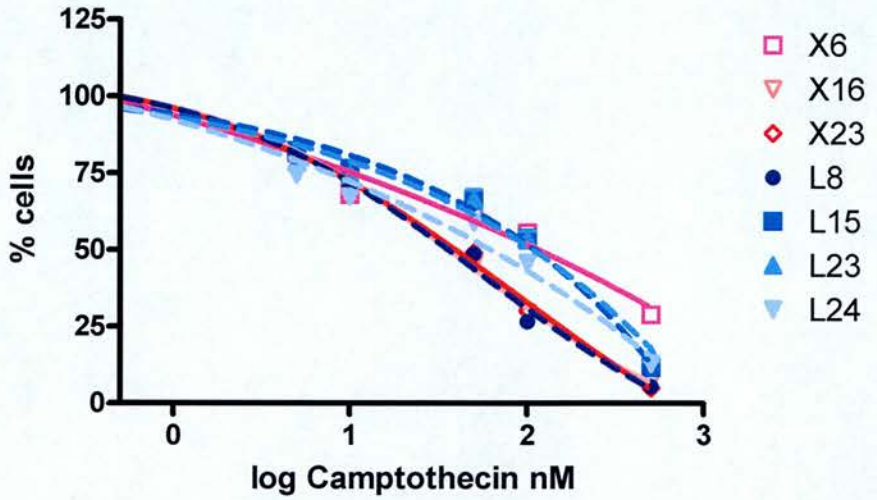

	Camptothecin
	IC50 (nM)
X6	112.2
X16	35.5
X23	38.9
L8	35.5
L15	107.2
L23	104.7
L24	60.3

Figure 59: Cytotoxic effect on clonal cell lines treated with camptothecin (0.5 - 500nM) for 72hrs by SRB assay. Error bars show standard error of the mean for 3 individual experiments.

The mean paclitaxel IC_{50} for three X cell lines was 5.5 (±0.35) nM compared to >8.1 nM for L cell lines. For docetaxel the mean IC50 was 2.2 (±0.56) nM for X cell lines and >5.9nM for L cell lines (Figure 60). Therefore at least a 2-fold increase in sensitivity to docetaxel treatment was identified in the XIAP knockdown cell lines. As the percentage cell death did not reach 50% in some of the L cell lines (L23, L24) at the highest treatment dose, an IC_{50} value cannot be accurately calculated and this also precludes statistical evaluation.

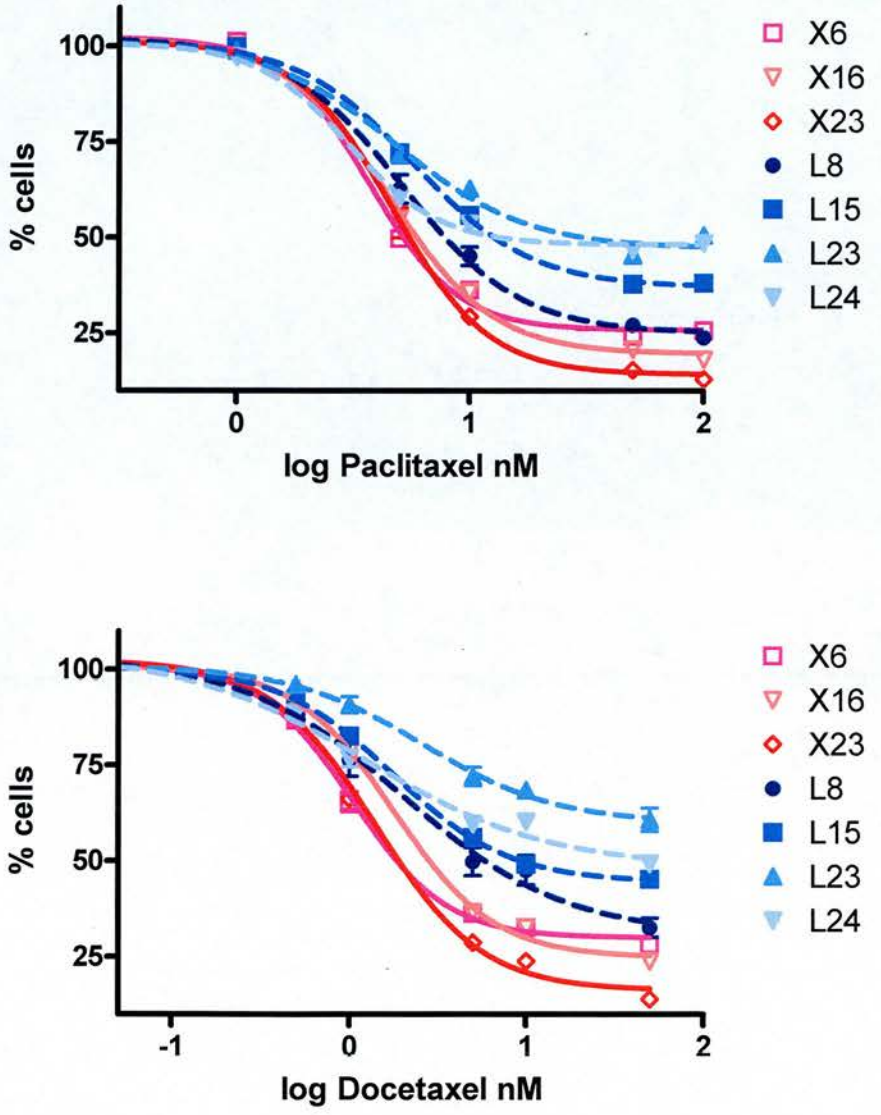

	Paclitaxel IC50 (nM)	Docetaxel IC50 (nM)
X6	5.0	1.9
X16	5.9	2.8
X23	5.4	1.7
L8	8.1	5.9
L15	13.3	9.1
L23	35.6	>50
L24	17.8	49.0

Figure 60: Cytotoxic effect on clonal cell lines treated with paclitaxel (1 -100nM) and docetaxel (0.5 – 50nM) for 72hrs by SRB assay. Error bars show standard error of the mean for 3 individual experiments.

8.3 Discussion

These data show a threefold increase in TRAIL cytotoxicity *in vitro* in a XIAP knockdown model. Cummins *et al* (131) were able to demonstrate a marked increase in sensitivity to TRAIL-mediated apoptosis and a corresponding decrease in clonogenic survival in a XIAP null HCT116 model. Our results therefore reproduce this effect though to a lesser degree and this may be explained by the 80% knock down of XIAP seen here compared with the complete knockout seen in the null system. In breast and pancreatic cancer cell lines (41) using the same short hairpin vector with similar levels of XIAP down regulation, a 100-fold increase in TRAIL cytotoxicity was seen. We could therefore hypothesise that a greater decrease in XIAP levels is required in a colorectal cancer model.

To investigate caspase activation in the two selected cell lines an earlier time-point was chosen as this is an earlier event in the apoptotic cascade. Cummins *et al* (131) were able to demonstrate cleaved caspase 3 at the 3 hour time point in the HCT116 colorectal cancer cell line. McManus *et al* used the identical rhTRAIL product at a dose of 5ng/ml therefore these conditions were also chosen for this study (41). A two fold increase in caspase 3/7 activity was demonstrated which confirms that the increase in TRAIL cytotoxicity is due to activation of the apoptotic cascade. A study of TRAIL receptor agonists in combination with radiotherapy in colorectal cancer models has shown promising results *in vitro* and *in vivo* (34).

Here we describe a 20% increase in sensitivity to γ radiation in the XIAP knockdown HCT116 cell line compared to the controls. Marini *et al* noted that a single fraction of γ radiation induced less than 10% apoptosis in the HCT116 wild type cell line. HCT116 was relatively resistant to radiotherapy compared to two other colorectal derivatives COLO205 and HCT15 though they used a lower dose of 10Gy (34). Radiotherapy studies performed with antisense oligonucleotides to XIAP transiently transfected *in vitro* into non small cell lung cancer cell lines led to a 20% increase in apoptotic cells after treatment with 2 Gy radiation (95). The differences in results

may therefore be explained by the differing sensitivities of cell lines and tumour types to γ radiation.

When treated with cytotoxic agents commonly used in the clinical treatment of colorectal cancer (5FU, camptothecin and oxaliplatin) there was no significant difference when comparing three X with four L cell lines. In the XIAP null system pilot experiments showed "small differences in cytotoxicity between XIAP null and wild type HCT116 cells when treated with cytotoxic agents such as 5FU" (Personal communication F. Bunz) (131). This implies that the sensitivity of these drugs is independent of XIAP in the HCT116 model.

Our data show at least a two fold increase in cytotoxicity of paclitaxel and docetaxel in the XIAP deficient cell lines. There is evidence that XIAP knock down sensitises to taxane therapy in prostate and lung cancer models (40) and the evidence presented here would concur. Taxanes are commonly used clinically in the treatment of both prostate and lung cancer but not colorectal cancer therefore this may provide a new therapeutic option. The effect may be due to the mechanism of action of taxanes rather than the characteristics of the tumour types. Chk1, a kinase involved in the DNA damage checkpoint response, has been shown to bind the BIR3 domain of XIAP during mitosis (143). This provides some evidence of cross-talk between cell cycle control and apoptosis although the precise mechanism remains to be clarified. Paclitaxel has been shown to induce caspase 10 dependent apoptosis (144) which is a component of the extrinsic pathway (involving the TRAIL receptors DR4 and DR5). It may be useful to investigate whether the effects of XIAP are more dependent on the extrinsic rather than the intrinsic pathway which is commonly associated with cytotoxic drugs. Another theory, continuing the theme of a threshold effect, is that treating with drugs known to be active in colorectal cancer does not show sensitisation because they have already crossed the threshold. Other drugs such as the taxanes may not have reached that threshold and therefore down regulating XIAP is effective.

A Phase 1 clinical trial is underway in solid tumours combining XIAP Antisense (Aegera Therapeutics Inc) and docetaxel (National Cancer Institute of Canada Clinical Trials Group). However, with such a narrow therapeutic index in colorectal models, it is unlikely these treatments will be of additional clinical benefit. Future work should focus on targeted agents such as rhTRAIL which directly stimulate the extrinsic apoptotic pathway. One such agent, a death receptor agonist, is in early clinical trial (145) and may show promise in combination with strategies to down regulate XIAP.

8.4 Conclusion

The XIAP deficient cell line X23 shows a 3-fold increase in sensitivity to rhTRAIL compared to L8. A 20% increase in sensitivity to radiotherapy and at least a two fold increase in sensitivity to docetaxel were seen in the X relative to the L cell lines. Further studies with these agents in an *in vivo* model are therefore warranted.

Chapter 9

shXIAP Cell Lines in a Mouse Xenograft Model

9 shXIAP Cell Lines in a Mouse Xenograft Model

9.1 Introduction

The initial *in vitro* and *in vivo* studies with XIAP antisense (AEG35156) failed to show a reproducible effect compared to the missense control (AEG35187) as described in Chapters 5 and 6. Therefore to establish whether down regulation of XIAP was a valuable strategy in colorectal cancer stable knockdown cell lines were developed as described in Chapter 7. This allowed an opportunity to test the efficacy of classical chemotherapeutic agents in combination with low XIAP levels in an isogenic system. The *in vitro* results of these studies are described in Chapter 8 and based on these data the model of stable XIAP knockdown was further developed for use *in vivo*.

The xenografts were established in female nude mice and growth pattern monitored prior to extraction of xenograft RNA to confirm the levels of XIAP and persistence of its down regulation in this model. Other IAPs and XAF1, the endogenous inhibitor of XIAP, were also investigated. Definitive chemotherapeutic studies with docetaxel were then performed to assess the effectiveness of a potential combination approach in colorectal cancer.

9.2 Results

9.2.1 In vivo xenograft establishment of clonal cell lines

All eight of the vector containing cell lines were successfully established in vivo (Figure 61A). In this model the growth pattern differed from the *in vitro* results as described in Chapter 7 Figure 51. Here, L8 and L23 grew faster than L24 and L15 which had a longer lag phase. The X clones had intermediate growth rates. The eight cell lines could be divided into two groups with a shorter (L8, L23, X23 and X16) or longer phase before exponential growth (X6, X10, L15 and L24). Therefore one X and one L cell line were selected for further investigation to overcome these difficulties. L8 and X23 had similar growth curves in this model, the growth of the individual xenografts is presented in Figure 61B, and were therefore selected as the pair of cell lines for chemotherapeutic studies in order to eliminate bias in comparison of cell growth patterns.

The take rate of the xenografts may be defined as the percentage of xenografts reaching a volume of $0.150cm^3$ by day 26. For the luciferase expressing cell lines these were L8 100%, L15 60%, L23 100%, L24 70% and for the shXIAP expressing cell lines X6 100%, X10 60%, X16 67%, X23 90%.

A

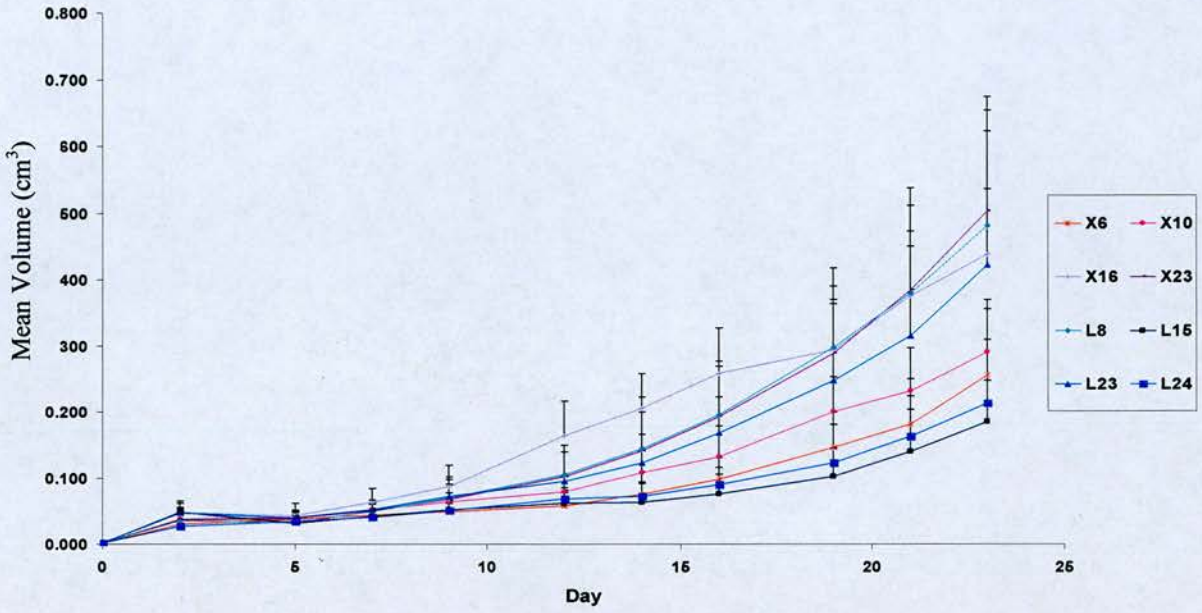

B

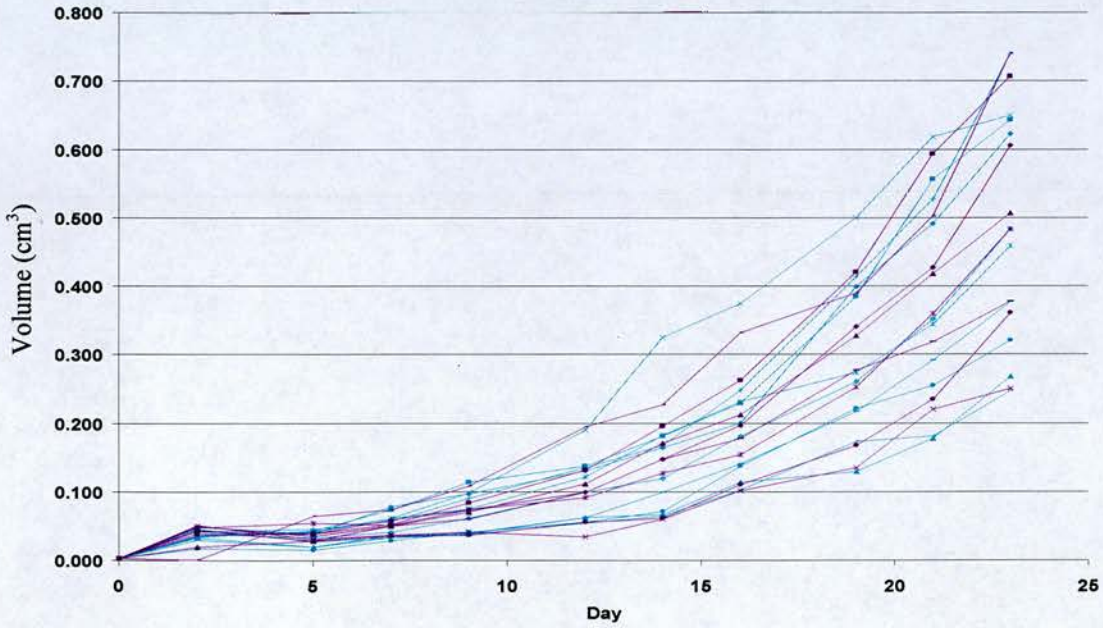

Figure 61: In vivo establishment of HCT116 XIAP knock down cell lines and luciferase expressing controls. A: Mean Volume (cm^3) and standard deviation for each group over time (days) with "no take" xenografts excluded. B: Growth curves for each individual xenograft in the L8 and X23 groups to show range of volumes.

9.2.2 Gene expression in xenografts

RNA was extracted from two xenografts (left and right flanks) in each cell line from the above establishment study, during the extraction process the tumours were noted to be cystic. This observation was not confined to either group of X or L cell lines though may explain some of the inconsistencies in growth. XIAP mRNA levels were investigated after 26 days in vivo growth (Figure 62). There was good correlation of the XIAP levels on the left compared to the right flank of each animal in all cell lines. The XIAP knockdown was X6 76%, X10 57%, X16 67%, X23 46% when the mean of left and right flank XIAP levels were expressed as a proportion of mean XIAP level in the eight samples of L clones (10.5 +/- 1.2). This implies that the X cell lines continue to express the short hairpin RNA despite the absence of G418 selection medium although there is less XIAP down regulation when compared to the *in vitro* model. A comparison of mean X23 and L8 XIAP levels, 5.6 and 10.1 respectively, shows 44% knockdown. The X23 cell line had the highest XIAP level of all the X lines which may be insufficient knockdown.

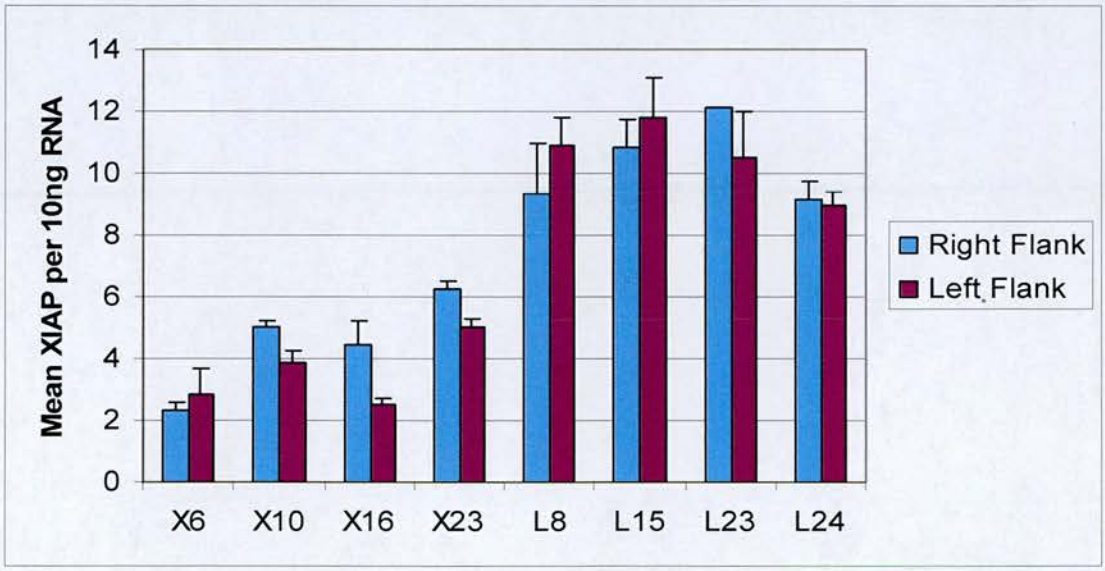

Figure 62: Mean XIAP mRNA levels by qRT-PCR from left and right xenografts of a single animal after 26 days of growth. Error bars show standard deviation for the triplicate RT-PCR reaction.

mRNA levels of three other members of the IAP family were investigated - CIAP1, CIAP2 and survivin (Figure 63). Comparison of the 4 X with 4 L clones revealed no significant differences in expression of any of these three endogenous inhibitors of apoptosis. In particular comparison of X23 and L8 showed similar IAP levels providing reassurance when interpreting the results of further experiments below.

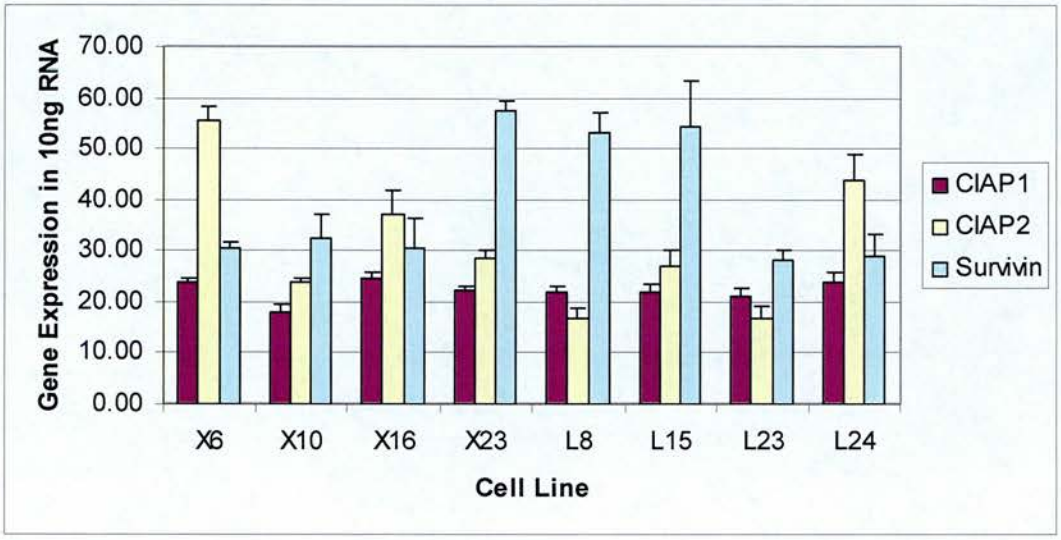

Figure 63: Other IAP family members mRNA levels by qRT-PCR. RNA extracted from right flank of xenograft on day 26. Error bars show standard deviation of the mean.

XAF1 levels cannot be directly compared with levels of the other IAPs as a different cell line was used for the standard curve in the qRT-PCR reaction (Figure 64). There is a tenfold variation in the XAF1 levels throughout the samples in this model which varies throughout the X and L cell lines. In particular there is more than a 5 fold difference in X23 and L8 levels, 29.0 and 5.5 respectively, which was not seen *in vitro* and may be functionally significant.

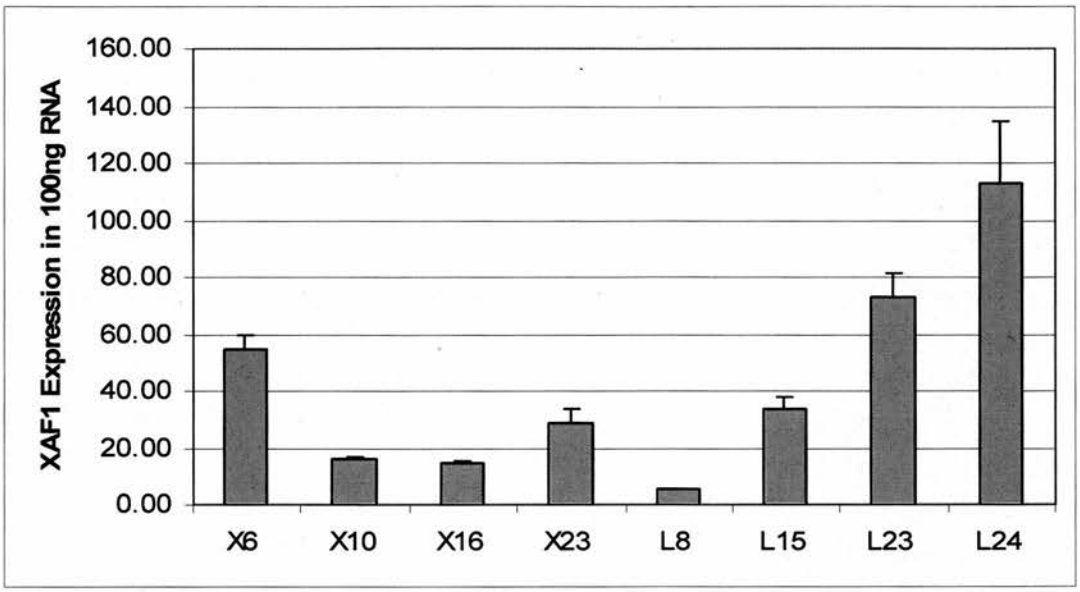

Figure 64: XAF1 RNA levels in 100ng total RNA by RT-PCR using COLO205 standard curve. Error bars show standard deviation of the mean for the triplicate RT-PCR reaction.

9.2.3 Clonal cell lines treated with docetaxel in vivo

For this study tumours were implanted on day -7 and the tumours were randomised by volume on day 0. There were 10 tumours per treatment group and 20 tumours per control group. The mice were treated with intraperitoneal docetaxel 5mg/kg on days 0, 4, 8, 11. Tumour volumes prior to randomisation (Figure 65) show no bias within the L8 groups and the X23 groups. However, there was a difference between the L8 and X23 groups which was not anticipated from the establishment study. This may be explained by the growth rates prior to randomisation (Figure 66); between day -5 and -3 the shXIAP expressing cell lines slow compared to the luciferase expressing cell lines. After randomisation (Day 0-2) the X23 group grows faster than the L8 group. This may have an impact on the initial response to treatment as the xenografts are in different phases of growth.

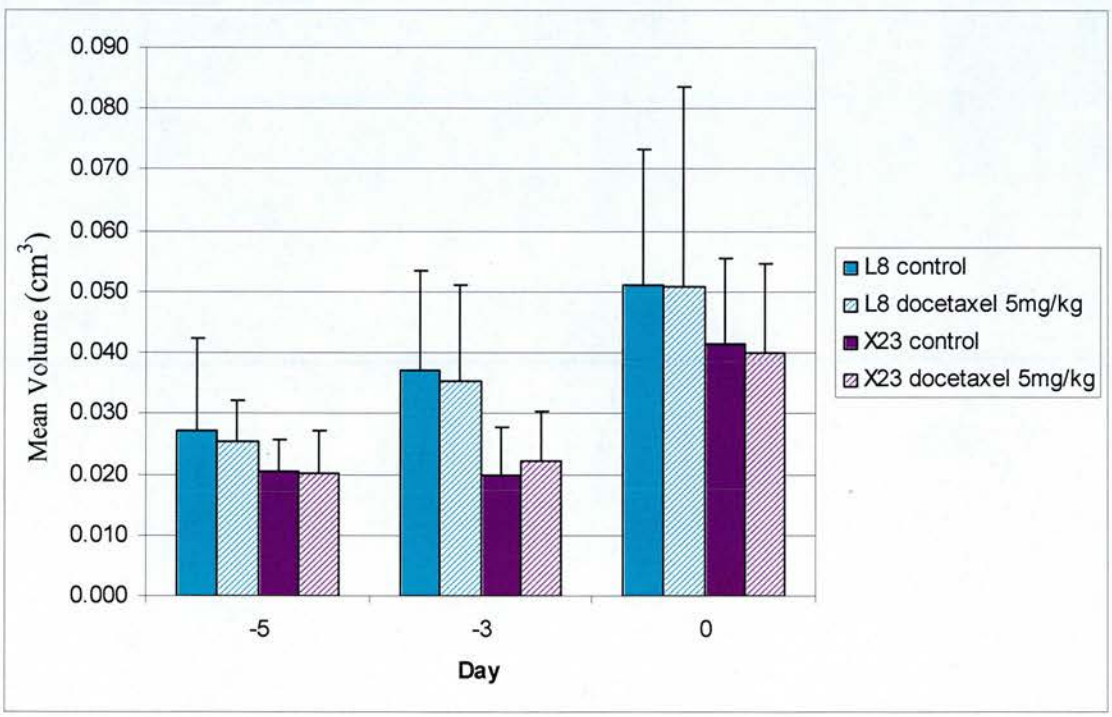

Figure 65: Pre-Treatment volumes prior to randomisation (Day 0). L8 is luciferase expressing cell line and X23 is shXIAP expressing cell line. Error bars show standard deviation from the mean for the group.

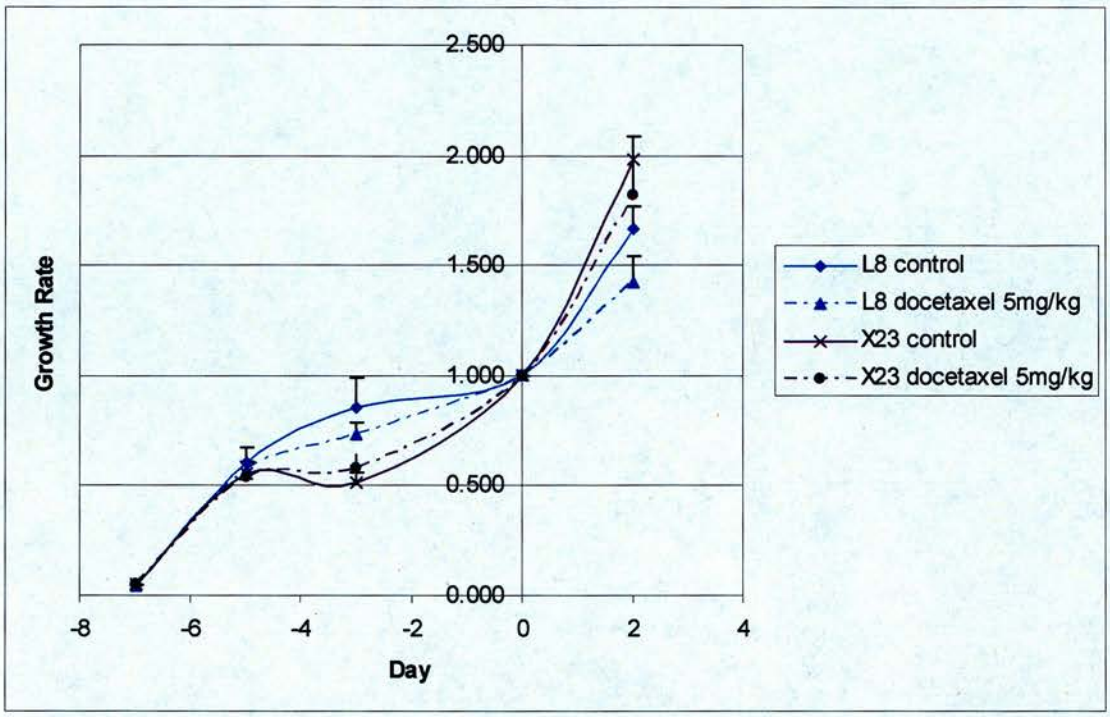

Figure 66: Growth rate of clonal cell line xenografts prior to randomisation. Error bars show standard error of the mean.

In the docetaxel treated xenografts (Figure 67) there was slowing of growth in the treated groups but this was not significant when compared to the control groups. As treatment progressed the L8 treated group grew more slowly than the X23 group though again this was not statistically significant.

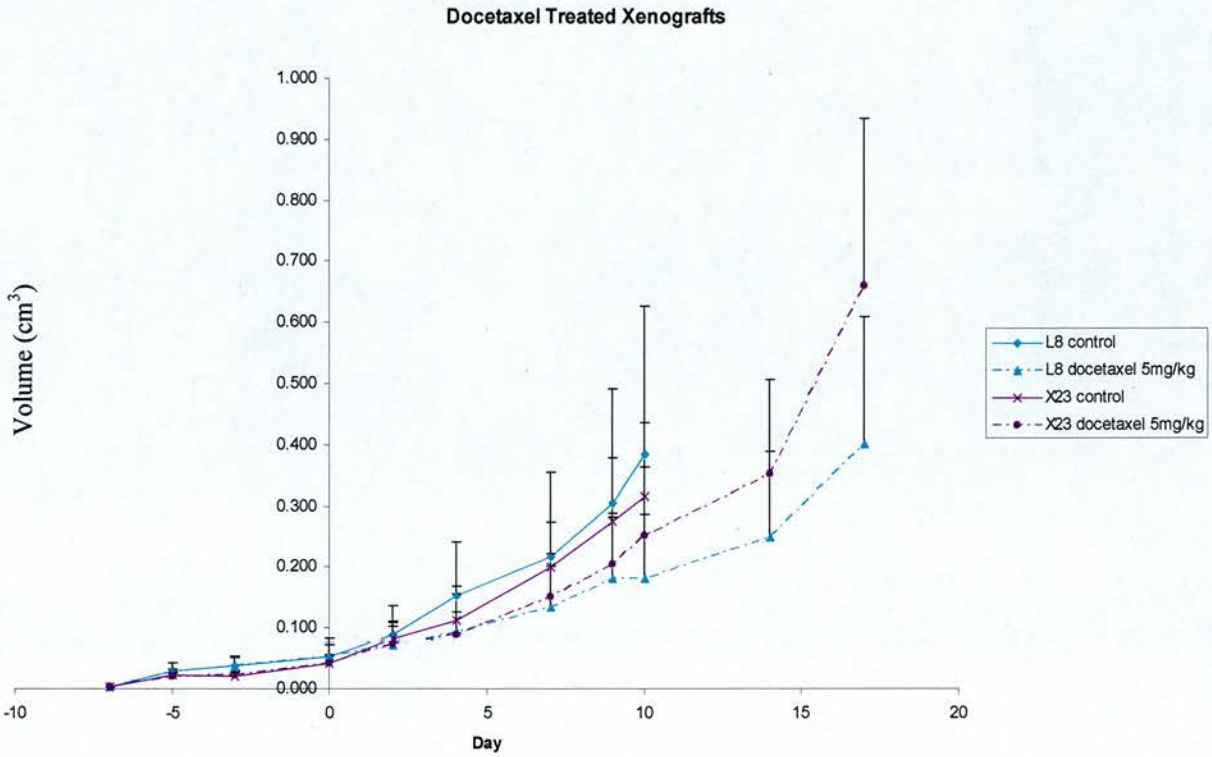

Figure 67: L8 and X23 xenografts treated with docetaxel 5mg/kg on days 0, 4, 8, 11. Error bars show standard deviation from the mean for the xenografts in that group.

9.3 Discussion

In this xenograft model the growth patterns differed from those *in vitro* where the X cell lines grew more slowly than their L controls (see Chapter 7). This may be due to differences in three dimensional structure in a xenograft compared to cells growing on a plate where the growth is two dimensional. The *in vitro* studies implied that more X cells were required to form the same growth curve and therefore the cell-cell interaction may be important. Another potential mechanism is that xenografts will be hypoxic relative to cells grown in tissue culture and therefore perform differently under these conditions. An end point of these studies was tumour volume but this does not necessarily equate to cell death. During this study tumours were noted to be cystic and further investigation may be useful to collect further samples for assessment of apoptosis.

The two cell lines selected for further study (L8 and X23) had good take rates which aids planning of further animal experiments in order to predict the numbers required.

Maintenance of XIAP knockdown at the RNA level is important to assure that the model remains stable over a period of time which is sufficient to perform further studies. The day 26 time point used in this study is well beyond that used in the chemotherapeutic studies described below and therefore maintenance of XIAP down regulation is validated in this xenograft system. The degree of X23 XIAP knockdown (46%) is less than is observed in the *in vitro* model (88%) which then decreased to 68% at passage 8. Given that the XIAP knock down in the X cell lines reduces over time following passage (seen also with microarray) it is perhaps not surprising that the *in vivo* model also loses a little of its XIAP down regulation when established as a xenograft. Further experiments to quantify XIAP mRNA levels in the short hairpin expressing cell lines over time in this xenograft model would also identify whether the effect decreases.

CIAP1, CIAP2 and survivin levels are similar between cell lines and do not appear to be associated with XIAP status. The levels of these three IAPs remain unchanged in breast cancer cells containing the identical vector as described by McManus *et al* (41) therefore our studies confirm these results in a second cell line from an alternative tumour type.

In this model it is relevant to consider the functional significance of XAF1 levels which are higher in the X23 cells which have decreased XIAP at the RNA level. XAF1 antagonises the anti-caspase activity of XIAP and reverses the protective effect of XIAP over expression by sequestration of XIAP in nuclear inclusions (81). Therefore high levels of XAF1 may enhance the effect of XIAP knockdown in the X23 cells, further increasing caspase activation. XIAP RNA levels would be similar as the total amount present has not changed but the cellular localisation prevents its function. If that were the case then perhaps the growth of X23 xenografts would be seen to slow, therefore it is likely that there are other important mechanisms which have not been investigated here.

In the chemotherapeutic study with docetaxel treatment the untreated groups had to be sacrificed on Day 10 before the end of cytotoxic treatment (Day 11). This leaves the later part of the experiment uncontrolled; however no significant difference was seen between the docetaxel treated groups. This may be due to the relative lack of XIAP down regulation in this model (46%, compared to 70-80% *in vitro*) or that a two-fold increase in cytotoxicity described *in vitro* for taxanes (Chapter 8) is not sufficient to translate to the *in vivo* system.

Our *in vitro* studies suggested that TRAIL may be a novel potential targeted therapy and further studies could be performed to explore this in an animal model. Radiotherapy is another potential therapeutic combination and could be developed though prior optimisation of the fractionation schedule would be required.

9.4 Conclusion

All eight short hairpin expressing cell lines may be established in an *in vivo* xenograft model, the L8 and X23 cell lines showing a similar growth pattern. XIAP knock down was maintained at the mRNA level for 26 days after implantation though the down regulation was less than that seen *in vitro*. There was no change in the levels of CIAP1, CIAP2 and survivin across the eight cell lines but XAF1 was increased in X23 compared to L8 which may be functionally relevant. Treatment of X23 and L8 xenografts with docetaxel showed no significant differential effect on growth.

Chapter 10

Summary

10 Summary

The aim of this project was to determine whether XIAP down regulation alone, or in combination with other therapeutic agents, is a potential treatment for patients with colorectal cancer. To achieve this aim, the following studies were undertaken and have been discussed in this thesis.

- The characterisation of colorectal cell lines according to p53, MLH1 and XIAP status.
- The effects of transient transfection of XIAP antisense (AEG35156) *in vitro* as a method of XIAP down regulation.
- The anti-tumour efficacy and pharmacodynamic effect of AEG35156 *in vivo* in a colorectal cancer xenograft model.
- The development and characterisation of stable XIAP knock down cell lines using short hairpin RNA.
- The *in vitro* response of stable XIAP knock down cell lines to therapeutic agents.
- The establishment and treatment of shXIAP-expressing cell lines as xenografts.

The HCT116 cell line is mismatch repair deficient (MLH1-) but has a normal functioning p53. Mismatch repair deficiency is a feature seen in 15% of patients with colorectal cancer (146) and has been reported to be associated with resistance to certain chemotherapeutic agents (130). It expresses XIAP at levels similar to the other cells in the colon cancer panel we used and is up regulated compared to normal tissue. It was particularly useful for my studies as it is a well characterised cell line; it grows well *in vitro* and *in vivo* and can be readily modified. Experimental results can also be compared with those generated using HCT116 XIAP null cell lines, in which Cummins *et al* demonstrated enhanced sensitivity to TRAIL (131).

A transient transfection method was used in the HCT116 colon cancer cell line and achieved 81% down regulation of XIAP mRNA using AEG35156. However, in the same experiment, down regulation (69%) of XIAP mRNA was also seen with the missense compound, AEG35187. LaCasse *et al* had also noted a reduction of up to 22% in XIAP mRNA levels with a non-sense control (AEG35185) indicating a non specific effect of the oligonucleotides (40). The use of a different control oligonucleotide may explain the magnitude of the difference in non-specific effect. It is essential to include control oligonucleotides in all experiments to assess whether the oligonucleotide is functioning by the prescribed mechanism i.e. complementary base pairing of the antisense to the XIAP mRNA. In the cytotoxicity experiments reported in this thesis, no significant therapeutic benefit of antisense over missense was seen; both showing a maximal cytotoxic effect of approximately 50% at concentrations greater than 400nM (one day protocol) and approximately 80% at concentrations greater than 200nM (two day protocol). These results suggest that AEG35156 is acting via an alternate mechanism other than RNase H degradation of the mRNA-antisense complex.

In order to achieve specific down regulation of XIAP only with the antisense (and not missense) a one day transfection at 400nM could be performed however the knockdown seen in this case is only 33%. Investigation of stimulation of the extrinsic apoptotic pathway with TRAIL following 33% XIAP down regulation does not confer a significant increase in apoptosis when compared to the missense control. Combination studies with other recognised cytotoxics are also unlikely to be effective with this level of selective down regulation of XIAP at the mRNA level. Therefore, it was decided to develop a stable siRNA model of XIAP knockdown and this will discussed later.

In an initial *in vivo* experiment, AEG35156 was associated with a significant effect on tumour growth in HCT116 xenografts compared to the missense control AEG35187, but subsequent studies did not confirm this. Weight loss was also observed in the antisense group identifying some toxicity in the animals. *In vivo*

efficacy studies were also performed with other colorectal cell lines (COLO205, HCT15, HT29 and SW620) but these results were not encouraging. It would therefore be difficult to justify single agent usage in colorectal cancer based on these studies. Lacasse et al have reported a 60% reduction in tumour volume *in vivo* in the LS174T colorectal cancer model (40). It would be interesting to obtain and establish the LS174T cell line to identify whether these data can be reproduced and compared with local HCT116 data.

Pharmacodynamic assays were performed in *in vivo* studies in the HCT116 xenograft model and mouse liver and tumour were analysed. Antisense directed against human XIAP caused mRNA target knock down in mouse liver despite a 3 base pair mismatch. Mouse liver XIAP down regulation of 43% appeared to be maximal 3 days after end of treatment. The effects of XIAP down regulation in mouse liver are cumulative in our study with 42% knock down seen 24 hours after 3 weeks of treatment. The tissue half life of AEG35156 is known to be approximately 14 days (personal communication, Aegera Therapeutics) and therefore these results would be consistent.

More concerning is the potential lack of specificity of the antisense and further pharmacodynamic studies would be useful to determine this. XIAP down regulation was not seen in the HCT116 human xenografts for which the mRNA sequence was designed although this could be due to the lack of drug delivery to the xenograft in this model. In clinical studies antisense molecules are known to cause liver transaminitis (112) which is thought to be a backbone effect of the oligonucleotide but here they also appear to be causing XIAP down regulation when the mRNA sequence was not specifically designed for this. The lack of specificity was also demonstrated in the *in vitro* studies where missense was shown to down regulate XIAP. This should be considered when designing clinical studies and would provide a rationale for including a missense control.

The Phase 1 study discussed in Chapter 2 demonstrated XIAP mRNA knock down of 82% and this coincided with an apparent clinical response to AEG35156 (147). In the same patient cleaved PARP and active caspase 3 are associated with reduced XIAP levels in lymphocytes confirming the mechanism of cell death was apoptosis. However, it is still possible that any oligonucleotide could have decreased XIAP levels and caused cell death by apoptosis, as again there was no missense control included in the study.

The ethics and practicality of including a missense control in Phase 1 trials are controversial as it would not be expected to benefit the patient and there would also be additional development costs, as separate toxicology would be required for the missense compound. An alternate strategy may be to analyse samples from other antisense phase 1 trials for decreased XIAP to assess whether this is a class effect of all antisense compounds; a BCL2 antisense oligonucleotide is in clinical trial (148).

In the laboratory, I used a different strategy to overcome the difficulties associated with the non-specific affects of antisense, by developing a stable colorectal cancer HCT116 cell line model incorporating short hairpin RNA targeting XIAP. This allowed potential combination regimens to be evaluated using XIAP down regulation in conjunction with known cytotoxic agents. XIAP is down regulated at the mRNA (82-93%) and protein levels (67-89%) in this model and knock down is maintained over at least 4 weeks; 79-85% at mRNA and 63-90% at protein level. The down regulation is also similar to levels which were achieved clinically (82% at the mRNA level) with antisense targeted to XIAP (147).

The isogenic nature of the short hairpin expressing cells was confirmed using microarray to identify any compensatory genetic changes. Compensatory changes had been observed in the XIAP knock out mouse (76) where CIAP1 and CIAP2 proteins were found to be up regulated. The microarray data confirmed down regulation of XIAP at early (4.3 fold) and late (2.4 fold) passage although some of

the down regulation was lost over time. The microarray data correlated well with qRT-PCR data, therefore validating the newer technique. There were no compensatory changes in genes currently documented to have an association with XIAP, other members of the bcl-2 family, the extrinsic pathway or the other six IAP family members. Therefore a colorectal cancer model has been developed using isogenic cell lines which differ only in the XIAP status at clinically relevant levels.

The *in vitro* characterisation of these stable knock down cell lines show differences in cell growth, plating efficiency and morphology in the XIAP deficient cells compared to their luciferase expressing controls. It is possible that further functions of XIAP exist which have not yet been clarified, for example XIAP binds to Chk1 implying a role in cell cycle (143) and another member of the IAP family, survivin also has a role in cell division (58). In addition, the enhanced cytotoxicity seen with taxanes following XIAP knockdown would be consistent with the differences in morphology and cell growth being related to the mitotic spindle and future studies are required to investigate this hypothesis.

In vitro cytotoxicity experiments with the XIAP deficient cell lines demonstrated a 2-fold increase in sensitivity to rhTRAIL and a 20% increase in sensitivity to radiotherapy. Cummins *et al* were able to demonstrate a greater increase in sensitivity to TRAIL in an HCT116 XIAP knock out model (131) which further suggests that maximising knockdown of XIAP would be beneficial.

It may be important to distinguish between knock "down" and knock "out". A small amount of XIAP, approximately 20%, may be enough to be functionally relevant and, as it is the most potent caspase inhibitor (55), this argument is plausible. A threshold may exist and greater than 80% XIAP down regulation may be required for the balance to favour apoptosis in a colorectal cancer model.

There was greater than 2-fold increase in sensitivity to paclitaxel and docetaxel *in vitro* in the XIAP knock down studies presented here; which is similar to the effect seen with rhTRAIL treatment. This suggests that the taxanes may have a mechanism of drug resistance which is dependent on XIAP in HCT116 cells. This class of drug acts by binding to tubulin and interfering with the function of the mitotic spindle blocking cells at the metaphase-anaphase junction (35). XIAP antisense has shown activity in prostate tumour xenografts in combination with docetaxel (40) and breast cancer RNAi XIAP cells were sensitised to taxanes (41) suggesting a rationale for combination of taxane therapy with XIAP knock down in a colorectal cancer model. However, a 2 fold enhancement of activity is probably not sufficiently convincing to encourage use in an unconventional tumour type.

Drugs commonly used in the treatment of colorectal cancer (5FU, oxaliplatin and irinotecan) failed to show sensitisation: they all act through the intrinsic pathway. The two compounds found to be effective in combination with XIAP down regulation (rhTRAIL and taxanes) are associated with the extrinsic pathway (6) (144). Further studies on the mechanism of action of taxanes may prove helpful in identifying additional therapeutic targets. Radiotherapy is usually described in relation to the intrinsic pathway but increasingly cross-talk between the two is described (2), with evidence for some involvement of the extrinsic pathway via Fas (26).

All eight short hairpin expressing cell lines have been established as *in vivo* xenograft models, the L8 and X23 cell lines showing a similar growth pattern. XIAP knockdown is maintained at the mRNA level for 26 days after implantation though the down regulation is less than that seen *in vitro*. However, treatment of X23 and L8 xenografts with docetaxel showed no significant change in growth. This may be related to the relatively small (2 fold) increase in sensitivity seen *in vitro*.

The overall aim of this project was to determine whether XIAP down regulation alone, or in combination with other therapeutic agents, is a potential treatment for patients with colorectal cancer. The data generated using the stable short hairpin RNA expressing HCT116 cell line suggest that the magnitude of sensitisation to docetaxel *in vitro* was insufficient for the effects to be translated to an *in vivo* model. The same outcome might be anticipated for radiotherapy, although was not formally assessed in these studies.

Further pre clinical evaluation of XIAP as a target might be relevant to colorectal cancer, if the magnitude of the XIAP knockdown can be increased to lower further the inhibition of apoptosis. Functional XIAP inhibitors may provide alternative strategies; for example polyphenylurea compounds (BIR2 domain) and smac peptidomimetics (BIR3 domain). However, difficulties with the development of these treatments may arise due to the specificity and sensitivity of these compounds. Additional challenges will also arise in assessing the pharmacodynamic effect as one advantage of antisense is the simplicity of its biomarker – a decrease in XIAP levels.

Therefore, the clinical development of AEG35156 should focus on alternative disease types. In the phase 1 clinical trial, efficacy was demonstrated in patients with refractory breast cancer and non-Hodgkin's lymphoma. During the phase I trial, the dose of 96mg/m^2/day was identified for further phase II evaluation as a seven day continuous intravenous infusion. However, the dose limiting toxicity of transaminitis may be overcome by shortening the duration of the intravenous infusion. Data are awaited from an ongoing clinical trial of infusion over 3 days to see whether this is feasible and an appropriate PD effect is achieved. Shorter still infusion regimens over 2 hours for 3 days are also being evaluated, in addition to combination regimes with docetaxel.

Chapter 11

References

11 References

1. Hanahan D, Weinberg RA. The hallmarks of cancer. Cell 2000;100(1):57-70.

2. Fulda S, Debatin KM. Extrinsic versus intrinsic apoptosis pathways in anticancer chemotherapy. Oncogene 2006;25(34):4798-811.

3. Schimmer AD. Inhibitor of apoptosis proteins: translating basic knowledge into clinical practice. Cancer research 2004;64(20):7183-90.

4. Debatin KM, Krammer PH. Death receptors in chemotherapy and cancer. Oncogene 2004;23(16):2950-66.

5. Zou H, Henzel WJ, Liu X, Lutschg A, Wang X. Apaf-1, a human protein homologous to C. elegans CED-4, participates in cytochrome c-dependent activation of caspase-3. Cell 1997;90(3):405-13.

6. Wang S, El-Deiry WS. TRAIL and apoptosis induction by TNF-family death receptors. Oncogene 2003;22(53):8628-33.

7. de Jong S, Timmer T, Heijenbrok FJ, de Vries EG. Death receptor ligands, in particular TRAIL, to overcome drug resistance. Cancer Metastasis Rev 2001;20(1-2):51-6.

8. Figueredo A, Germond C, Maroun J, Browman G, Walker-Dilks C, Wong S. Adjuvant therapy for stage II colon cancer after complete resection. Provincial Gastrointestinal Disease Site Group. Cancer Prev Control 1997;1(5):379-92.

9. Efficacy of adjuvant fluorouracil and folinic acid in colon cancer. International Multicentre Pooled Analysis of Colon Cancer Trials (IMPACT) investigators. Lancet 1995;345(8955):939-44.

10. Schmoll HJ, Arnold D. Update on capecitabine in colorectal cancer. Oncologist 2006;11(9):1003-9.

11. Andre T, Boni C, Mounedji-Boudiaf L, *et al.* Oxaliplatin, fluorouracil, and leucovorin as adjuvant treatment for colon cancer. N Engl J Med 2004;350(23):2343-51.

12. Vaisman A, Varchenko M, Umar A, *et al.* The role of hMLH1, hMSH3, and hMSH6 defects in cisplatin and oxaliplatin resistance: correlation with replicative bypass of platinum-DNA adducts. Cancer research 1998;58(16):3579-85.

13. Temmink OH, Hoebe EK, van der Born K, Ackland SP, Fukushima M, Peters GJ. Mechanism of trifluorothymidine potentiation of oxaliplatin-induced cytotoxicity to colorectal cancer cells. British journal of cancer 2007;96(2):231-40.

14. Fink D, Zheng H, Nebel S, *et al.* In vitro and in vivo resistance to cisplatin in cells that have lost DNA mismatch repair. Cancer research 1997;57(10):1841-5.

15. Jonker DJ, Maroun JA, Kocha W. Survival benefit of chemotherapy in metastatic colorectal cancer: a meta-analysis of randomized controlled trials. British journal of cancer 2000;82(11):1789-94.

16. Douillard JY, Cunningham D, Roth AD, *et al.* Irinotecan combined with fluorouracil compared with fluorouracil alone as first-line treatment for metastatic colorectal cancer: a multicentre randomised trial. Lancet 2000;355(9209):1041-7.

17. Colucci G, Gebbia V, Paoletti G, *et al.* Phase III randomized trial of FOLFIRI versus FOLFOX4 in the treatment of advanced colorectal cancer: a multicenter study of the Gruppo Oncologico Dell'Italia Meridionale. J Clin Oncol 2005;23(22):4866-75.

18. Takimoto CH, Wright J, Arbuck SG. Clinical applications of the camptothecins. Biochim Biophys Acta 1998;1400(1-3):107-19.

19. Hayward RL, Macpherson JS, Cummings J, Monia BP, Smyth JF, Jodrell DI. Antisense Bcl-xl down-regulation switches the response to topoisomerase I inhibition from senescence to apoptosis in colorectal cancer cells, enhancing global cytotoxicity. Clin Cancer Res 2003;9(7):2856-65.

20. Cunningham D, Pyrhonen S, James RD, *et al.* Randomised trial of irinotecan plus supportive care versus supportive care alone after fluorouracil failure for patients with metastatic colorectal cancer. Lancet 1998;352(9138):1413-8.

21. de Gramont A, Figer A, Seymour M, *et al.* Leucovorin and fluorouracil with or without oxaliplatin as first-line treatment in advanced colorectal cancer. J Clin Oncol 2000;18(16):2938-47.

22. Rich TA, Skibber JM, Ajani JA, *et al.* Preoperative infusional chemoradiation therapy for stage T3 rectal cancer. Int J Radiat Oncol Biol Phys 1995;32(4):1025-9.

23. Janjan NA, Crane C, Feig BW, *et al.* Improved overall survival among responders to preoperative chemoradiation for locally advanced rectal cancer. Am J Clin Oncol 2001;24(2):107-12.

24. Spanos WJ, Jr., Perez CA, Marcus S, *et al.* Effect of rest interval on tumor and normal tissue response--a report of phase III study of accelerated split course palliative radiation for advanced pelvic malignancies (RTOG-8502). Int J Radiat Oncol Biol Phys 1993;25(3):399-403.

25. Shinomiya N. New concepts in radiation-induced apoptosis: 'premitotic apoptosis' and 'postmitotic apoptosis'. J Cell Mol Med 2001;5(3):240-53.

26. Reap EA, Roof K, Maynor K, Borrero M, Booker J, Cohen PL. Radiation and stress-induced apoptosis: a role for Fas/Fas ligand interactions. Proc Natl Acad Sci U S A 1997;94(11):5750-5.

27. Cunningham D, Humblet Y, Siena S, *et al.* Cetuximab monotherapy and cetuximab plus irinotecan in irinotecan-refractory metastatic colorectal cancer. N Engl J Med 2004;351(4):337-45.

28. Sobrero AF, Fehrenbacher, L., Rivera F., Steinhauer, E. U., Prausova, J., Borg, C., Abubakr Y., Zubel, A., Langer, C., Burris, H. Randomized Phase III trial of cetuximab plus irinotecan versus irinotecan alone for metastatic colorectal cancer in 1298 patients who have failed prior oxaliplatin-based therapy: The EPIC trial. Proc Amer Assoc Cancer Res 2007.

29. Hochster HS. Bevacizumab in combination with chemotherapy: first-line treatment of patients with metastatic colorectal cancer. Semin Oncol 2006;33(5 Suppl 10):S8-14.

30. Tappenden P, Jones R, Paisley S, Carroll C. Systematic review and economic evaluation of bevacizumab and cetuximab for the treatment of metastatic colorectal cancer. Health Technol Assess 2007;11(12):1-146.

31. de Vries EG, Gietema JA, de Jong S. Tumor necrosis factor-related apoptosis-inducing ligand pathway and its therapeutic implications. Clin Cancer Res 2006;12(8):2390-3.

32. Kanzler S TT, Heinemann V, et al. Results of a phase 2 trial of HGS-ETR1 (agonistic human monoclonal antibody to TRAIL receptor 1) in subjects with relapsed or refractory colorectal cancer (CRC) [abstract 630]. Eur J Cancer Suppl 2005;3:177.

33. Attard G PR, de Bono JS, et al. Phase 1 and pharmacokinetic study of HGS-ETR2, a human monoclonal antibody to TRAIL-R2, in patients with advanced solid malignancies [abstract B114]. Clin Cancer Res 2005;11:9060S.

34. Marini P, Denzinger S, Schiller D, *et al.* Combined treatment of colorectal tumours with agonistic TRAIL receptor antibodies HGS-ETR1 and HGS-ETR2 and radiotherapy: enhanced effects in vitro and dose-dependent growth delay in vivo. Oncogene 2006;25(37):5145-54.

35. Gligorov J, Lotz JP. Preclinical pharmacology of the taxanes: implications of the differences. Oncologist 2004;9 Suppl 2:3-8.

36. Aggarwal BB, Shishodia S, Takada Y, *et al.* Curcumin suppresses the paclitaxel-induced nuclear factor-kappaB pathway in breast cancer cells and inhibits lung metastasis of human breast cancer in nude mice. Clin Cancer Res 2005;11(20):7490-8.

37. Ajani JA, Pazdur R, Dumas P, Fairweather J. Phase II study of prolonged infusion of Taxol in patients with metastatic colorectal carcinoma. Invest New Drugs 1998;16(2):175-7.

38. Casazza AM, Fairchild CR. Paclitaxel (Taxol): mechanisms of Resistance. Cancer Treat Res 1996;87:149-71.

39. Tortora G, Caputo R, Damiano V, *et al.* Oral administration of a novel taxane, an antisense oligonucleotide targeting protein kinase A, and the epidermal growth factor receptor inhibitor Iressa causes cooperative antitumor and antiangiogenic activity. Clin Cancer Res 2001;7(12):4156-63.

40. LaCasse EC, Cherton-Horvat GG, Hewitt KE, *et al.* Preclinical characterization of AEG35156/GEM 640, a second-generation antisense oligonucleotide targeting X-linked inhibitor of apoptosis. Clin Cancer Res 2006;12(17):5231-41.

41. McManus DC, Lefebvre CA, Cherton-Horvat G, *et al.* Loss of XIAP protein expression by RNAi and antisense approaches sensitizes cancer cells to functionally diverse chemotherapeutics. Oncogene 2004;23(49):8105-17.

42. Bast RC, Jr., Lilja H, Urban N, *et al.* Translational crossroads for biomarkers. Clin Cancer Res 2005;11(17):6103-8.

43. Lynch HT, de la Chapelle A. Hereditary colorectal cancer. N Engl J Med 2003;348(10):919-32.

44. Lynch HT, de la Chapelle A. Genetic susceptibility to non-polyposis colorectal cancer. J Med Genet 1999;36(11):801-18.

45. Peltomaki P. Deficient DNA mismatch repair: a common etiologic factor for colon cancer. Hum Mol Genet 2001;10(7):735-40.

46. Funaioli C, Pinto C, Mutri V, Di Fabio F, Ceccarelli C, Martoni AA. Does biomolecular characterization of stage II/III colorectal cancer have any prognostic value? Clin Colorectal Cancer 2006;6(1):38-45.

47. Magrini R, Bhonde MR, Hanski ML, *et al.* Cellular effects of CPT-11 on colon carcinoma cells: dependence on p53 and hMLH1 status. Int J Cancer 2002;101(1):23-31.

48. Borresen-Dale AL, Lothe RA, Meling GI, Hainaut P, Rognum TO, Skovlund E. TP53 and long-term prognosis in colorectal cancer: mutations in the L3 zinc-binding domain predict poor survival. Clin Cancer Res 1998;4(1):203-10.

49. Clahsen PC, van de Velde CJ, Duval C, *et al.* p53 protein accumulation and response to adjuvant chemotherapy in premenopausal women with node-negative early breast cancer. J Clin Oncol 1998;16(2):470-9.

50. Ahnen DJ, Feigl P, Quan G, *et al.* Ki-ras mutation and p53 overexpression predict the clinical behavior of colorectal cancer: a Southwest Oncology Group study. Cancer research 1998;58(6):1149-58.

51. Watanabe T, Wu TT, Catalano PJ, *et al.* Molecular predictors of survival after adjuvant chemotherapy for colon cancer. N Engl J Med 2001;344(16):1196-206.

52. Wallace-Brodeur RR, Lowe SW. Clinical implications of p53 mutations. Cell Mol Life Sci 1999;55(1):64-75.

53. Lowe SW, Cepero E, Evan G. Intrinsic tumour suppression. Nature 2004;432(7015):307-15.

54. Wright CW, Duckett CS. Reawakening the cellular death program in neoplasia through the therapeutic blockade of IAP function. J Clin Invest 2005;115(10):2673-8.

55. Deveraux QL, Takahashi R, Salvesen GS, Reed JC. X-linked IAP is a direct inhibitor of cell-death proteases. Nature 1997;388(6639):300-4.

56. Takahashi R, Deveraux Q, Tamm I, *et al.* A single BIR domain of XIAP sufficient for inhibiting caspases. The Journal of biological chemistry 1998;273(14):7787-90.

57. Crook NE, Clem RJ, Miller LK. An apoptosis-inhibiting baculovirus gene with a zinc finger-like motif. J Virol 1993;67(4):2168-74.

58. Verhagen AM, Coulson EJ, Vaux DL. Inhibitor of apoptosis proteins and their relatives: IAPs and other BIRPs. Genome Biol 2001;2(7):REVIEWS3009.

59. Li X, Yang Y, Ashwell JD. TNF-RII and c-IAP1 mediate ubiquitination and degradation of TRAF2. Nature 2002;416(6878):345-7.

60. Bolton MA, Lan W, Powers SE, McCleland ML, Kuang J, Stukenberg PT. Aurora B kinase exists in a complex with survivin and INCENP and its kinase activity is stimulated by survivin binding and phosphorylation. Mol Biol Cell 2002;13(9):3064-77.

61. Conte D, Holcik M, Lefebvre CA, *et al.* Inhibitor of apoptosis protein cIAP2 is essential for lipopolysaccharide-induced macrophage survival. Mol Cell Biol 2006;26(2):699-708.

62. Liston P, Roy N, Tamai K, *et al.* Suppression of apoptosis in mammalian cells by NAIP and a related family of IAP genes. Nature 1996;379(6563):349-53.

63. Holcik M, Lefebvre C, Yeh C, Chow T, Korneluk RG. A new internal-ribosome-entry-site motif potentiates XIAP-mediated cytoprotection. Nat Cell Biol 1999;1(3):190-2.

64. Borden KL. RING domains: master builders of molecular scaffolds? J Mol Biol 2000;295(5):1103-12.

65. Sun C, Cai M, Meadows RP, *et al.* NMR structure and mutagenesis of the third Bir domain of the inhibitor of apoptosis protein XIAP. The Journal of biological chemistry 2000;275(43):33777-81.

66. Shin S, Sung BJ, Cho YS, *et al.* An anti-apoptotic protein human survivin is a direct inhibitor of caspase-3 and -7. Biochemistry 2001;40(4):1117-23.

67. Deveraux QL, Reed JC. IAP family proteins--suppressors of apoptosis. Genes & development 1999;13(3):239-52.

68. Huang Y, Lu M, Wu H. Antagonizing XIAP-mediated caspase-3 inhibition. Achilles' heel of cancers? Cancer Cell 2004;5(1):1-2.

69. Lewis J, Burstein E, Reffey SB, Bratton SB, Roberts AB, Duckett CS. Uncoupling of the signaling and caspase-inhibitory properties of X-linked inhibitor of apoptosis. The Journal of biological chemistry 2004;279(10):9023-9.

70. Yang Y, Fang S, Jensen JP, Weissman AM, Ashwell JD. Ubiquitin protein ligase activity of IAPs and their degradation in proteasomes in response to apoptotic stimuli. Science 2000;288(5467):874-7.

71. Stehlik C, de Martin R, Kumabashiri I, Schmid JA, Binder BR, Lipp J. Nuclear factor (NF)-kappaB-regulated X-chromosome-linked iap gene expression protects endothelial cells from tumor necrosis factor alpha-induced apoptosis. J Exp Med 1998;188(1):211-6.

72. Bubici C, Papa S, Pham CG, Zazzeroni F, Franzoso G. NF-kappaB and JNK: an intricate affair. Cell Cycle 2004;3(12):1524-9.

73. Dan HC, Sun M, Kaneko S, *et al.* Akt phosphorylation and stabilization of X-linked inhibitor of apoptosis protein (XIAP). The Journal of biological chemistry 2004;279(7):5405-12.

74. Asselin E, Mills GB, Tsang BK. XIAP regulates Akt activity and caspase-3-dependent cleavage during cisplatin-induced apoptosis in human ovarian epithelial cancer cells. Cancer research 2001;61(5):1862-8.

75. Burstein E, Ganesh L, Dick RD, *et al.* A novel role for XIAP in copper homeostasis through regulation of MURR1. The EMBO journal 2004;23(1):244-54.

76. Harlin H, Reffey SB, Duckett CS, Lindsten T, Thompson CB. Characterization of XIAP-deficient mice. Mol Cell Biol 2001;21(10):3604-8.

77. Du C, Fang M, Li Y, Li L, Wang X. Smac, a mitochondrial protein that promotes cytochrome c-dependent caspase activation by eliminating IAP inhibition. Cell 2000;102(1):33-42.

78. van Loo G, Saelens X, van Gurp M, MacFarlane M, Martin SJ, Vandenabeele P. The role of mitochondrial factors in apoptosis: a Russian roulette with more than one bullet. Cell Death Differ 2002;9(10):1031-42.

79. Wu G, Chai J, Suber TL, *et al.* Structural basis of IAP recognition by Smac/DIABLO. Nature 2000;408(6815):1008-12.

80. Liu Z, Sun C, Olejniczak ET, *et al.* Structural basis for binding of Smac/DIABLO to the XIAP BIR3 domain. Nature 2000;408(6815):1004-8.

81. Liston P, Fong WG, Kelly NL, *et al.* Identification of XAF1 as an antagonist of XIAP anti-Caspase activity. Nat Cell Biol 2001;3(2):128-33.

82. Fong WG, Liston P, Rajcan-Separovic E, St Jean M, Craig C, Korneluk RG. Expression and genetic analysis of XIAP-associated factor 1 (XAF1) in cancer cell lines. Genomics 2000;70(1):113-22.

83. Silke J, Kratina T, Chu D, *et al.* Determination of cell survival by RING-mediated regulation of inhibitor of apoptosis (IAP) protein abundance. Proc Natl Acad Sci U S A 2005;102(45):16182-7.

84. Clem RJ, Sheu TT, Richter BW, *et al.* c-IAP1 is cleaved by caspases to produce a proapoptotic C-terminal fragment. The Journal of biological chemistry 2001;276(10):7602-8.

85. Hegde R, Srinivasula SM, Datta P, *et al.* The polypeptide chain-releasing factor GSPT1/eRF3 is proteolytically processed into an IAP-binding protein. The Journal of biological chemistry 2003;278(40):38699-706.

86. Tamm I, Kornblau SM, Segall H, *et al.* Expression and prognostic significance of IAP-family genes in human cancers and myeloid leukemias. Clin Cancer Res 2000;6(5):1796-803.

87. Krajewska M, Krajewski S, Banares S, *et al.* Elevated expression of inhibitor of apoptosis proteins in prostate cancer. Clin Cancer Res 2003;9(13):4914-25.

88. Krajewska M, Kim H, Kim C, *et al.* Analysis of apoptosis protein expression in early-stage colorectal cancer suggests opportunities for new prognostic biomarkers. Clin Cancer Res 2005;11(15):5451-61.

89. Shrikhande SV, Kleeff J, Kayed H, *et al.* Silencing of X-linked inhibitor of apoptosis (XIAP) decreases gemcitabine resistance of pancreatic cancer cells. Anticancer Res 2006;26(5A):3265-73.

90. Yamamoto K, Abe S, Nakagawa Y, *et al.* Expression of IAP family proteins in myelodysplastic syndromes transforming to overt leukemia. Leuk Res 2004;28(11):1203-11.

91. Liu Z, Li H, Wu X, *et al.* Detachment-induced upregulation of XIAP and cIAP2 delays anoikis of intestinal epithelial cells. Oncogene 2006.

92. Takeuchi H, Kim J, Fujimoto A, *et al.* X-Linked inhibitor of apoptosis protein expression level in colorectal cancer is regulated by hepatocyte growth factor/C-met pathway via Akt signaling. Clin Cancer Res 2005;11(21):7621-8.

93. Berezovskaya O, Schimmer AD, Glinskii AB, *et al.* Increased expression of apoptosis inhibitor protein XIAP contributes to anoikis resistance of circulating human prostate cancer metastasis precursor cells. Cancer research 2005;65(6):2378-86.

94. Yang X, Xing H, Gao Q, *et al.* Regulation of HtrA2/Omi by X-linked inhibitor of apoptosis protein in chemoresistance in human ovarian cancer cells. Gynecol Oncol 2005;97(2):413-21.

95. Cao C, Mu Y, Hallahan DE, Lu B. XIAP and survivin as therapeutic targets for radiation sensitization in preclinical models of lung cancer. Oncogene 2004;23(42):7047-52.

96. Agrawal S, Kandimalla ER. Role of Toll-like receptors in antisense and siRNA [corrected]. Nat Biotechnol 2004;22(12):1533-7.

97. Orr RM. Technology evaluation: fomivirsen, Isis Pharmaceuticals Inc/CIBA vision. Curr Opin Mol Ther 2001;3(3):288-94.

98. Jabs DA, Griffiths PD. Fomivirsen for the treatment of cytomegalovirus retinitis. Am J Ophthalmol 2002;133(4):552-6.

99. Storey A, Oates D, Banks L, Crawford L, Crook T. Anti-sense phosphorothioate oligonucleotides have both specific and non-specific effects on cells containing human papillomavirus type 16. Nucleic Acids Res 1991;19(15):4109-14.

100. Hannon GJ, Rossi JJ. Unlocking the potential of the human genome with RNA interference. Nature 2004;431(7006):371-8.

101. McIntyre GJ, Fanning GC. Design and cloning strategies for constructing shRNA expression vectors. BMC Biotechnol 2006;6:1.

102. Yan H, Frost P, Shi Y, *et al.* Mechanism by which mammalian target of rapamycin inhibitors sensitize multiple myeloma cells to dexamethasone-induced apoptosis. Cancer research 2006;66(4):2305-13.

103. Schimmer AD, Welsh K, Pinilla C, *et al.* Small-molecule antagonists of apoptosis suppressor XIAP exhibit broad antitumor activity. Cancer Cell 2004;5(1):25-35.

104. Karikari CA, Roy I, Tryggestad E, *et al.* Targeting the apoptotic machinery in pancreatic cancers using small-molecule antagonists of the X-linked inhibitor of apoptosis protein. Molecular cancer therapeutics 2007;6(3):957-66.

105. Oost TK, Sun C, Armstrong RC, *et al.* Discovery of potent antagonists of the antiapoptotic protein XIAP for the treatment of cancer. J Med Chem 2004;47(18):4417-26.

106. Li L, Thomas RM, Suzuki H, De Brabander JK, Wang X, Harran PG. A small molecule Smac mimic potentiates TRAIL- and TNFalpha-mediated cell death. Science 2004;305(5689):1471-4.

107. Agrawal S, Jiang Z, Zhao Q, *et al.* Mixed-backbone oligonucleotides as second generation antisense oligonucleotides: in vitro and in vivo studies. Proc Natl Acad Sci U S A 1997;94(6):2620-5.

108. Ranson M. A Phase 1 Trial of AEG35156 (XIAP antisense) Administered as a 7-day Continuous Intravenous Infusion in Patients with Advanced Tumors. Clinical Cancer Research 2005;11(24, part 2):8965s-9216s.

109. Ranson M, Ward T, Cummings J, Connolly K, Evans S, Robson L, Durkin J, Jolivet J, Jodrell D. A phase I trial of AEG35156 (XIAP antisense) administered as a continuous intravenous infusion in patients with advanced tumors. Journal of Clinical Oncology 2006;24(18S):3059.

110. Cummings J, Ward TH, LaCasse E, *et al.* Validation of pharmacodynamic assays to evaluate the clinical efficacy of an antisense compound (AEG 35156) targeted to the X-linked inhibitor of apoptosis protein XIAP. British journal of cancer 2005;92(3):532-8.

111. Agrawal S, Zhao Q, Jiang Z, *et al.* Toxicologic effects of an oligodeoxynucleotide phosphorothioate and its analogs following intravenous administration in rats. Antisense Nucleic Acid Drug Dev 1997;7(6):575-84.

112. Mani S, Goel S, Nesterova M, *et al.* Clinical studies in patients with solid tumors using a second-generation antisense oligonucleotide (GEM 231) targeted against protein kinase A type I. Ann N Y Acad Sci 2003;1002:252-62.

113. Lacasse EC, Kandimalla ER, Winocour P, *et al.* Application of XIAP antisense to cancer and other proliferative disorders: development of AEG35156/ GEM640. Ann N Y Acad Sci 2005;1058:215-34.

114. Waters JS, Webb A, Cunningham D, *et al.* Phase I clinical and pharmacokinetic study of bcl-2 antisense oligonucleotide therapy in patients with non-Hodgkin's lymphoma. J Clin Oncol 2000;18(9):1812-23.

115. Cummings J, Ranson M, Lacasse E, *et al.* Method validation and preliminary qualification of pharmacodynamic biomarkers employed to evaluate the clinical efficacy of an antisense compound (AEG35156) targeted to the X-linked inhibitor of apoptosis protein XIAP. British journal of cancer 2006;95(1):42-8.

116. Macpherson JS, Jodrell DI, Guichard SM. Validation of real-time reverse-transcription-polymerase chain reaction for quantification of capecitabine-metabolizing enzymes. Anal Biochem 2006;350(1):71-80.

117. Gentleman RC, Carey VJ, Bates DM, *et al.* Bioconductor: open software development for computational biology and bioinformatics. Genome Biol 2004;5(10):R80.

118. Team RDC. R: A language and environment for statistical computing. 2006 Available from: http://www.R-project.org

119. Gautier L, Cope L, Bolstad BM, Irizarry RA. affy--analysis of Affymetrix GeneChip data at the probe level. Bioinformatics 2004;20(3):307-15.

120. Smyth G. Limma: linear models for microarray data. New York: Springer; 2005.

121. Irizarry RA, Bolstad BM, Collin F, Cope LM, Hobbs B, Speed TP. Summaries of Affymetrix GeneChip probe level data. Nucleic Acids Res 2003;31(4):e15.

122. Smyth G. Linear models and empirical Bayes methods for assessing differential expression in microarray experiments. Statistical Applications in Genetics and Molecular Biology 2004;3, No 1:Article 3.

123. Benjamini YH, Y. Controlling the false discovery rate: a practical and powerful approach to multiple testing. Journal of the Royal Statistical Society Series 1995;B(57):289-300.

124. Wilson CL, Miller CJ. Simpleaffy: a BioConductor package for Affymetrix Quality Control and data analysis. Bioinformatics 2005;21(18):3683-5.

125. Liu T-Y. hgu133plus2: Affymetrix Human Genome U133 Plus 2.0 Array Annotation Data. R package version 1.12.0. [cited; Available from:

126. Skehan P, Storeng R, Scudiero D, *et al.* New colorimetric cytotoxicity assay for anticancer-drug screening. J Natl Cancer Inst 1990;82(13):1107-12.

127. Sewell JM, Mayer I, Langdon SP, Smyth JF, Jodrell DI, Guichard SM. The mechanism of action of Kahalalide F: variable cell permeability in human hepatoma cell lines. Eur J Cancer 2005;41(11):1637-44.

128. Alley MC, Scudiero DA, Monks A, *et al.* Feasibility of drug screening with panels of human tumor cell lines using a microculture tetrazolium assay. Cancer research 1988;48(3):589-601.

129. Workman P, Twentyman, P, Balkwill F, United Kingdom Co-Ordinating Committee on Cancer Reasearch (UKCCCR). Guidelines for the welfare of animals in experimental neoplasia. British journal of cancer 1998;77:1-10.

130. Meyers M, Wagner MW, Hwang HS, Kinsella TJ, Boothman DA. Role of the hMLH1 DNA mismatch repair protein in fluoropyrimidine-mediated cell death and cell cycle responses. Cancer research 2001;61(13):5193-201.

131. Cummins JM, Kohli M, Rago C, Kinzler KW, Vogelstein B, Bunz F. X-linked inhibitor of apoptosis protein (XIAP) is a nonredundant modulator of tumor

necrosis factor-related apoptosis-inducing ligand (TRAIL)-mediated apoptosis in human cancer cells. Cancer research 2004;64(9):3006-8.

132. Zou B, Chim CS, Zeng H, *et al.* Correlation between the single-site CpG methylation and expression silencing of the XAF1 gene in human gastric and colon cancers. Gastroenterology 2006;131(6):1835-43.

133. Hu Y, Cherton-Horvat G, Dragowska V, *et al.* Antisense oligonucleotides targeting XIAP induce apoptosis and enhance chemotherapeutic activity against human lung cancer cells in vitro and in vivo. Clin Cancer Res 2003;9(7):2826-36.

134. Farman CA, Kornbrust DJ. Oligodeoxynucleotide studies in primates: antisense and immune stimulatory indications. Toxicol Pathol 2003;31 Suppl:119-22.

135. Spee B, Jonkers MD, Arends B, Rutteman GR, Rothuizen J, Penning LC. Specific down-regulation of XIAP with RNA interference enhances the sensitivity of canine tumor cell-lines to TRAIL and doxorubicin. Mol Cancer 2006;5:34.

136. Suzuki Y, Imai Y, Nakayama H, Takahashi K, Takio K, Takahashi R. A serine protease, HtrA2, is released from the mitochondria and interacts with XIAP, inducing cell death. Mol Cell 2001;8(3):613-21.

137. Vagnarelli P, Earnshaw WC. Chromosomal passengers: the four-dimensional regulation of mitotic events. Chromosoma 2004;113(5):211-22.

138. Geisbrecht ER, Montell DJ. A role for Drosophila IAP1-mediated caspase inhibition in Rac-dependent cell migration. Cell 2004;118(1):111-25.

139. Vogler M, Giagkousiklidis S, Genze F, Gschwend JE, Debatin KM, Fulda S. Inhibition of clonogenic tumor growth: a novel function of Smac contributing to its antitumor activity. Oncogene 2005;24(48):7190-202.

140. Welman A, Cawthorne C, Barraclough J, *et al.* Construction and characterization of multiple human colon cancer cell lines for inducibly regulated gene expression. J Cell Biochem 2005;94(6):1148-62.

141. Olayioye MA, Kaufmann H, Pakusch M, Vaux DL, Lindeman GJ, Visvader JE. XIAP-deficiency leads to delayed lobuloalveolar development in the mammary gland. Cell Death Differ 2005;12(1):87-90.

142. Buchsbaum DJ, Zhou T, Grizzle WE, *et al.* Antitumor efficacy of TRA-8 anti-DR5 monoclonal antibody alone or in combination with chemotherapy and/or radiation therapy in a human breast cancer model. Clin Cancer Res 2003;9(10 Pt 1):3731-41.

143. Galvan V, Kurakin AV, Bredesen DE. Interaction of checkpoint kinase 1 and the X-linked inhibitor of apoptosis during mitosis. FEBS Lett 2004;558(1-3):57-62.

144. Park SJ, Wu CH, Gordon JD, Zhong X, Emami A, Safa AR. Taxol induces caspase-10-dependent apoptosis. The Journal of biological chemistry 2004;279(49):51057-67.

145. de Bono JS, Calvert, H. A Phase 1 Safety and Pharmacokinetic (PK) Study of an Agonistic, Fully Human Monoclonal Antibody, HGS-ETR2, to the TNF-Related Apoptosis-Inducing Ligand Receptor 2 (TRAIL-R2) in Patients with Advanced

Cancer. 16th EORTC-NCI-AACR Symposium on Molecular Targets and Cancer Therapeutics 2004:Abstract #197.

146. Jo WS, Carethers JM. Chemotherapeutic implications in microsatellite unstable colorectal cancer. Cancer Biomark 2006;2(1-2):51-60.

147. Ranson M, Ward TH, Cummings J, Connolly K, Evans S, Robson L, Durkin J, Jolivet J, Jodrell DI. A Phase I Trial of AEG35156 (XIAP antisense)Administered as a 7-day Continuous Intravenous Infusion in Patients with Advanced Tumors. Clin Cancer Res 2005;11(9116s):C9172.

148. O'Brien S, Moore JO, Boyd TE, *et al.* Randomized phase III trial of fludarabine plus cyclophosphamide with or without oblimersen sodium (Bcl-2 antisense) in patients with relapsed or refractory chronic lymphocytic leukemia. J Clin Oncol 2007;25(9):1114-20.